ARMY RESEARCH LABORATORY

Material Optimization and Manufacturing Development of Reduced Cost Powder Metal Titanium Alloy Components for Gas Turbine Engine Application, Phase II - SBIR

Stanley Abkowitz, Robert Djingheuzian, Susan M. Abkowitz,
Harold Heussi, and Paul Weihrauch

ARL-CR-110 November 1993

prepared by

Dynamet Technology, Inc.
Eight A Street
Burlington, MA 01803

under contract

DAAL04-91-C-0046

The findings in this report are not to be construed as an official Department of the Army position unless so designated by other authorized documents.

Citation of manufacturer's or trade names does not constitute an official endorsement or approval of the use thereof.

Destroy this report when it is no longer needed. Do not return it to the originator.

DISCLAIMER NOTICE

THIS DOCUMENT IS BEST QUALITY AVAILABLE. THE COPY FURNISHED TO DTIC CONTAINED A SIGNIFICANT NUMBER OF COLOR PAGES WHICH DO NOT REPRODUCE LEGIBLY ON BLACK AND WHITE MICROFICHE.

REPORT DOCUMENTATION PAGE

Form Approved
OMB No. 0704-0188

1. AGENCY USE ONLY (Leave blank)	2. REPORT DATE	3. REPORT TYPE AND DATES COVERED
	November 1993	Final Report - 10/91 - 5/93

4. TITLE AND SUBTITLE
Material Optimization and Manufacturing Development of Reduced Cost Powder Metal Titanium Alloy Components for Gas Turbine Engine Application, Phase II - SBIR

5. FUNDING NUMBERS
DAAL04-91-C-0046

6. AUTHOR(S)
Stanley Abkowitz, Robert Djingheuzian, Susan M. Abkowitz, Harold Heussi, and Paul Weihrauch

7. PERFORMING ORGANIZATION NAME(S) AND ADDRESS(ES)
Dynamet Technology, Inc.
Eight A Street
Burlington, MA 01803

8. PERFORMING ORGANIZATION REPORT NUMBER
AD B173-752L

9. SPONSORING/MONITORING AGENCY NAME(S) AND ADDRESS(ES)
U.S. Army Research Laboratory
Watertown, MA 02172-0001
ATTN: AMSRL-OP-PR-WT

10. SPONSORING/MONITORING AGENCY REPORT NUMBER
ARL-CR-110

11. SUPPLEMENTARY NOTES
Martin G. H. Wells, COR

12a. DISTRIBUTION/AVAILABILITY STATEMENT
Approved for public release; distribution unlimited.

12b. DISTRIBUTION CODE

13. ABSTRACT (Maximum 200 words)

This Small Business Innovation Research (SBIR) program has demonstrated the economic benefits of the cold-hot isostatic pressing (CHIP) powder metallurgy (P/M) materials and manufacturing technology to produce light-weight titanium alloy components. Tooling was developed and a turbine engine bearing housing preform and a tank track pin were produced. The study also established a data base of the static and dynamic mechanical properties as a function of the chloride impurity level of the commercially available elemental titanium powders and their associated costs.

14. SUBJECT TERMS
Titanium, Powder metallurgy, Bearing housing, Mechanical properties

15. NUMBER OF PAGES
115

16. PRICE CODE

17. SECURITY CLASSIFICATION OF REPORT	18. SECURITY CLASSIFICATION OF THIS PAGE	19. SECURITY CLASSIFICATION OF ABSTRACT	20. LIMITATION OF ABSTRACT
Unclassified	Unclassified	Unclassified	UL

ACKNOWLEDGEMENTS

The authors wish to thank Dr. Dan Rosenthal of Textron Lycoming and Professor Harold Margolin of Polytechnic Institute of New York for their very valuable participation in the many aspects of this work. Special acknowledgement is due to Dr. Geza Szonyi who was responsible for that portion of the program concerned with experimental design, statistical analysis and mathematical modeling.

At Dynamet Technology, we express our sincere thanks to Laural Buckman, whose contribution throughout the program and especially in preparation of this final report, is gratefully acknowledged. In addition, we wish to express our appreciation to Dr. Martin G.H. Wells of the Army Research Laboratory for his continued guidance and encouragement in the conduct of this program.

TABLE OF CONTENTS

FIGURES

FIGURES

FIGURES

FIGURES

TABLES

TABLES IN APPENDIX B

PROGRAM SUMMARY

This Small Business Innovation Research (SBIR) Phase II program has demonstrated the economic benefits of the Cold-Hot Isostatic Pressing (CHIP) powder metallurgy (P/M) materials and manufacturing technology to produce lightweight titanium alloy components for aircraft gas turbine engines and other applications at lower cost than by conventional methods without any sacrifice in the technical performance of the components.

The manufacturing development work included the design of tooling and the evaluation of CHIP processing conditions for manufacturing near-net shape gas turbine engine bearing housing preforms. By a series of iterations, a prototype preform was developed, manufactured and tested. The final preform weighed a little more than 7 pounds, was fully dense and of uniform microstructure throughout. Test samples machined from the CHIP preforms performed as well as test material machined from the currently manufactured forgings. In contrast, the ring forging needed to manufacture the same bearing housing weighs more than 2¼ times the CHIP produced preform. Since the finish machined bearing housing weighs 3.53 pounds the Dynamet P/M approach represents a buy-to-fly ratio of 2 to 1 compared to a ratio of 4.5 to 1 when manufactured from a forging.

In addition, a study was conducted to establish a comprehensive and reliable data base of the static and dynamic mechanical properties as related to the chloride impurity level of the commercially available elemental titanium powders and their associated costs. This was accomplished by a designed experiment at various chloride levels, and, from this data, the development of a statistical model to predict these properties across all chloride levels.

This model of properties along with corresponding material cost estimates will allow designers and planners to consider components for application of CHIP fabricated P/M titanium alloys. The model was applied to the gas turbine engine bearing housing described above, as well as to a replacement titanium Army tank track pin, currently manufactured from steel, which was also the subject of preliminary manufacturing development studies aimed at producing near-net shape preforms.

The report also contains a discussion of the economic advantages offered by the technology developed in this SBIR program and compares projected costs of CHIP produced titanium alloy components to those produced by conventional methods. The report concludes with suggestions for further development and follow-through with this manufacturing technology through a preproduction phase on an appropriate component such as the bearing housing, a tank track pin or other tank components.

INTRODUCTION

Developments in titanium alloy P/M at Dynamet Technology have indicated significant economic advantage in producing fully dense, near-net shape preforms from compactable blends of elemental powders by cold isostatic pressing (CIP), vacuum sintering and containerless hot isostatic pressing (HIP). Commercially known as the CHIP process, this manufacturing technology offers significant cost savings over other P/M methods by avoiding the use of more expensive pre-alloyed powders and by eliminating the need for a HIP enclosure or "can". Near-net CHIP processed components can also compete with wrought material by reducing both expensive machining time and the amount of material machined away associated with conventional starting stock.

Utilizing inexpensive titanium sponge fines, containing about 1500 ppm chloride impurity (designated StCl for standard chloride) as the starting powder, CHIP process technology offers static mechanical properties superior to castings and comparable to wrought product. Using extra low chloride (ELCl) titanium powder with less than 10 ppm chloride, produced by the hydride-dehydride process results in further improvements with both static and dynamic mechanical properties equivalent to wrought titanium alloys.

With the price of StCl titanium at $6-$8 per pound and that of ELCl powder 3 to 4 times higher. Any improved performance of ELCl-based materials is achieved at significantly higher cost. Despite the cost premium associated with ELCl powder, CHIP P/M manufacturing is still competitive with wrought materials in those component shapes which take full advantage of the economics offered by near-net-shape manufacturing; large, thin-walled axisymmetric shapes with a closed end, for example.

This report presents the results of Phase II of a Small Business Innovation Research (SBIR) program, initially sponsored by the Air Force Materials Laboratory (Phase I program) and later by the Army Research Laboratory, Materials Directorate (Phase II Program). The overall objective of the program was to overcome the remaining technical and economic barriers to the more widespread use of P/M titanium alloys in aircraft engine components including those with the most demanding performance criteria. To accomplish this, a manufacturing feasibility study was conducted, using a Ti-6Al-4V helicopter gas turbine engine support bearing housing as a prototypical component to demonstrate that near-net shape titanium alloy P/M can result in substantial cost savings without compromising structural properties or performance level. In addition, because the cost-performance trade-off in P/M titanium alloys is largely controlled by the chloride impurity level, a major effort was devoted to developing a predictive mathematical model to quantify the relationship between the chloride impurity level and the critical mechanical properties, including fatigue and fracture toughness, of Ti-6Al-4V.

To achieve these objectives the Phase II program plan was divided into six subtasks:

I Evaluation of Preform and Final Component Properties
II Optimization of Bearing Housing Preform Design
III Optimization of Chloride Impurity Level
IV Manufacture and Test of Optimal Bearing Housing
V Application of Process/Model to New Component
VI Economic Evaluation

The work performed is summarized in the report which follows.

EVALUATION OF PREFORM AND FINAL COMPONENT PROPERTIES

The component that was initially chosen for development as a P/M preform in Phase I was the main engine bearing support housing for the T55 gas turbine engine produced by Textron-Lycoming Division.

A drawing of the turbine support bearing housing is shown in Figure 1. With a maximum outside diameter (OD) flange dimension of just under 7 inches and a minimum inside diameter (ID) of more than 4 inches, it is a relatively complex shape with a wall thickness of about ½-inch over most of its 3-inch length.

This component is currently made by machining from a 16 pound ring forging of Ti-6Al-4V[1] which utilizes a substantial amount of excess material and requires additional costly machining to obtain final dimensions. The material must meet the requirements specified by ASM4928, Titanium 6Al-4V Alloy Bars, Forgings, and Rings in the Solution Annealed and Aged Condition with Yield Strength of 120,000 psi minimum.

In the Phase I effort, tooling was designed and used to fabricate three (3) prototype bearing housing P/M preforms. A conservative approach was used, designing the preform intentionally oversize to ensure that a finished component could be machined to specification regardless of exact shrinkage rate or distortion.

The target dimensions of the Phase I preform are shown in Figure 2. The dimensions of the three Ti-6Al-4V ELCl bearing housing preforms manufactured at the end of the Phase I program are shown in Figure 3. The actual dimensions were very uniform among the three preforms with variations limited to a range of less than 1 percent; the dimensions generally were within 2-3 percent of the target dimensions of Figure 2. The total weight was slightly above 9 pounds, representing a significant reduction in material usage from the 16 pound forging used in current manufacturing operation.

These three Phase I bearing housing preforms were delivered to Textron Lycoming at the conclusion of the Phase I program. These preforms, manufactured from Ti-6Al-4V StCl powder, were evaluated as the first task of the Phase II effort.

The three preforms were heat treated by solution annealing for 1 hour at 1750°F followed by water quenching and aging for 4 hours at 1050°F. Test results of tensile samples machined from one of the heat treated preforms are shown in Table I. As indicated the properties met the requirements of AMS specification 4996 for Ti-6Al-4V made by powder metallurgy.

---

[1] Specified dimensions of the ring forging are 7.34 inches minimum OD x 3.82 inches maximum ID and 3.20 inches minimum length

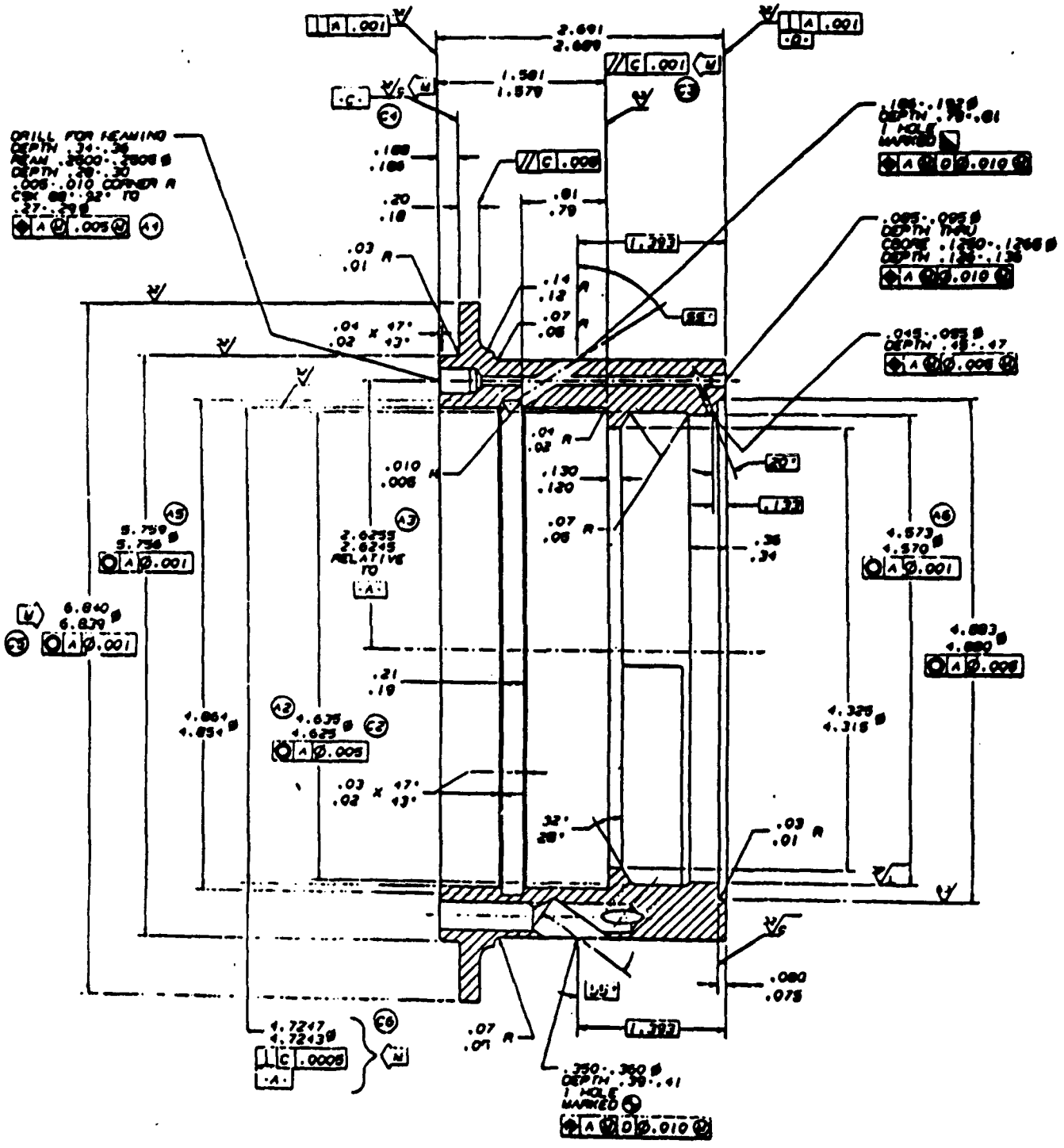

Figure 1. TEXTRON LYCOMING TURBINE SUPPORT BEARING HOUSING CURRENTLY MACHINED FROM FORGED RING.

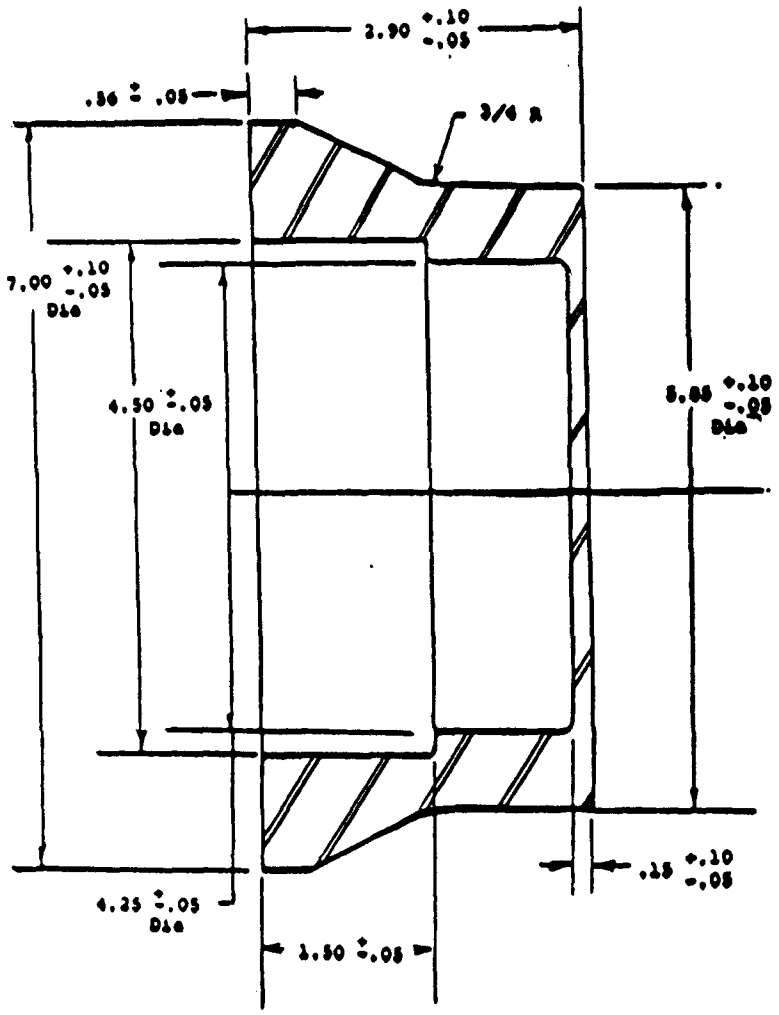

Figure 2. DESIGN OF PHASE I PREFORM FOR MANUFACTURE OF TURBINE ENGINE SUPPORT BEARING HOUSING OF FIGURE 1.

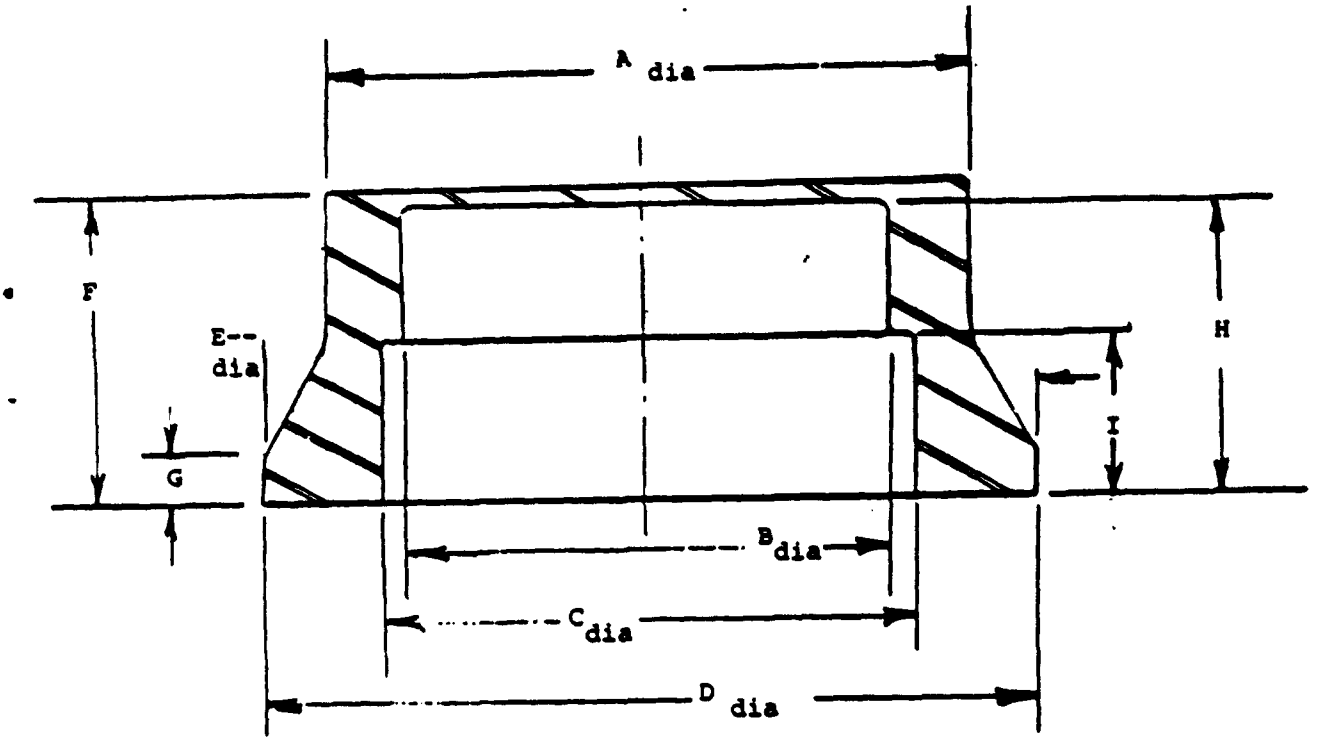

1597-1	
A dia	6.15
B dia	4.22
C dia	4.45
D dia	7.075
E dia	6.85
F	2.935
G	.75
H	2.675
I	1.485
WEIGHT	9.1#

1597-2	
A dia	6.15
B dia	4.215
C dia	4.40
D dia	7.15
E dia	6.92
F	2.93
G	.75
H	2.685
I	1.475
WEIGHT	9.2#

1597-3	
A dia	6.12
B dia	4.22
C dia	4.40
D dia	7.195
E dia	6.85
F	2.937
G	.76
H	2.677
I	1.48
WEIGHT	9.1#

Figure 3. DIMENSIONAL MEASUREMENTS AND WEIGHTS OF THREE PHASE I PROTOTYPE PREFORMS DELIVERED TO TEXTRON LYCOMING.

TABLE I

TENSILE PROPERTIES OF TEST BARS MACHINED
FROM HEAT TREATED Ti-6AL-4V StCL

BEARING HOUSING PREFORM

Test Bar	Ultimate Tensile Strength (psi)	0.2% Offset Yield Strength (psi)	% Elongation	% Reduction of Area
1	155,500	140,100	5.5	10.2
2	157,300	139,900	5.5	10.5
3	158,900	140,800	6.0	12.5
Specified AMS 4996 Minimum	130,000	120,000	5.0	10.0

A second heat treated preform was finish machined to the final component configuration shown in Figure 1. This finished bearing housing was then non-destructively tested by fluorescent penetrant inspection and functionally tested by leak testing under pressure. As indicated by the appended Certificate of Conformance, the bearing housing met all specified requirements.

OPTIMIZATION OF BEARING HOUSING PREFORM DESIGN

The objective of this task was to demonstrate that, with an optimized tool design, the weight of a titanium alloy bearing housing preform could be further reduced from the 9-10 pounds achieved in Phase I to less than 7.5 pounds. An iterative process of successive tooling modifications, using the Phase I tool design as the baseline, was used to achieve further reduction in preform weight.

At the start of the Phase II program, it was hoped that a simple modification to the Phase I bearing housing tooling could be made to achieve the target 2 - 2½ pound weight reduction. By eliminating the end closure and refining the shape of the flange end of the preform, as shown in Figure 4, the program goal would be achieved without a major change in the wall thickness of the Phase I preform. However, manufacturing of a prototype preform proved otherwise. Without the end closure to act as a constraint, significant control over dimensions was lost. Severe distortion developed during sintering and was further exaggerated by HIPing so that the final out-of-roundness exceeded the acceptable level.

Based on this result, the basic tool design philosophy was re-examined. To aim for a preform weight approaching 7 pounds would necessitate reducing the wall thickness significantly by restricting the preform to smaller external dimensions, as well as radically changing the tooling design so as to minimize preform distortion during sintering and/or HIPing.

Figure 5a depicts the basic Phase I tool design where the elastomeric mold walls are constrained from any lateral movement by a rigid steel base plate and an elastomeric top cap. Figure 5b represents a tool design in which the mold walls are free to move between lubricated top and bottom steel plates. This latter design was developed in this Phase II program as a possibility with the potential to achieve more uniform and reduced wall thickness in the bearing housing preform.

Another tool design approach was also evaluated based on the idea of applying the pressing pressure from within the mold, as shown conceptually in Figure 6. A potential advantage of this method is that the final outside dimensions and distortion might be better controlled, yielding a preform closer to net shape that is less costly to produce. Moreover, by this pressing route the incorporation of shape details into the inner wall might become possible. This added manufacturing flexibility, though not crucial to the bearing housing application, might be of benefit in fabricating other complex components.

Developmental work was done with both novel pressing approaches of Figures 5b and 6, but efforts were concentrated on the more established route of pressing from the outside.

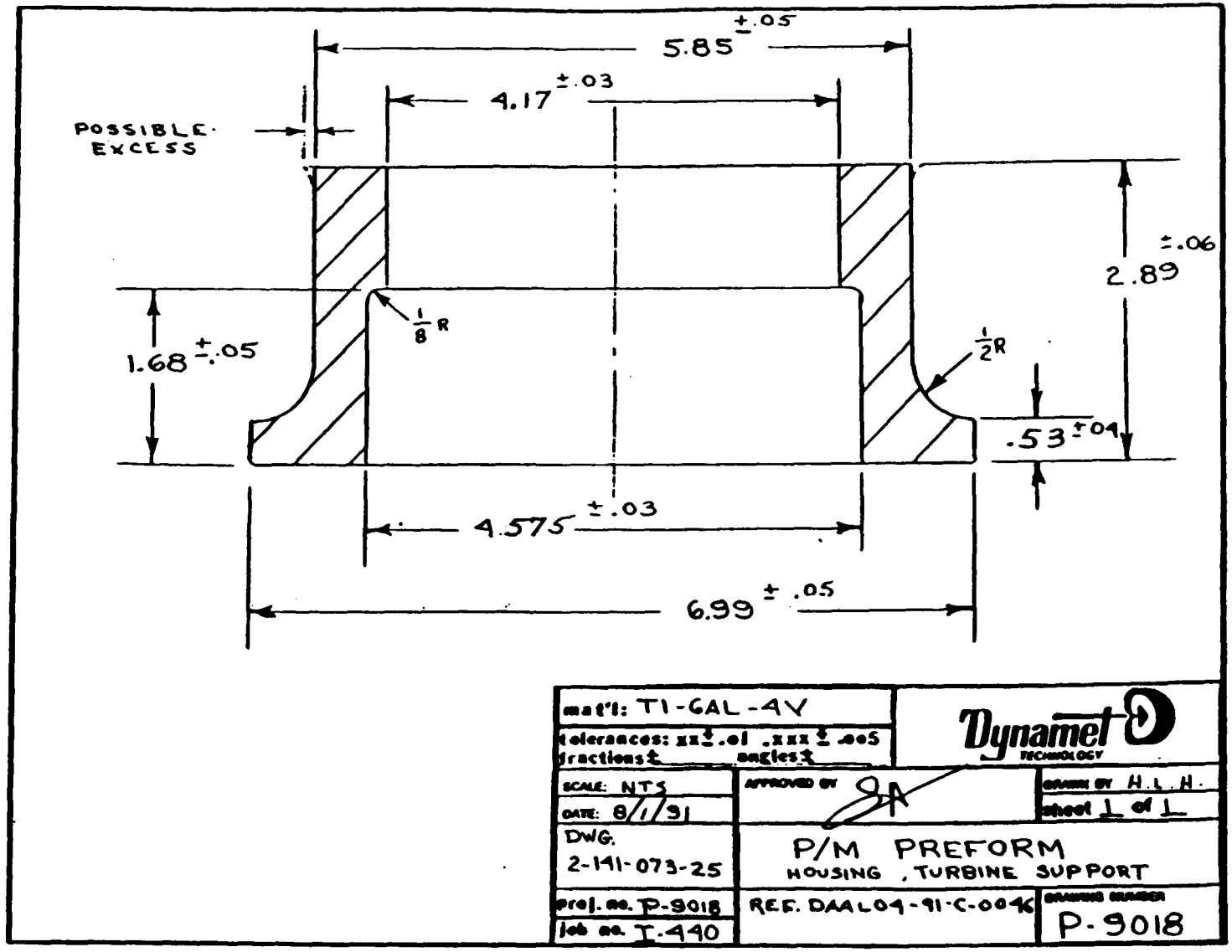

Figure 4. MODIFIED DESIGN OF P/M PREFORM FOR MANUFACTURE OF A REDUCED WEIGHT (7 POUND) TURBINE ENGINE SUPPORT BEARING HOUSING.

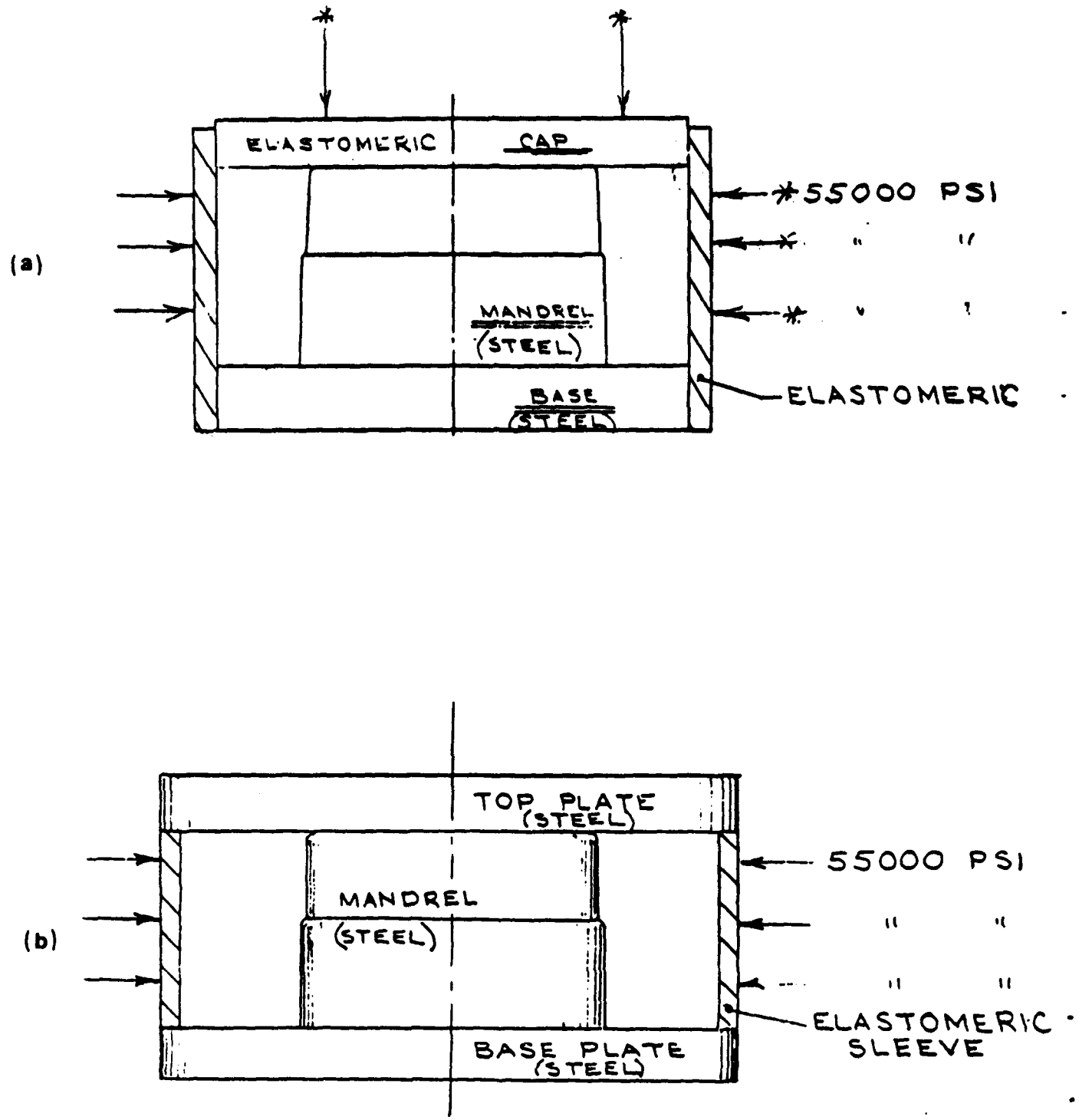

Figure 5. CONCEPTUAL SKETCH OF TOOL DESIGNS COMPARING (a) THE CONVENTIONAL APPROACH USING AN ELASTOMERIC END CAP WITH ELASTOMERIC MOLD WALLS LATERALLY CONSTRAINED AT BOTH ENDS AND (b) A DESIGN DEVELOPED IN THIS PROGRAM WHERE THE SIDE WALLS ARE FREE TO MOVE BETWEEN RIGID STEEL PLATES.

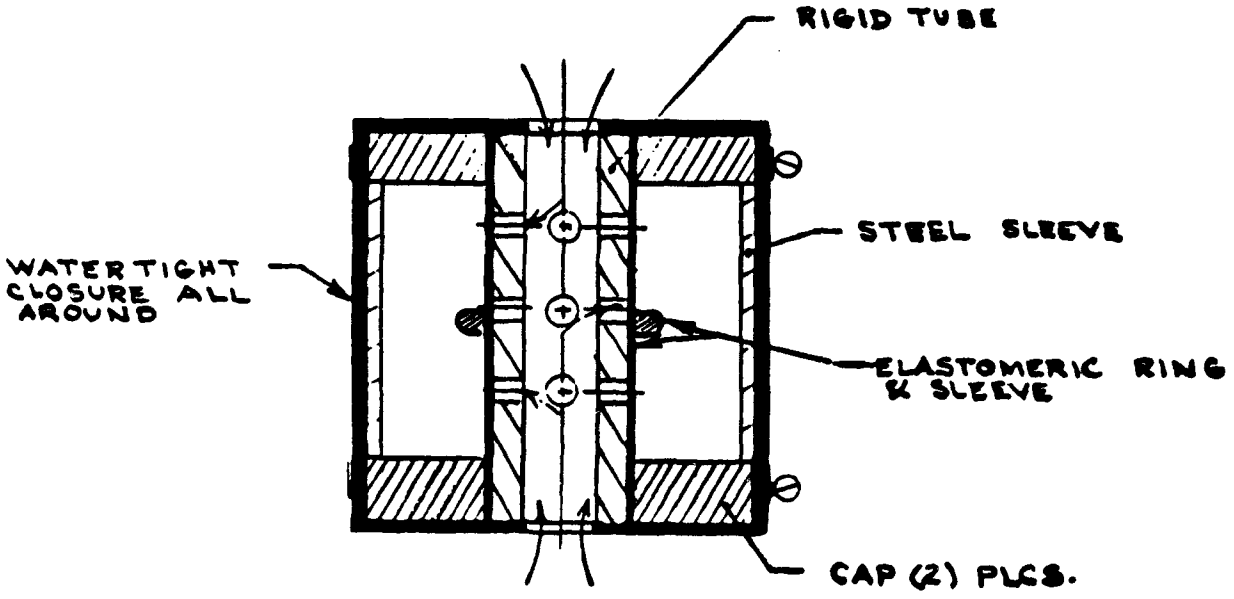

Figure 6. CONCEPTUAL SKETCH OF TOOL DESIGN FOR CIPING A CYLINDRICAL PREFORM BY APPLYING PRESSURE FROM THE INSIDE DIAMETER SURFACE.

Sub-size tooling for pressing in the tool configuration of Figure 5b was designed and built, and an experimental pressing without the end closure was made. Figure 7 shows typical dimensions as-CIPed and after sintering and HIPing. These results were considered promising since distortion was limited to a maximum of ±0.040 inches in the larger 4.90 inch diameter dimension (Figure 7).

Although this experimental pressing demonstrated much better control of the wall dimensions and more uniformity of the inner and outer diameters along the total length of the preform than with the Figure 5a tooling, some out-of-roundness developed during sintering, which was further exaggerated in HIPing. This result reaffirmed the necessity of retaining the end closure to minimize distortion (see Figure 7).

A series of tooling modifications were systematically introduced and tested with experimental pressings. First was the re-introduction of the end closure and the replacement of the elastomeric mold cover with a rigid steel cap lined with a thin elastomeric layer, as illustrated in Figure 8. Preliminary pressings indicated that these changes helped to maintain better diametrical constancy along the length of the preform and to reduce distortion near the end closure. This accomplishment is important in that it would permit a longer part with reduced wall thickness to be pressed with more reliable dimensional control.

When the end closure was reduced in thickness to 0.090 inch in an effort to minimize the preform weight, cracking developed in the blend radius between the interior side wall and the thin end cap. This problem was corrected by a minor tool modification to increase the blend radius tc about 0.25 inch (from about 0.10 inch).

A series of three simplified but full scale bearing housing preform shapes (without a flange but otherwise full size) were pressed crack-free using the refined mold/mandrel combination (Figure 9). All were vacuum sintered according to standard practice (2250°F for 2 hours) and HIPed in argon using a standard commercial cycle of 1650°F for 2 hours at 15,000 psi pressure.

The final full density experimental preforms, each weighing about 5.6 pounds, still displayed some tendency for the end closure to deform into a dome shape and for the wall to flare 2near the closed end (Figures 10 and 11).

An additional series of tooling modifications were undertaken to reduce the end closure distortion and wall flaring (Figure 10). First, the elastomeric layer was replaced with one that was thinner and of higher hardness. With this change the end distortion was reduced, as shown in Figure 11.

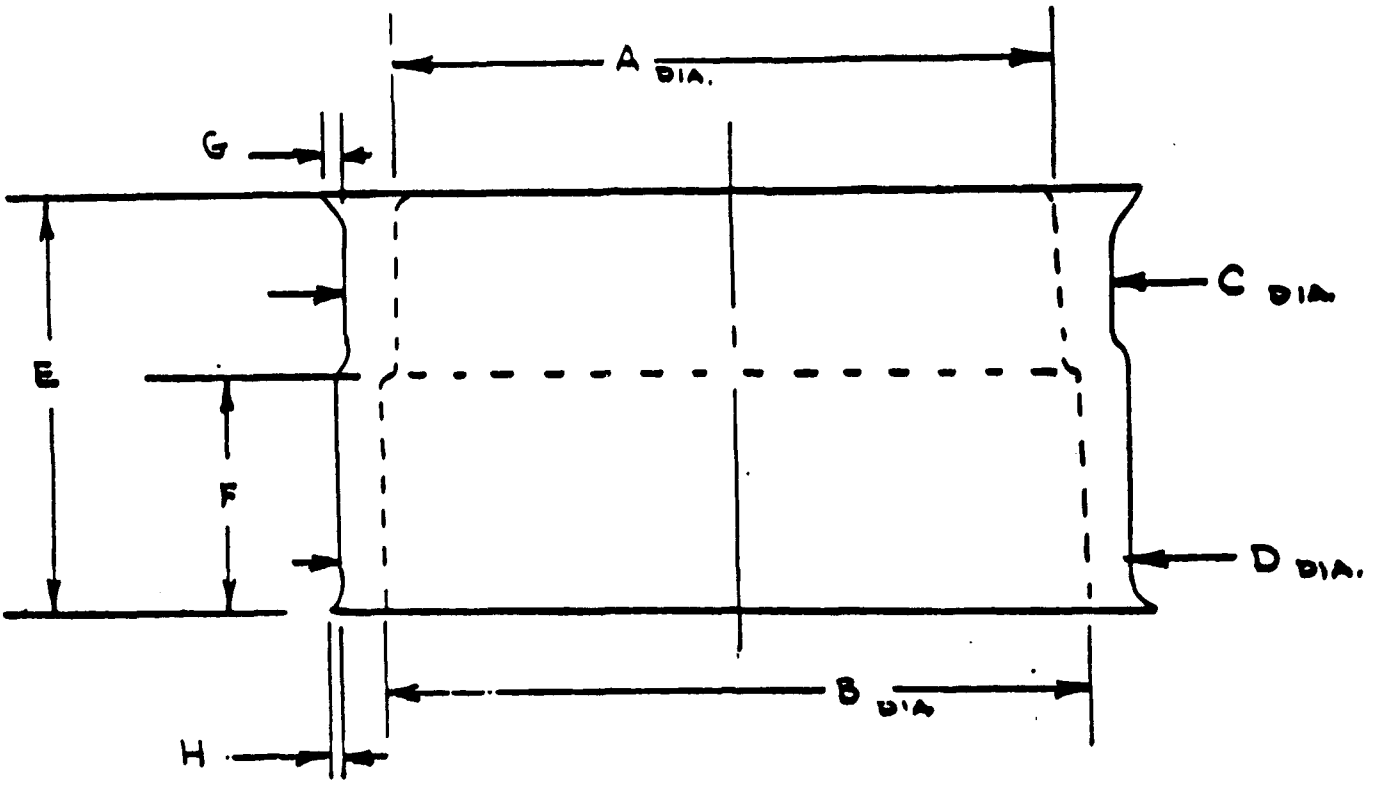

PRESSED	
A	4.464
B	4.735
C	4.4475
D	5.125
E	2.915
F	1.57
G	0.125
H	0.09
PRESS	55000 PSI
MAT'L	Ti-6Al-4V
WT.	597.4 gms

SINTERED*	
A	4.267/4.311
B	4.506/4.579
C	4.700/4.760
D	4.890/4.945
E	2.785
F	1.5
G	-
H	-
TEMP.	2250 F
TIME	2 HRS
DENSITY	95.10%

HIP*	
A	4.255/4.183
B	4.447/4.499
C	4.709/4.652
D	4.877/4.817
E	2.739/2.744
F	1.532
G	0.106
H	0.093
TEMP	1650 F
TIME	2 HRS
PRESS	15000 PSI
DENSITY	99.93%

* Diameters indicate out of roundness if shown with (2) Measurements

Figure 7. DIMENSIONS, WEIGHT AND DENSITY OF SUB-SIZE PREFORM USED TO PRELIMINARILY EVALUATE THE PRESSING APPROACH OF FIGURE 5b.

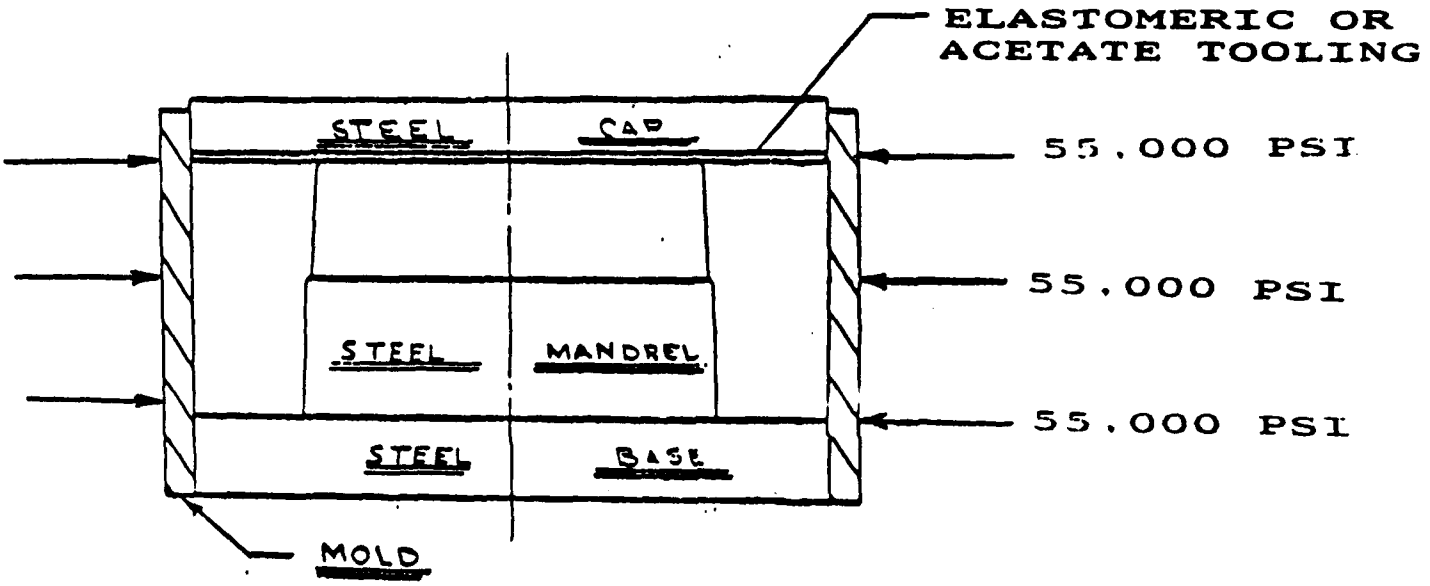

Figure 8. CONCEPTUAL SKETCH OF IMPROVED TOOLING CONFIGURATION COMBINING FEATURES OF THE PREVIOUS DESIGNS, AND UTILIZING AN ADDITIONAL ELASTOMERIC OR ACETATE LINER.

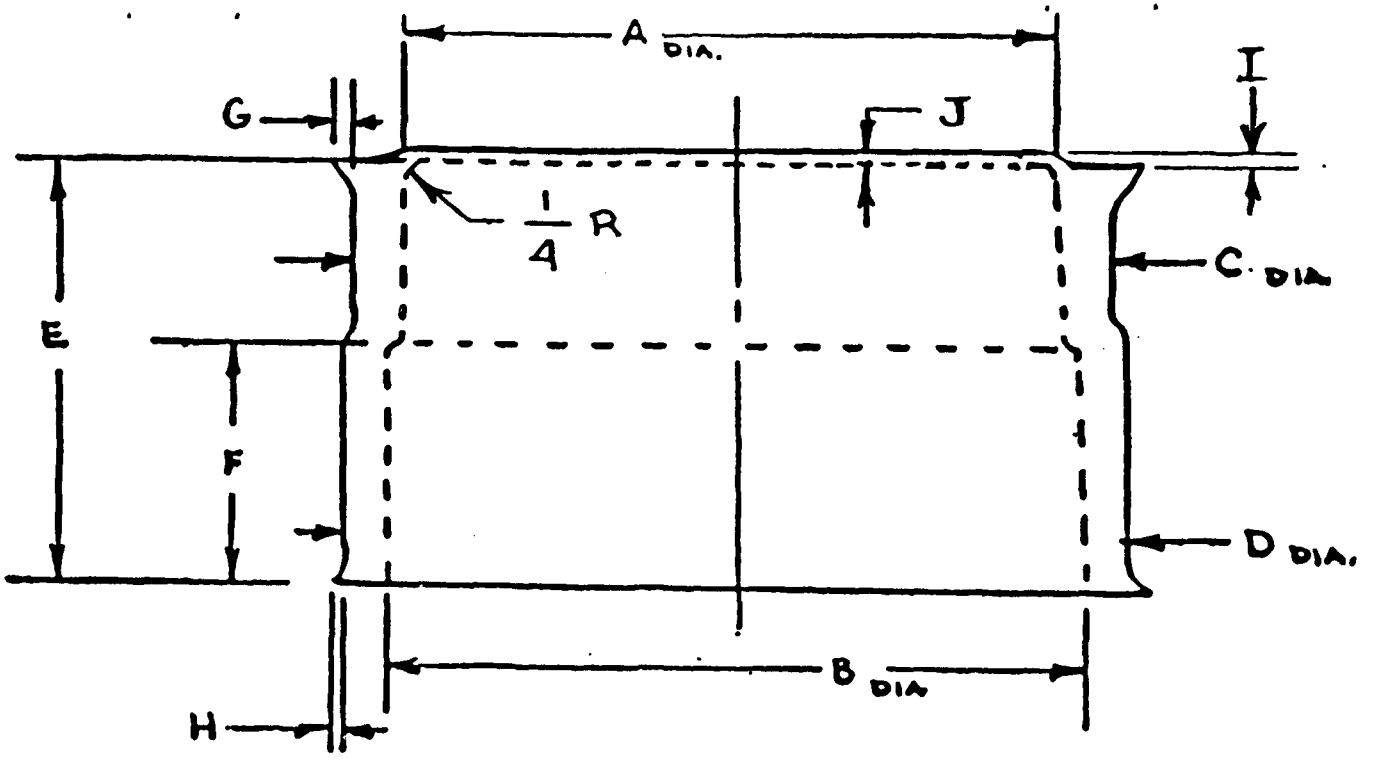

	PREFORM #3			PREFORM #4			PREFORM #5		
DIMENSION	CIP	SINTER	HIP	CIP	SINTER	HIP	CIP	SINTER	HIP
A Dia	4.470	4.336	4.271	4.473	4.331	4.274	4.474	4.330	4.259
B Dia	4.741	4.564	4.502	4.742	4.553	4.472	4.746	4.550	4.492
C Dia	6.230/6.335	6.112/6.365	5.936/5.979	6.325/6.338	6.133	5.998/6.046	6.442/6.438	6.121	6.162/5.967
D Dia	6.208	5.978	5.918	6.245/6.265	6.007	5.964	6.205	5.962	5.903
E	2.703/2.730	2.614/2.646	2.622	2.636/2.713	2.544/2.627	2.521	2.650	2.674/2.701	2.682
F	1.621/1.618	1.554/1.550	1.531	1.587/1.595	1.529/1.561	1.524	1.582/1.580	1.518/1.543	1.652
G	.040	Nil	.0375	Nil	Nil	.019	.112	Nil	.022
H	.050	.051	.035	.029	.020	.039	.059	.035	.038
I	.275	.223/.261	.416	.327/.362	.225/.279	.025	.396/.416	.200/.232	.025
J	.076/.084	.073/.086	.096	.073/.088	.070/.082	.084	.080	.063/.072	.075
WEIGHT	5.62#	-	-	5.57#	-	-	5.66#	-	-
DENSITY	-	96.1%	99.8%	-	95.5%	99.8%	-	95.8%	99.7%

Figure 9. WEIGHT, DENSITY AND DIMENSIONS OF THREE (3) DEVELOPMENTAL BEARING HOUSING PREFORMS AFTER CIP, SINTER AND HIP.

Figure 10. INITIAL PREFORM PRESSED WITH TOOLING CONFIGURATION OF FIGURE 8 WITH AN ELASTOMERIC LINER. NOTE DISTORTION OF END CLOSURE AND FLARING OF SIDE WALL.

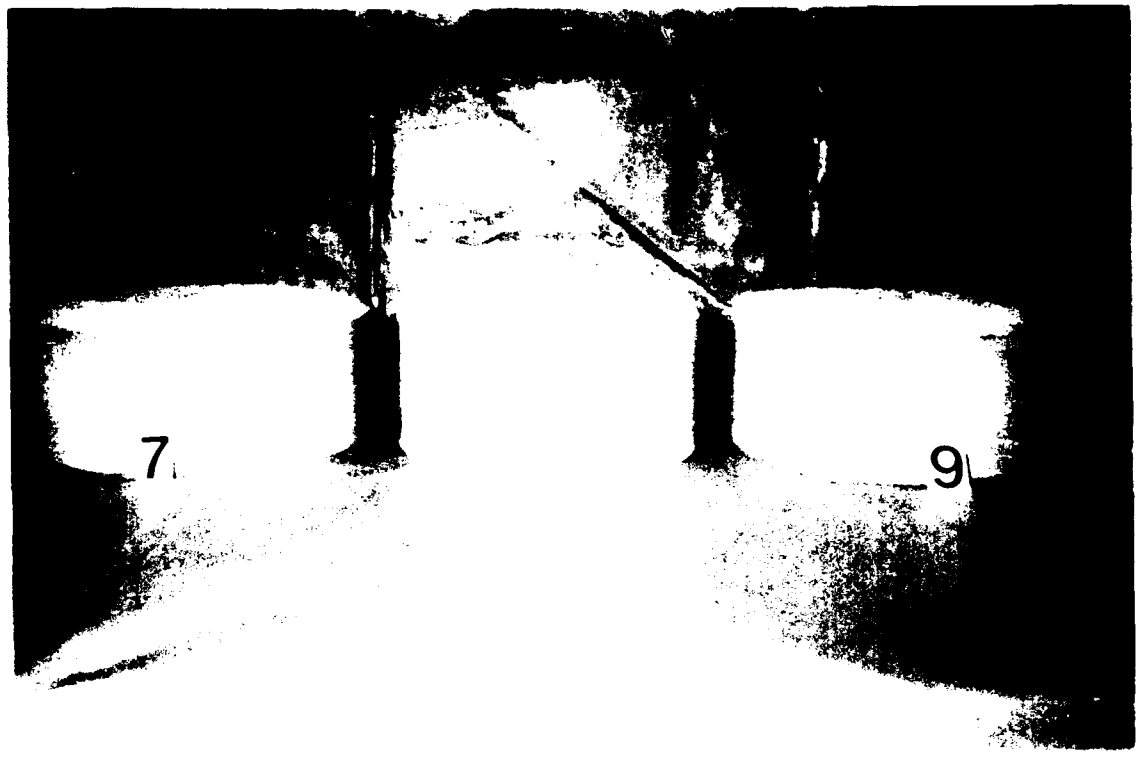

Figure 11. PREFORMS PRESSED AS IN FIGURE 8 BUT WITH A THINNER AND HARDER ELASTOMERIC LINER MATERIAL. NOTE SIGNIFICANT REDUCTION OF DISTORTION AND FLARING.

In successive tooling iterations, the elastomeric liner was replaced with a harder, less compliant acetate liner and a slightly enlarged steel end cap. As shown in Figure 12, these tooling changes virtually eliminated any tendency for the end closure to distort or the side wall to flare.

These tooling developments made possible the manufacture of a thinner walled bearing housing preform meeting the program's target of under 7½ pounds. A final tooling configuration for pressing the final bearing housing preform was built, incorporating the features described above.

Using the optimized tooling, four bearing housing preforms were cold isostatically pressed (CIPed) at 55,000 psi from a Ti-6Al-4V alloy blend (designation B-2151) based on StCl titanium powder. The preforms were vacuum sintered and HIPed using standard processing cycles as follows:

- Sintering Cycle - 2250°F for 2½ hours
- HIP Cycle - 1650°F/2 hours/15,000 psi

The preform configuration with pressed, sintered and HIPed dimensions of the four preforms are shown in Figure 13. Also included in Figure 13 are preform weights and densities after sintering and HIPing. All four preforms met the target weight of 7½ pounds with actual weights of approximately 7 to 7¼ pounds (3232 grams to 3302 grams).

Sintered density in all cases exceeded 94.5% of theoretical density indicating that the preforms had achieved closed porosity and would reach virtual full 100% density after HIPing. The four preforms displayed highly consistent and reproducible dimensions with differences in initial dimensions after sintering amounting to less than ± 0.5%.

HIPed density in all cases (Figure 13) exceeded 99.6% of theoretical wrought product density. This is considered full density for Ti-6Al-4V powder based alloys using standard chloride (StCl) commercially pure titanium powder, because of the relatively low density of any included chloride contaminant particles (absent in wrought titanium alloys).

Consistent with the results after sintering, the four HIPed preforms displayed highly consistent and reproducible dimensions with very little distortion (Figure 13). Dimensional variations after HIPing are in a range of about 2% (± 1%) compared to the 1% (±0.5%) variation in dimensions measured after sintering. Considering the size and complexity of the preform shape, this level of variation is considered near optimum.

The thickness of the end closure (dimension "J" in Figure 13) was intentionally varied from 0.073 inch (preforms A and C as pressed) to 0.092 inch (preform B as pressed) to see if this difference would affect dimensional control and distortion. The thinner end closure did not seem to measurably degrade the dimensional control or increase the distortion.

Figure 12 PREFORMS PRESSED WITH FURTHER TOOLING MODIFICATIONS INCLUDING THE REPLACEMENT OF THE ELASTOMERIC LINER WITH AN ACETATE LINER. NOTE THAT BOTH END CLOSURE DISTORTION AND SIDE WALL FLARING HAVE BEEN VIRTUALLY ELIMINATED.

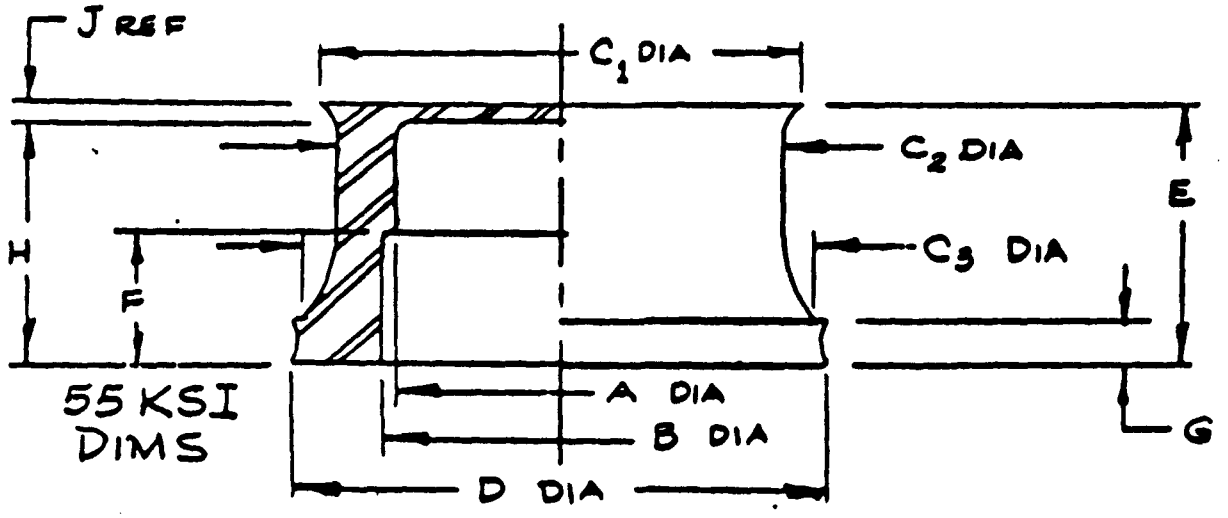

PREFORM (A) DIMENSIONS	PRESSED	SINTERED	HIPED
A DIA.	4.457	4.265	4.211
B DIA.	4.843	4.630	4.553
C1 DIA.	6.60	6.052	N/A
C2 DIA.	6.255	5.994	5.885
C3 DIA.	6.860	N/A	N/A
D DIA.	7.400--7.460	7.125	6.950--7.025
E	3.150	3.018	2.934--2.960
F	1.601	1.526	1.495
G	0.682	N/A	N/A
H	3.077	2.944	2.905
J (REF.)	0.073	0.064	N/A
	WEIGHT:3302 gms	DENSITY:94.65%	DENSITY:99.91%

PREFORM (C) DIMENSIONS	PRESSED	SINTERED	HIPED
A DIA.	4.451	4.202	4.211
B DIA.	4.843	4.608	4.553
C1 DIA.	6.519	6.000	N/A
C2 DIA.	6.217	5.961--5.980	5.853
C3 DIA.	6.912	N/A	N/A
D DIA.	7.488	7.110	6.975--7.000
E	3.149	3.011	2.945--2.970
F	1.598	1.532	1.487
G	0.672	N/A	N/A
H	3.076	2.949	2.873
J (REF.)	0.073	0.062	N/A
	WEIGHT:3232 gms	DENSITY:94.73%	DENSITY:99.60%

PREFORM (B) DIMENSIONS	PRESSED	SINTERED	HIPED
A DIA.	4.446	4.196	4.211
B DIA.	4.843	4.609	4.553
C1 DIA.	6.382	6.014	N/A
C2 DIA.	6.205	5.936--5.969	5.872
C3 DIA.	6.868	N/A	N/A
D DIA.	7.488	7.021	6.665--6.990
E	3.168	3.033	2.959--2.980
F	1.601	1.531	1.490
G	0.662	N/A	N/A
H	3.076	2.950	2.940
J (REF.)	0.092	0.082	N/A
	WEIGHT:3258 gms	DENSITY:94.95%	DENSITY:99.72%

PREFORM (D) DIMENSIONS	PRESSED	SINTERED	HIPED
A DIA.	4.451	4.259	4.211
B DIA.	4.845	4.624	4.553
C1 DIA.	6.599	6.028	N/A
C2 DIA.	6.200	5.951	5.850
C3 DIA.	6.931	N/A	N/A
D DIA.	7.519	7.059	7.000--7.010
E	3.157	3.040	2.936--3.013
F	1.601	1.531	1.480--1.498
G	0.673	N/A	N/A
H	3.076	2.966	2.849
J (REF.)	0.082	0.074	N/A
	WEIGHT:3288 gms	DENSITY:94.57%	DENSITY:99.60%

Figure 13. FINAL TASK II BEARING HOUSING PREFORM DESIGN WITH WEIGHT, DENSITY AND DIMENSIONS OF FOUR PREFORMS AFTER CIP, SINTER AND HIP.

Tensile test results of witness bars manufactured from the same alloy blend as the preforms (designation B-2151) and processed with the four preforms are shown in Table II. The tensile properties met Dynamet's typical properties for CHIP processed Ti-6Al-4V StCl alloy.

TABLE II
TENSILE PROPERTIES OF Ti-6Al-4V WITNESS BARS

Specimen No.	Ultimate Tensile Strength (psi)	Yield Strength (psi)	Percent Elongation	Percent Reduction in area
1	123,100	107,700	8.9	15.9
2	122,800	110,000	6.8	18.7
ASTM B-817 (typical properties)	123,000	108,000	8	14

The second pressing approach described earlier (Figure 6), based on the idea of applying pressure from inside the elastomeric mold, was also evaluated. The major problem encountered in the experimental pressings was the development of a concave or barrel shape on the inside surface. Tooling variations were tried in the effort to minimize the distortion. It was concluded that a tooling design using a rigid inner tube with a perforated wall to allow pressure transmission to an inside elastomeric liner (rather than a completely elastomeric inner tube) was more effective in controlling the barreling.

Based on the preliminary developmental work with small shapes, tooling was designed and built for pressing two simple, thin-walled geometric shapes: a flanged cup with end closure as shown in Figure 14 and a flanged tubular shape as shown in Figure 15. A single preform of each shape was CIPed, sintered and HIPed

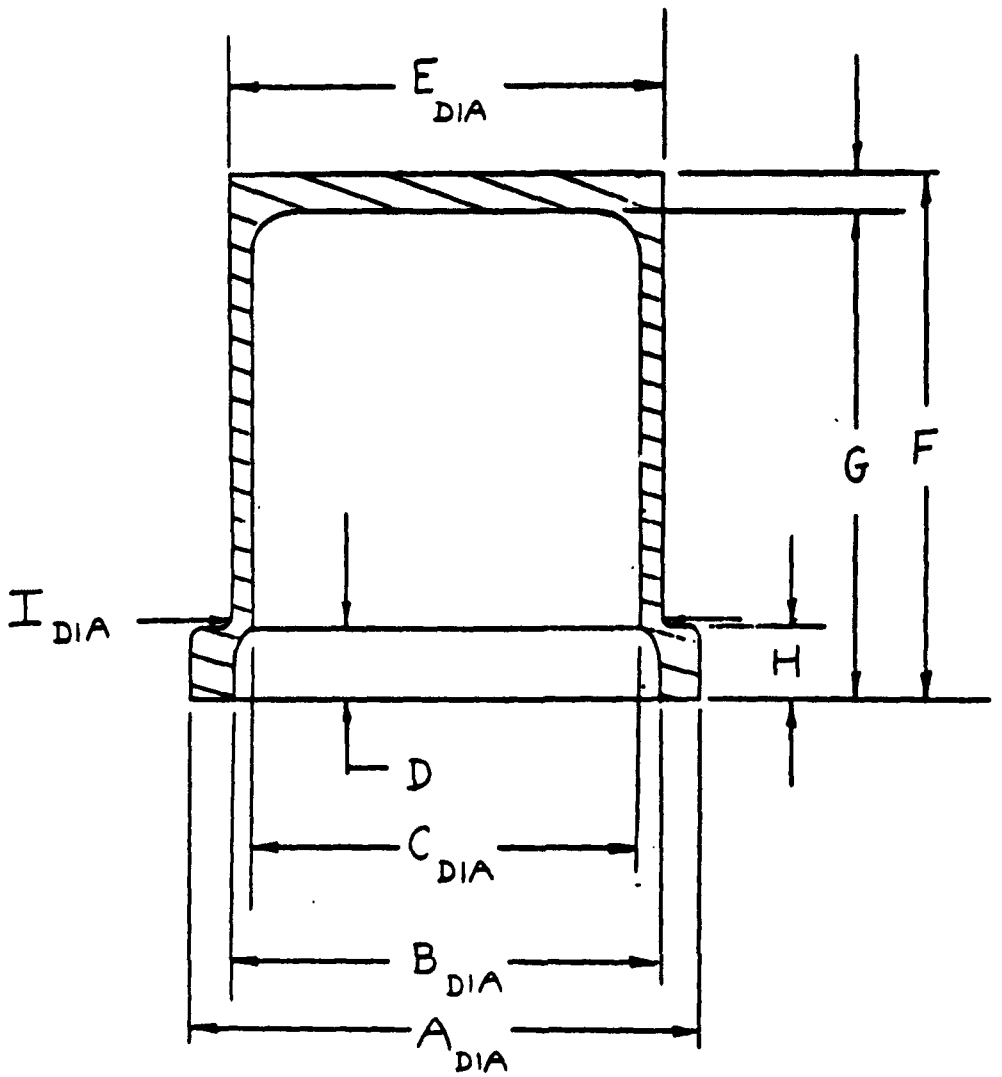

PREFORM (B) DIMENSIONS	PRESSED	SINTERED	HIPED
A DIA.	2.561	2.472--2.485	2.438--2.457
B DIA.	2.332	2.233--2.245	2.202--2.224
C DIA.	2.220	2.148--2.157	2.146
D	0.63	0.604	0.604
E DIA.	2.380	2.286--2.290	2.255
F	2.510	2.420	2.387
G	2.345	2.252	2.180
H	0.580	0.562	0.550
I DIA.	2.405	2.320--2.326	2.283--2.293
	WEIGHT: 136 gms	DENSITY:96.15%	DENSITY:99.87%

Figure 14. CONFIGURATION, WEIGHT, DENSITY AND DIMENSIONS OF AN EXPERIMENTAL CLOSED-END CUP PRESSED USING PRESSURE APPLIED FROM INSIDE THE MOLD.

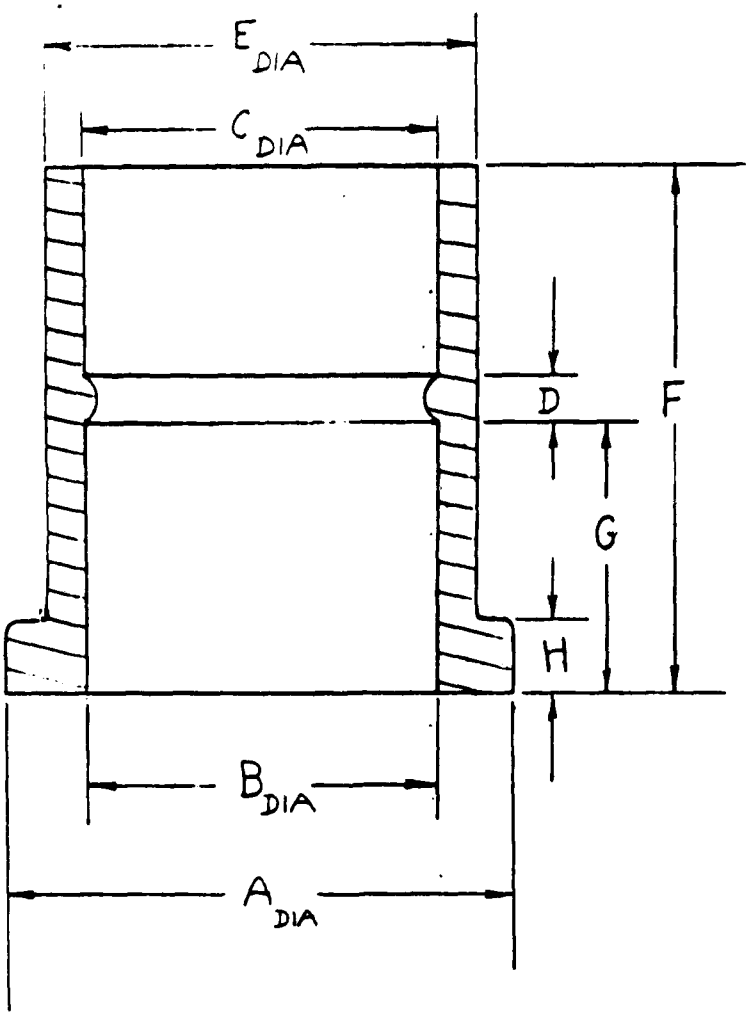

PREFORM (A) DIMENSIONS	PRESSED	SINTERED	HIPED
A DIA.	2.556	2.432--2.450	2.402--2.415
B DIA.	2.195	2.092--2.112	2.062--2.082
C DIA.	2.085	1.971--1.990	1.951--1.975
D	0.23	0.195	0.145
E DIA.	2.380	2.270--2.283	2.235--2.261
F	3.011	2.874--2.876	2.837
G	1.410	1.385	1.340
H	0.583	0.552	0.543
	WEIGHT: 193 gms	DENSITY:95.96%	DENSITY:99.61%

Figure 15. CONFIGURATION, WEIGHT, DENSITY AND DIMENSIONS OF A FLANGED TUBULAR SHAPE PRESSED WITH PRESSURE APPLIED FROM INSIDE THE MOLD.

using the same standard processing described earlier. In both cases pressing was accomplished with no cracking and no apparent barreling. Sintered and HIPed dimensions were uniform diametrically and along the length of the preforms with variations in the final HIPed preforms falling within a range of less than 2%. As expected dimensional variations were slightly greater in the open ended tubular shape but the differences were well within the 2% range.

Both experimental preforms achieved full density and the effort to incorporate geometric features into the inside walls was successful. The latter achievement demonstrates that P/M isostatic pressing technology can also provide internal dimensional control of thin-walled, fully dense, distortion-free preform shapes not possible by other fabricating routes including other P/M methods, casting and forging. The inside-out pressing method has been refined as a result of this program and could be effectively used for future manufacturing of military component preforms.

OPTIMIZATION OF CHLORIDE IMPURITY LEVEL

This task, which comprises a major focus of the Phase II program, addressed the optimization of the chloride impurity level in P/M Ti-6Al-4V alloys.

In Phase I a comparison was made between titanium powder with the standard level of chloride contaminant (about 1500 ppm, designated StCl) and titanium powder with an extra low level of chloride contaminant (less than 10 ppm, designated ELCl). While proving the feasibility of the process at both levels, Phase I demonstrated that the chloride impurity level has a significant effect on mechanical properties, particularly fatigue, with improved properties resulting with reduced chloride level. The trade-off is increased cost. In order to most efficiently select the proper chloride level for specific applications, a predictive model is needed.

To develop this predictive model, Dynamet conducted a statistically designed experiment to quantify the relationship of chloride level and trace element variables with critical mechanical properties. To adequately cover the full range of chloride levels (and alloy costs) the seven (7) specific design points, shown in Table III, were tested.

TABLE III
COMPOSITIONS OF Ti-6Al-4V ALLOY BLENDS
OF THE EXPERIMENTAL DESIGN

Design Point	ELCl content	StCl content	Alloy Cl content target	Blend Designation
1	100%	0%	<10 ppm	ELCl
2	80%	20%	300	LCl-80
3	60%	40%	600	LCl-60
4	50%	50%	750	LCl-50
5	40%	60%	900	LCl-40
6	20%	80%	1200	LCl-20
7	0%	100%	1500	StCl

Processing Studies

The seven (7) alloy blends corresponding to the design point compositions of Table III were prepared. Each of the blends weighed six pounds, the amount of alloy powder needed to fabricate all of the test samples of the experimental design.

Starting materials were selected from standard powder lots from Dynamet's commercial suppliers and included powders of StCl titanium (lot designation R-1803), ELCl titanium (lot designation R-1596) and master alloy powder of nominal 60Al-40V composition (lot designation R-1871). The chemical compositions and particle size distributions of the starting powders are shown in Table IV.

TABLE IV
CHEMICAL COMPOSITION AND PARTICLE SIZE DISTRIBUTION
OF STARTING POWDER MATERIALS FOR
EXPERIMENTAL ALLOY BLENDS

Element	StCl Titanium Lot R-1803	ELCl Titanium Lot R-1596	60Al-40V Master Alloy R-187
	Chemical Composition (%)		
Oxygen	0.08	0.19	0.07
Nitrogen	0.01	0.03	0.005
Hydrogen	--	0.04	0.004
Carbon	0.01	0.01	0.04
Chloride	0.18	0.0007	--
Iron	0.01	0.14	0.20
Silicon	--	--	0.262
Aluminum	--	--	57.06
Vanadium	--	--	42.28
Molybdenum	--	--	0.028
Total Other	--	--	<0.040
	Particle Size Distribution		
Mesh Size	% Finer Than		
60	--	100	--
80	--	97	--
100	100	76.6	--
200	30	38.2	--
270	--	--	100
325	11	12.3	--

Based on Table III, chloride levels for the StCl and ELCl blends of Table IV should be 1800 ppm and 7 ppm, respectively. The lower chloride target levels of Table III reflect the expected 15-20% partial removal of chloride which occurs in the vacuum sintering step.

The ELC1 and StC1 titanium powder mixtures of Table III were blended in a V-blender for 1 hour. The blended powders were then fabricated into test bars by cold isostatic pressing (CIP) at 55,000 psi in the appropriately shaped elastomeric tooling. The CIP cycle time is several minutes and depends on the press design, but the dwell at the maximum pressure is specified at 20 seconds minimum. Two test bar shapes were made; Dynamet's standard 5/8 inch diameter by 5 inch long test bar to be used for tensile and fatigue test specimens and rectangular bars 1 inch x 1 inch x 2½ inches long for fracture toughness test samples.

The CIPed test bars were vacuum sintered (10^{-5} Torr vacuum pressure). Sintering was for 2½ hours at 2250°F followed by furnace cooling in vacuum. Density measurements were made on all sintered test bars with the results shown in appended Table B-1.

The sintered densities exceed 97% of theoretical in the blends with high chloride content and decrease to about 96% of theoretical density in the ELC1 blend. This difference in densification is attributed principally to the differences in particle size distribution between the StC1 and ELC1 powder (see Table IV) and perhaps also due to chemical differences. The greater specific surface area of the finer StC1 powders provides the increased thermodynamic driving force for densification. It is also postulated that the chloride in StC1 powder promotes diffusion (and densification) by removing inhibiting surface films, while the extra oxygen of ELC1 powder may have the opposite effect by reducing diffusion rates.

The next processing step was to HIP the test bars to full (100% of theoretical) density. There are two commercial HIP cycles used for titanium alloys, and it was a goal of this program to determine which of the two provides the better performance. The alternative commercial HIP cycles are as follows:

1. 1650°F for 2 hours in argon at 15,000 psi
2. 2165°F for 4 hours in argon at 25,000 psi

Both cycles are followed by (slow) furnace cooling to produce fully annealed microstructures.

Clearly, the first cycle is preferred based on economic considerations providing that there is no substantial performance advantage to the higher temperature, longer time second cycle.

In order to choose between the alternative cycles, two sets of test bars from each of the seven blends were HIPed, one set processed through each of the two cycles. These test bars were evaluated by density measurements and tensile testing with the results comparing the two HIP cycles plotted in Figures 16, 17 and 18 (the data are tabulated in Appendix B). In addition, a sample of each alloy was taken from a HIPed test bar for chemical analysis. The results are shown in Table V and the chloride and oxygen levels plotted against the % ELC1 titanium in the initial alloy powder blend shown in Figure 19.

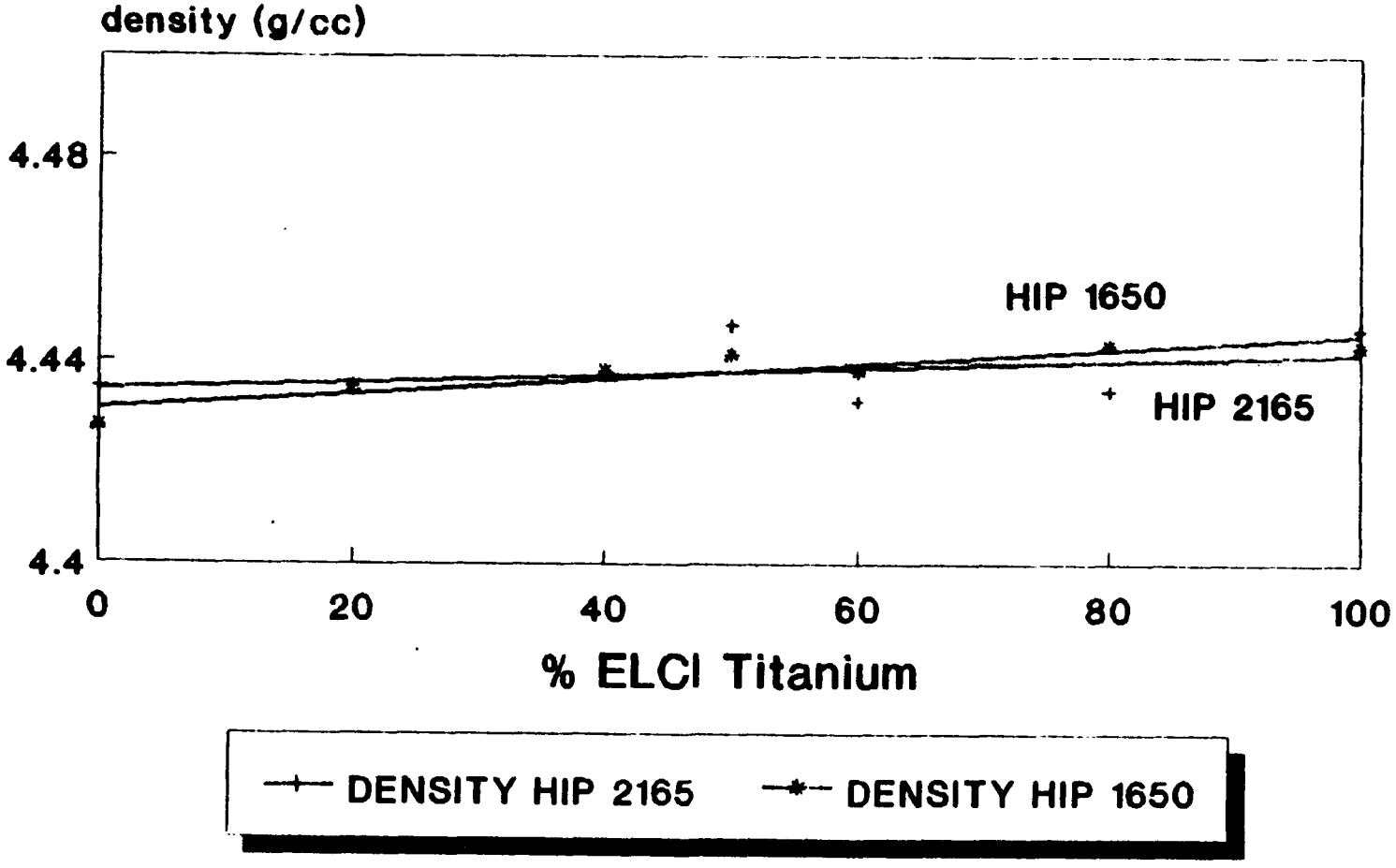

Figure 16. DENSITY VS. CHLORIDE, HIP CYCLE COMPARISON.

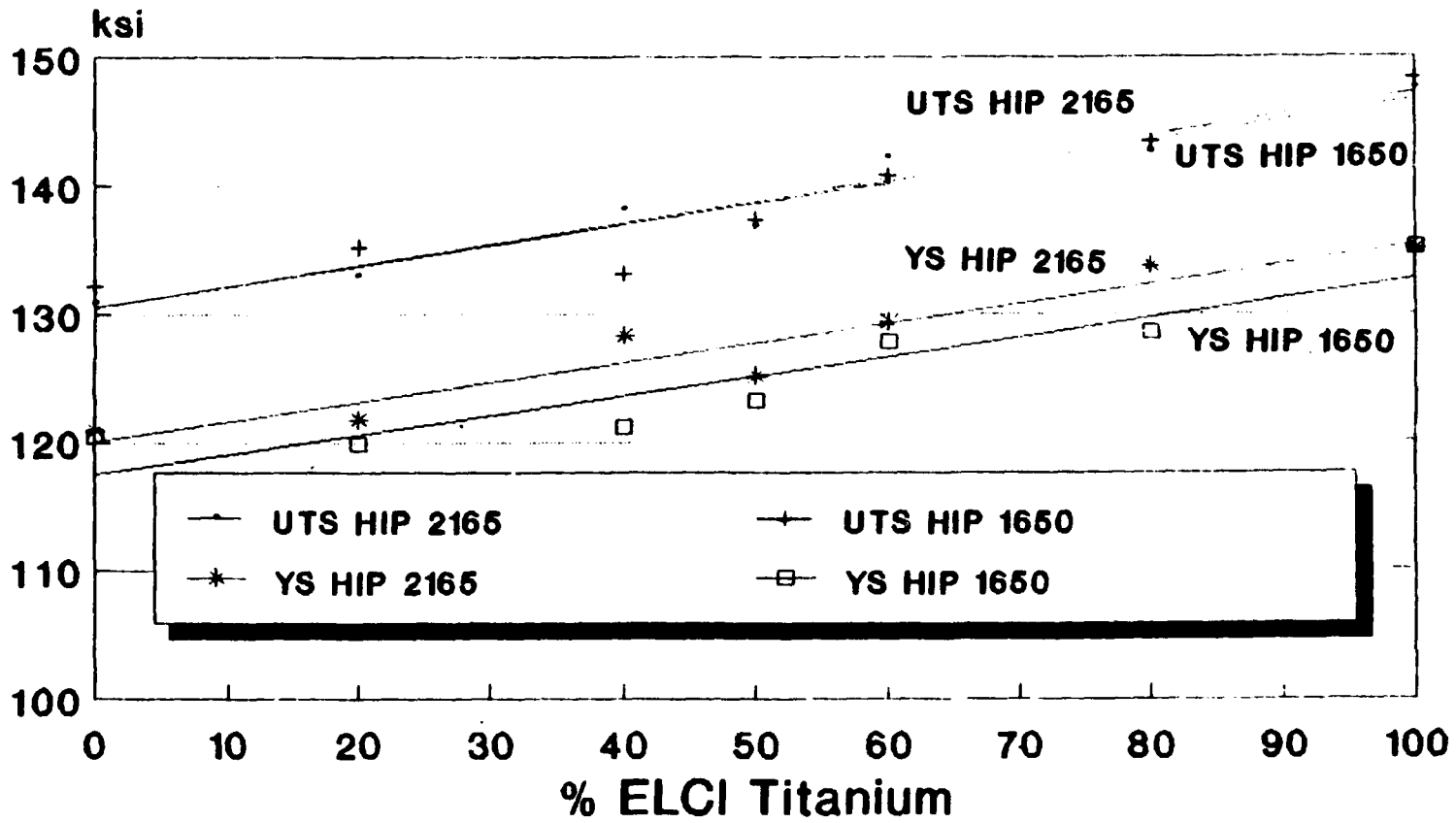

Figure 17. HIP CYCLE COMPARISON, ULTIMATE TENSILE AND YIELD STRENGTH AT ALL CHLORIDE LEVELS.

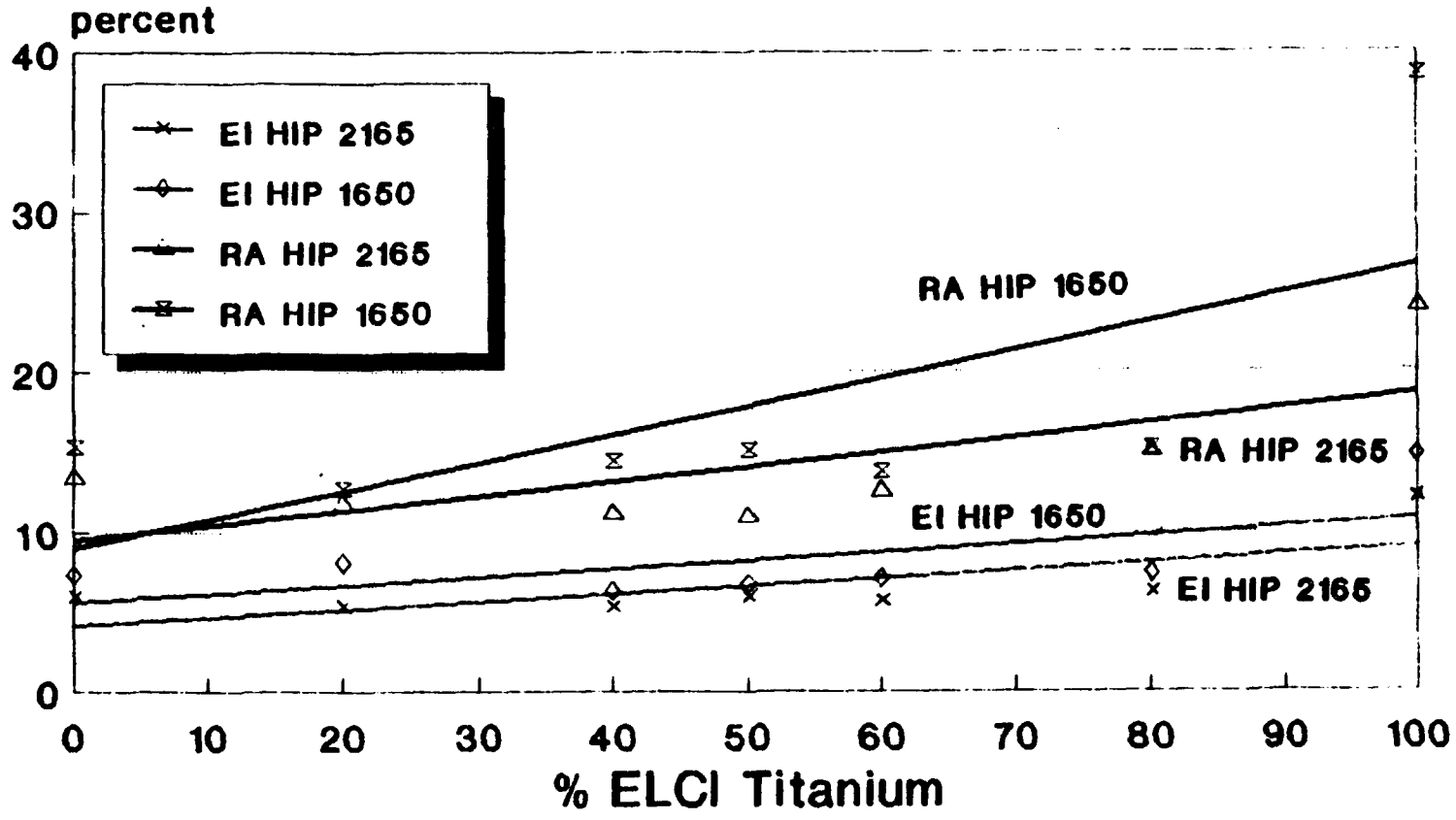

Figure 18. HIP CYCLE COMPARISON, ELONGATION AND REDUCTION OF AREA AT ALL CHLORIDE LEVELS.

TABLE V

COMPOSITION OF HIPed TEST BARS

Blend	Blend #	Al	V	Fe	Si	C	H	N	O	Na	Cl
StCl	1994	6.07	4.13	0.23	0.02	0.01	0.0138	0.0145	0.1560	.07	0.1000
LCl-20	2000	6.06	4.14	0.25	0.01	0.02	0.0119	0.0123	0.1847	.06	0.0840
LCl-40	1999	5.91	4.16	0.28	0.03	0.02	0.0115	0.0135	0.2051	.05	0.0540
LCl-50	1998	5.93	4.04	0.26	0.03	0.02	0.0105	0.0133	0.2216	.04	0.0390
LCl-60	1997	5.71	3.98	0.27	<.01	0.02	0.0154	0.0181	0.2344	.03	0.0310
LCl-80	1996	5.89	3.99	0.28	0.01	0.02	0.0089	0.0155	0.2498	.02	0.0200
ELCl	1995	5.89	4.10	0.31	0.02	0.02	0.0119	0.0200	0.2492	<.01	<.0050

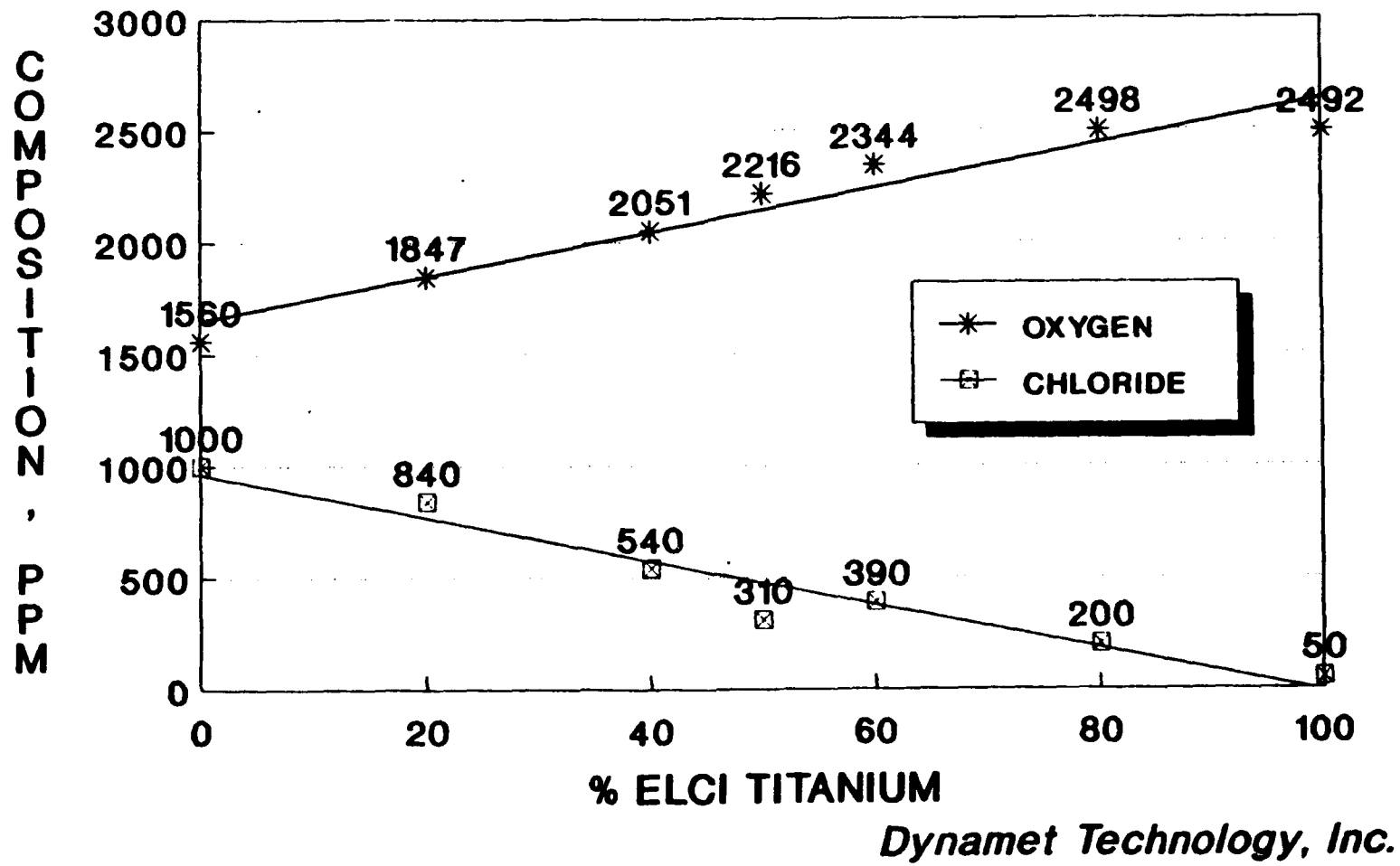

Figure 19. CHLORIDE & OXYGEN LEVELS OF EXPERIMENTAL BLENDS.

In Figure 16 the densities for the two HIP cycles, reported as percent theoretical density, are compared. As expected the density increases with the %ELCl titanium in the alloy blend, primarily as a result of a reduction in chloride content (Figure 19) and the reduction in the concentration of lower density chloride inclusions (the densities of the sodium and titanium chloride compounds most likely to be present have densities below 3g/cc compared to 4.43g/cc for the Ti-6Al-4V alloy). Most importantly, both HIP cycles result in virtual full density with no apparent difference due to the differences in the HIP temperature, pressure and time.

The comparisons of tensile properties in Figures 17 and 18 also indicate an improvement in both strength and ductility with the increase in the %ELCl titanium in the blend. This is consistent with the increase in density (and reduction in chloride inclusions) with % ELCl titanium described earlier (Figure 16). However, the increase in strength properties is more strongly related to the increase in oxygen content associated with the higher %ELCl titanium in the blend (Figure 19). Oxygen is a very effective interstitial strengthener of titanium while it tends to lower ductility. The fact that the ductility seems to be relatively insensitive to the increases in %ELCl titanium until the blend contains nearly 100% ELCl titanium could be a result of the opposing effects of increased oxygen and reduced chloride (Figure 19) canceling each other out until the ductility limiting chloride inclusions have been virtually eliminated.

Metallographic samples were prepared from the HIPed test bars. Selected as-HIPed microstructures for the 1650°F and 2165°F cycles are shown in the sets of photomicrographs of Figures 20 and 21. Both HIP cycles resulted in the expected phase distribution of acicular alpha with intergranular beta. For each HIP cycle the average grain size increased with increasing %ELCl. This is attributed to the reduction in the number of chloride inclusions (dark particles in the microstructures), which form barriers to grain growth. The other significant chemical difference, the increase in oxygen content with increasing %ELCl is not expected to have a comparable effect on grain growth, since the oxygen is in solid solution. The increase in grain size with increasing %ELCl also may be related, in part, to the larger starting particle size of ELCl powder (see Table IV). At fixed %ELCl the grain size was always larger when HIPing was done with the 2165°F cycle, consistent with the effect of higher temperature (and longer time at temperature) on grain size.

The comparison of the alternative HIP cycles in Figures 16, 17 and 18 indicates no clear advantage related to the HIP processing conditions. The yield and ultimate strengths are virtually identical with the higher temperature HIP cycle showing a slight advantage on average of about 2000 psi in the yield strength (Figure 17). On the other hand, the tensile ductility

is slightly but consistently higher when HIPing was done by the 1650°F cycle. This is consistent with the smaller grain size of material HIPed at the lower temperature and below the alpha beta transformation temperature. With all other factors (density, chemical composition and microstructure) the same, finer grained material should have higher ductility.

Based on the test results, there is no clear advantage in using one HIP cycle rather than the other. However, based on the slight improvement in ductility, the similarity of the density and strength properties and lower cost, the 1650°F HIP cycle was selected for manufacturing of test bars for mechanical testing and statistical analysis.

All remaining test bars were HIPed using the 1650°F, 2 hrs., 15 ksi cycle. Measurements of density were made and are shown in appended Table B-1, while mean sintered density values and corresponding standard deviations for each blend and sample geometry are listed in Table VI. The HIPed densities increase with increasing %ELCl in the same way as the samples of the experimental HIP comparisons (see Figure 16). As discussed earlier, this dependence of density on chloride content is related to the lower concentration of low density chloride inclusions with increased %ELCl.

All of the HIPed cylindrical and rectangular test bars from each blend were given a strengthening heat treatment. The heat treatment consisted of solution annealing at 1750°F for one hour, followed by water quenching and ageing at 1050°F for four hours. Metallographic samples were also prepared from selected heat treated test bars.

Photomicrographs of the heat treated samples, which are shown in Figure 22, displayed the same dependence of grain size on %ELCl with a grain size at each %ELCl intermediate between the two corresponding as-HIPed microstructures and consistent with the intermediate 1750°F heat treating (solution annealing) temperature. However, the phase composition of the heat treated microstructures consisted of a matrix of acicular alpha and transformed beta with fine alpha needles precipitated from the beta during ageing. These microstructural features are typical of Ti-6Al-4V in the solution annealed, water quenched and aged condition. The fine scale distribution of precipitates is responsible for the higher strength to the alloy relative to the strength of the material as-CHIP'd.

The heat treated test bars were low stress machined into test specimens for tensile, fatigue and fracture toughness testing. The specimen for the tensile and fatigue tests, which is shown in Figure 23, consisted of a 0.750 inch gage length of 0.200 inch diameter with threaded shoulders for gripping. For fracture toughness testing a sub-size Charpy impact specimen was used with a 60° notch of 1-mm depth, as shown in Figure 24. This specimen was tested in 4-point bending in the configuration shown in Figure 25.

TABLE VI

MEAN DENSITY VALUES AND STANDARD DEVIATIONS
OF SINTERED TEST BARS OF SEVEN ALLOY BLENDS

Blend	ELC1 Titanium Powder Content	CYLINDRICAL TEST BARS Density (% Theo)	Standard Deviation	RECTANGULAR TEST BARS Density (% Theo)	Standard Deviation
StC1	0 %	97.4	0.115	97.3	0.085
LC1-20	20 %	97.3	0.097	97.4	0.0129
LC1-40	40 %	97.3	0.078	97.4	0.075
LC1-50	50 %	97.2	0.251	97.1	0.067
LC1-60	60 %	96.7	0.138	97.0	0.046
LC1-80	80 %	96.4	0.176	96.5	0.131
ELC1	100 %	96.2	0.299	96.0	0.115

(a) StCl

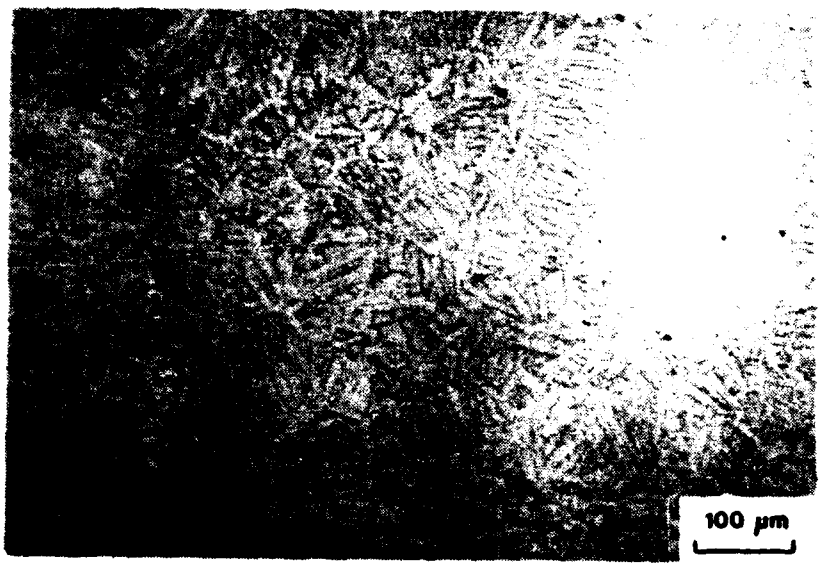

(b) LCl-50

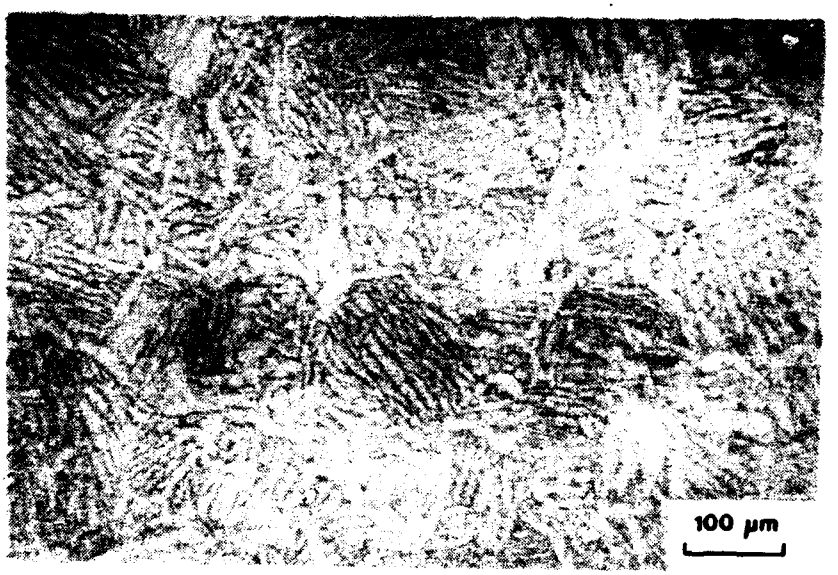

(c) ELCl Material

Figure 20. MICROSTRUCTURES OF AS HIPed SAMPLES FROM 1650°F/2 HOUR/15,000 PSI CYCLE. SAMPLES INCLUDE (a) StCl, (b) LCl-50 AND (c) ELCl MATERIAL.

(a) StCI

(b) LCI-50

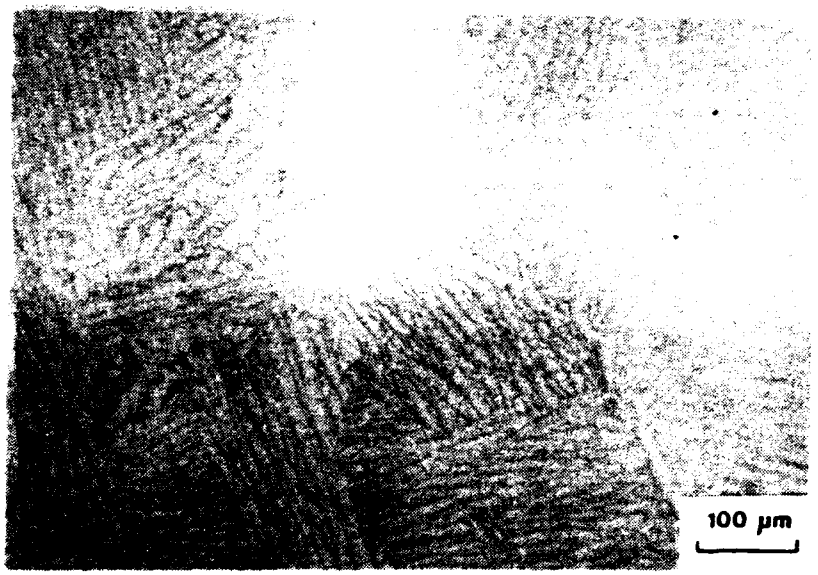

(c) ELCI Material

Figure 21. MICROSTRUCTURES OF AS HIPed SAMPLES FROM 2165°F/4 HOUR/25,000 PSI HIP CYCLE. SAMPLES INCLUDE (a) StCI, (b) LCI-50 AND (c) ELCI MATERIAL.

(a) StCI

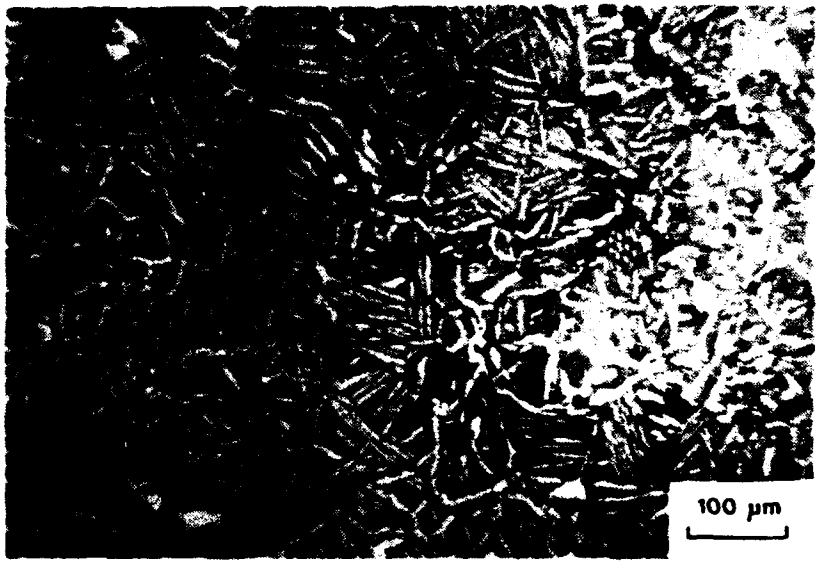

(b) LCI-50

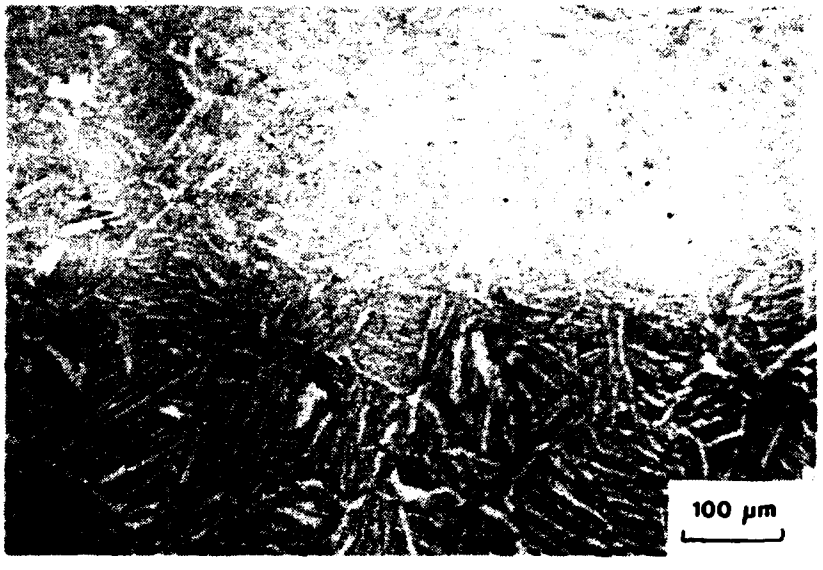

(c) ELCI Material

Figure 22. MICROSTRUCTURES OF HEAT TREATED SAMPLES (HIPed WITH 1650°F/2 HOUR/15,000 PSI CYCLE). SAMPLES INCLUDE (a) StCI, (b) LCI-50 AND (c) ELCI MATERIAL.

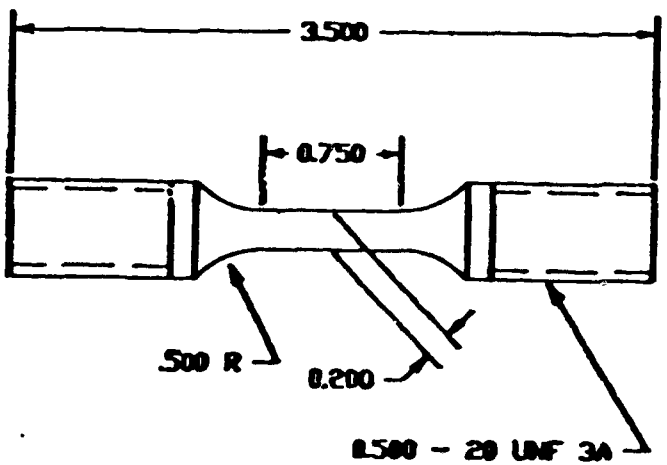

Figure 23. GEOMETRY OF TEST SPECIMEN FOR TENSILE AND FATIGUE TESTING.

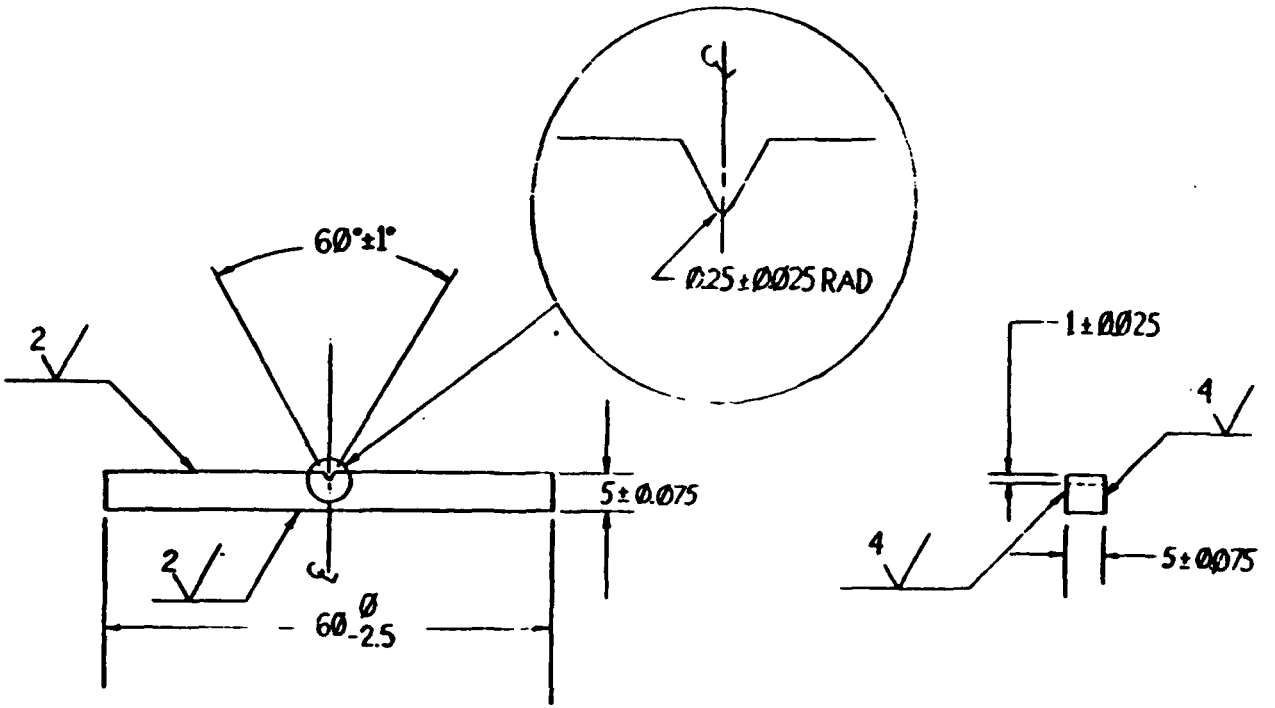

NOTE: ALL DIMENSIONS IN MILLIMETERS UNLESS OTHERWISE NOTED.
SURFACE TEXTURE DIMENSIONS IN MICROMETERS

Figure 24. NOTCHED TEST SPECIMEN FOR FRACTURE TOUGHNESS TESTING.

mat'l:		Dynamet TECHNOLOGY
tolerances: xx ± .01 .xxx ± .005 fractions ± angles ±		
SCALE: NTS	APPROVED BY	DRAWN BY
DATE:		sheet __ of __
	FOUR POINT BEND TEST SPECIMEN	
proj. no.		DRAWING NUMBER
job no.		

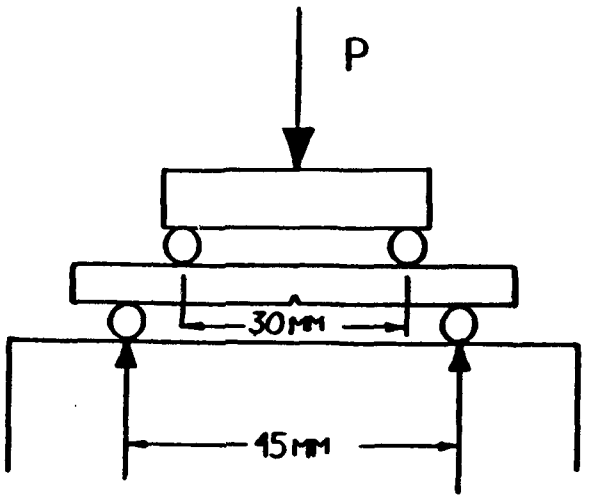

Figure 25. FOUR-POINT BEND TEST CONFIGURATION FOR FRACTURE TOUGHNESS TESTING OF SPECIMEN OF FIGURE 24.

Testing, Modeling and Statistical Analysis

Testing consisted of measurements of density (Table B-1), Rockwell C hardness (Table B-2), tensile properties (B-3), fracture toughness (Table B-4) and fatigue properties (Table B-5).

These data were analyzed with respect to their dependence on the measured chloride and oxygen content[2] of the fully processed alloys (Table V and Figure 19). The density, hardness and tensile data were also analyzed with respect to processing conditions comparing results after the low temperature HIP cycle, the high temperature HIP cycle and, excluding the density data, after heat treatment of samples HIPed by the lower temperature cycle. Fracture toughness and fatigue test data were analyzed only in the HIPed plus heat treated process condition. The analyses were mainly performed by plotting and curve fitting of the plots.

For analysis with Cl-content all 7 of the alloy blends were used, whereas with O-content 6 of the 7 alloys were used. Data for the ELCl material, the alloy with the highest expected O-content, was not used, because the measured oxygen concentration was about the same as for the LCl-80 alloy and, as a result, the plots of properties which included the value for ELCl material would have two property values corresponding to the same (approximate) level of oxygen.

Details of the various analyses are described in the following sections.

Density Measurements

The average density was investigated for samples of both cylindrical and rectangular shapes and for both sintered and HIPed[3] process conditions. Plots of average density vs. Cl-content and O-content are presented in Figures 26-29 with the corresponding fitting equations as follows:

Avg. Density Cylinders	Y = 4.26+0.0000641*X Sintered
	X = Cl ppm
	Y = 4.40-0.0000457*X
	X = O ppm
	Y = 4.45-0.0000214*X HIPed
	X = Cl ppm
	Y = 4.40+0.0000178*X
	X = O ppm

---

[2] It should be noted that the chloride and oxygen are interrelated by virtue of the fact that the starting titanium powder with the higher chloride level (StCl) has a lower oxygen content than ELCl titanium.

[3] HIPed data were for the 1650°F/2 hours/15,000 psi HIP cycle.

Avg. Density
Rectangles

Y = 4.27+0.0000591*X Sintered
X = Cl ppm
Y = 4.38-0.0000366*X
X = O ppm

Y = 4.44-0.0000184*X HIPed
X = Cl ppm
Y = 4.41+0.0000114*X
X = O ppm

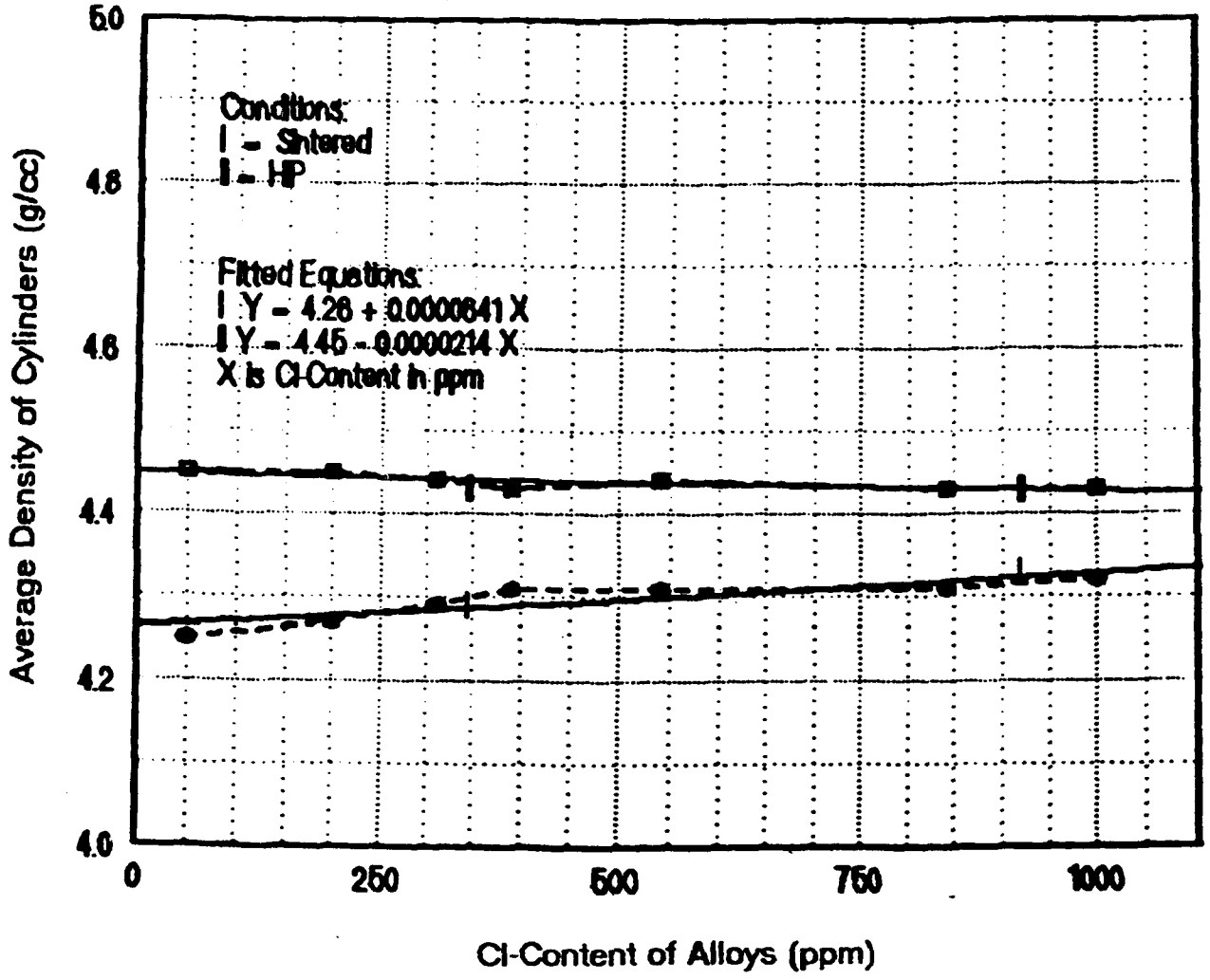

Figure 26 AVERAGE DENSITY OF CYLINDERS VS. CI-CONTENT FOR 7 ALLOYS AT 2 DIFFERENT CONDITIONS.

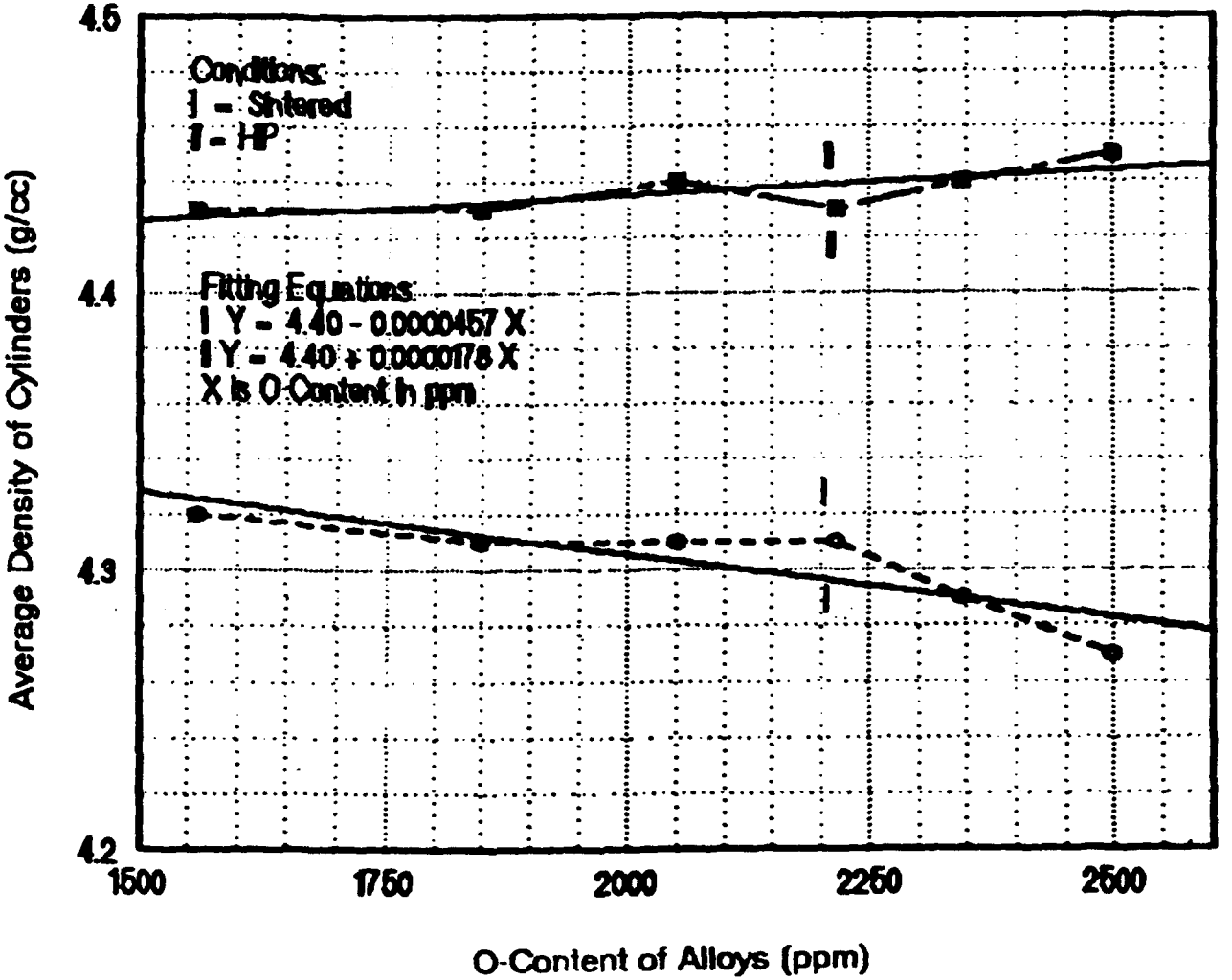

Figure 27. AVERAGE DENSITY OF CYLINDERS VS. O-CONTENT FOR 6 ALLOYS AT 2 DIFFERENT CONDITIONS.

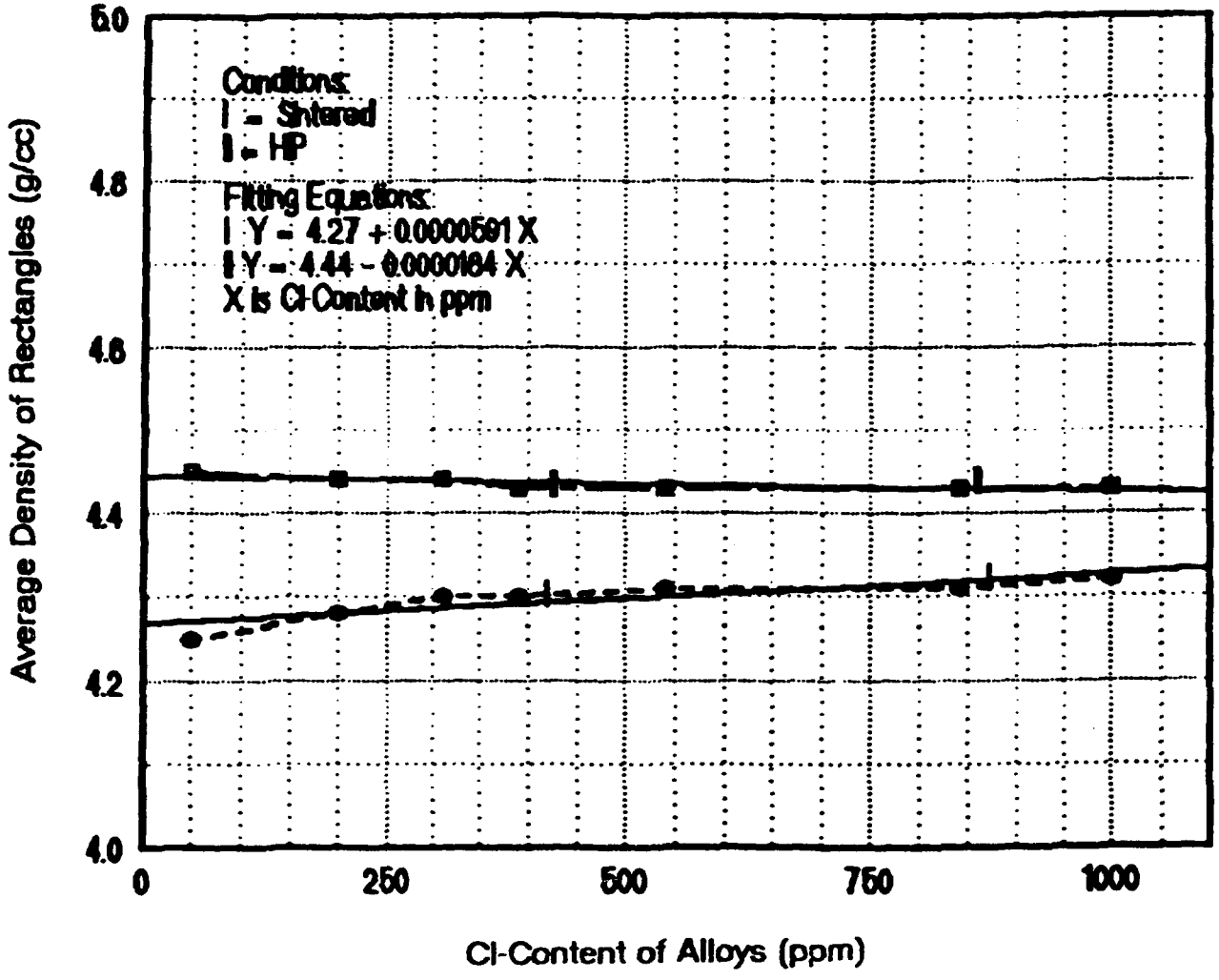

Figure 28. AVERAGE DENSITY OF RECTANGLES VS. CI-CONTENT FOR 7 ALLOYS AT 2 DIFFERENT CONDITIONS.

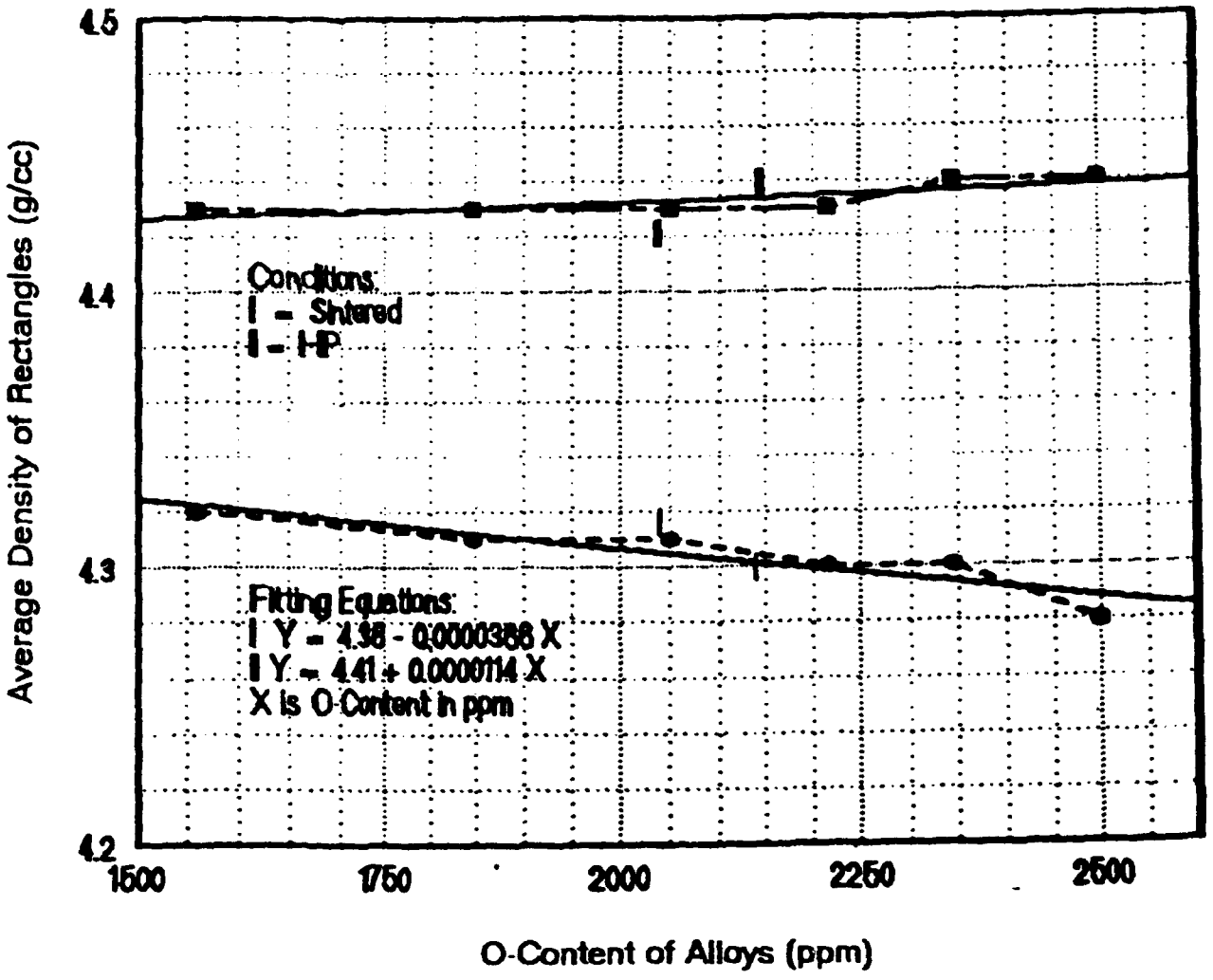

Figure 29 AVERAGE DENSITY OF RECTANGLES VS. O-CONTENT FOR 6 ALLOYS AT 2 DIFFERENT CONDITIONS.

The plots show that with increasing Cl-content average density for cylinders increases for sintered specimens and decreases for HIPed specimens (Figure 26), and with O-content these trends are reversed (Figure 27). For rectangles the same trends apply (Figures 28 and 29).

The detailed statistical difference analysis of the seven alloys offered some insight into the significance of the effect of various parameters on density. The following comparisons were made:

Cylinders, Sintered vs. HIPed
Rectangles, Sintered vs. HIPed
Cylinders vs. Rectangles, Sintered
Cylinders vs. Rectangles, HIPed
Alloys compared, Sintered (Cylinders and Rectangles)
Alloy Compared, HIPed (Cylinders and Rectangles)

These analyses confirmed the already well-documented conclusion that there is a statistically significant difference between the averages of both cylinders and rectangles in the sintered condition and those in the HIPed condition. Although geometry would not be expected to have a significant effect on density, the initial statistical analysis was not clear.

A more direct statistical approach was suggested. An experimental design with 3 independent variables was simulated using the available data. The variables were:

X1 = Process Sintered or HIPed
X2 = Geometry Cylinder or rectangle
X3 = Cl ppm 200 or 540

This experimental design is described in Table VII.

On evaluating this design, the following two regression equations were obtained.

For the Average:

$$Y=4.336+0.0735*X1+0.00648*X3-0.0127*X1*X3$$

For the Standard Deviation:

$$Y=0.00531-0.00253*X1+0.00188*X1*X2-0.00065*X1*X3 - 0.00106*X2*X3+0.000593*X1*X2*X3$$

A comparison of calculated and actual values of average density and standard deviation is shown in Table VIII.

The first equation indicates that the most important variable is the process (X1=Sintered or HIP) and that process-Cl-content interaction (X1*X3) and Cl-content (X3) are also important. To get the highest average of the average density, the process must be: HIP, and the Cl-content low.

TABLE VII

AVERAGE DENSITY
EXPERIMENTAL DESIGN

Design Used:

X1	X2	X3
-1	-1	-1
1	-1	-1
-1	1	-1
1	1	-1
-1	-1	1
1	-1	1
-1	1	1
1	1	1

Designations:

	-1	0	1
X1=Process	Sintered		HIP
X2=Geometry	Cylinder		Rectangle
X3=Cl ppm	200	370	540

Results:

X1	X2	X3	Ave.	Std. Dev.
-1	-1	-1	4.27045	0.00743
1	-1	-1	4.244827	0.00110
-1	1	-1	4.27633	0.00641
1	1	-1	4.44317	0.00523
-1	-1	1	4.31092	0.01257
1	-1	1	4.43517	0.00127
-1	1	1	4.31250	0.00495
1	1	1	4.43150	0.00354

TABLE VIII

AVERAGE DENSITY AND STANDARD DEVIATION COMPARING RESULTS FROM MEASUREMENTS TO CALCULATED VALUES BASED ON EXPERIMENTAL DESIGN

A) Averages

$$Y=4.336+0.0735*X1+0.00648*X3-0.0127*X1*X3$$

Actual	Calculated
4.27045	4.27332
4.44827	4.44572
4.27633	4.28628
4.44317	4.38740
4.31092	4.31168
4.43517	4.43328
4.43150	4.43328

B) Standard Deviations

$$Y=0.00531-0.00253*X1+0.00188*X1*X2-0.00065*X1*X3 -0.00106*X2*X3+0.000593*X1*X2*X3$$

Actual	Calculated
0.00743	0.00742
0.00110	0.00108
0.00641	0.00696
0.00523	0.00578
0.01257	0.01202
0.00127	0.00072
0.00495	0.00496
0.00354	0.00354

The second equation indicates that the standard deviation (i.e., the variability of the average density) depends mainly on the process (X1) and that all variable interactions are important. The lowest standard deviation is obtained when the process is HIP; the Geometry, Cylinder; and the Cl-content, 540.

From these equations, geometry is shown to not be a factor in the average density values and only plays a minor role in the standard deviation.

Rockwell C Hardness

The Rockwell C hardness values (Table B-2) plotted against Cl-content and O-content for the three process conditions are shown in Figures 30 and 31, respectively. In all conditions, the hardness increases with decreased Cl-content and increased O-content. Hardness is highest in the HIPed plus heat treated condition and lowest in samples as-HIPed at the lower HIPing temperature (1650°F). The fitting equations for the plots of Figures 30 and 31 are as follows:

Property	Equations	Process Condition
Rockwell C Hardness	Y = 33.0-0.00236*X X = Cl ppm Y = 26.9+0.00227*X X = O ppm	1650°F, 2 hrs, 15,000 psi
	Y = 35.2-0.00319*X X = Cl ppm Y = 30.1+0.00137*X X = O ppm	2165°F, 4 hrs, 25,000 psi
	Y = 41.8-0.00236*X X = Cl ppm Y = 29.6+0.00435*X X = O ppm	HIPed and Heat Treated

Tensile Properties

The room temperature tensile properties plotted against Cl-content and O-content for the three process conditions are shown in Figures 32 thru 39. The corresponding equations are listed below:

FITTING EQUATIONS OF TENSILE PROPERTIES

Tensile Property	Fitting Equation	Process Condition
Ultimate Tensile Strength	Y=146.0-0.153*X X=Cl ppm Y=112.0+0.121*X X=O ppm	1650°F,2hrs,15,000 psi
	Y=147.0-0.0165*X X=Cl ppm Y=111.0+0.0128*X X=O ppm	2165°F,4hrs,25,000 psi
	Y=171.0-0.0306*X X=Cl ppm Y=112.0+0.0127*X X=O ppm	HIPed and Heat Treated

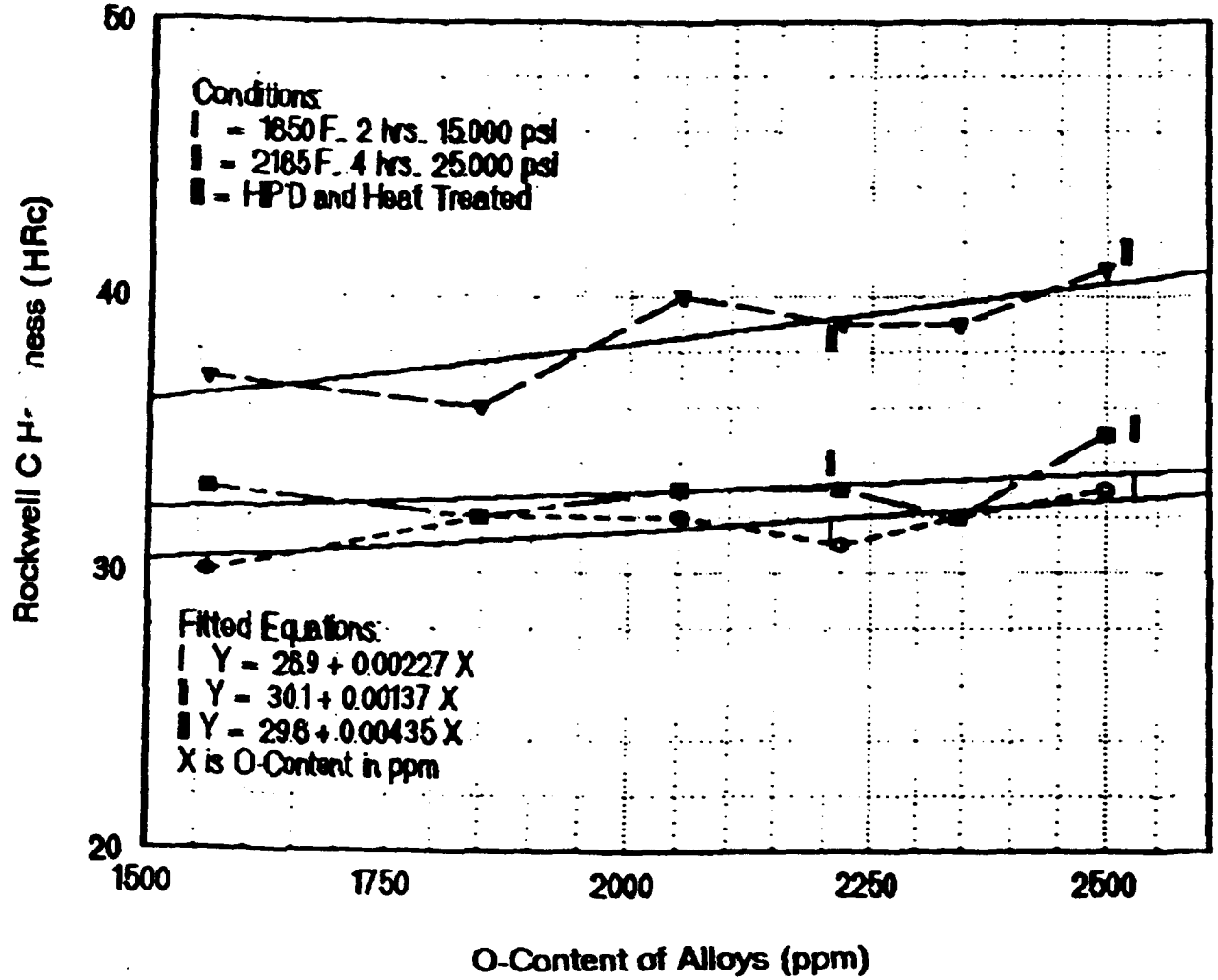

Figure 30. ROCKWELL C HARDNESS VS. CI-CONTENT FOR 7 ALLOYS AT 3 DIFFERENT CONDITIONS.

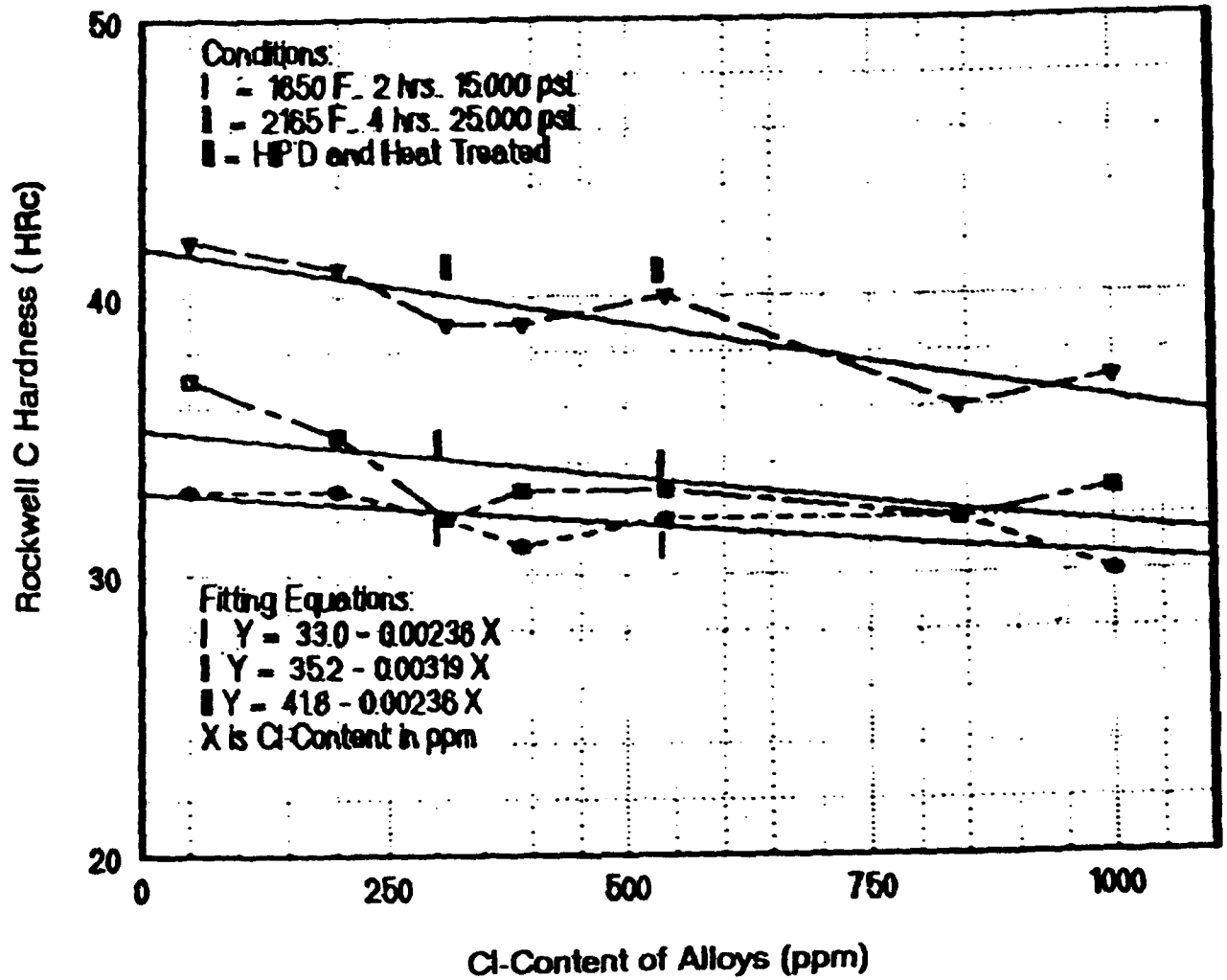

Figure 31. ROCKWELL C HARDNESS VS. O-CONTENT FOR 6 ALLOYS AT 3 DIFFERENT CONDITIONS.

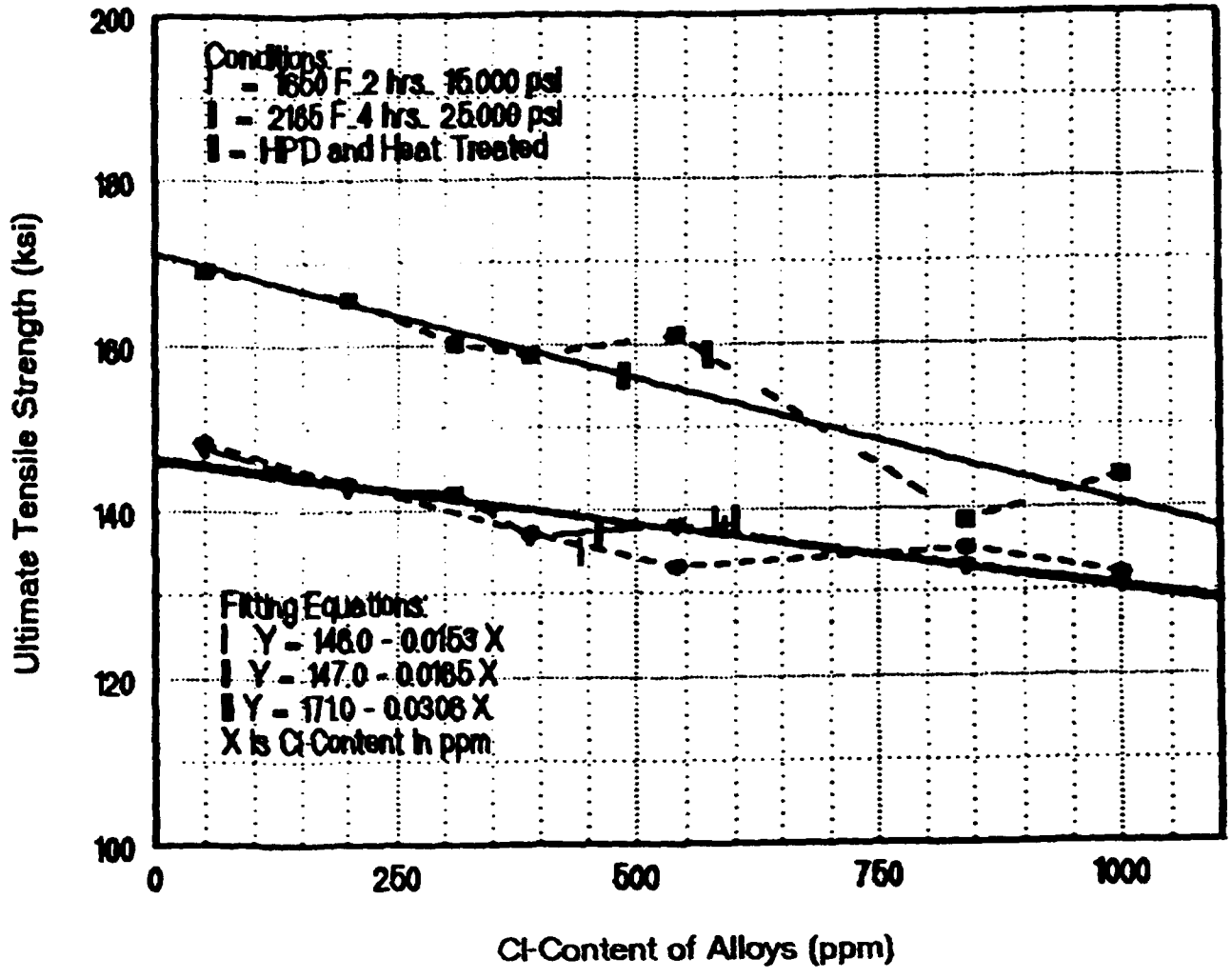

Figure 32. ULTIMATE TENSILE STRENGTH VS. CI-CONTENT FOR 7 ALLOYS AT 3 DIFFERENT CONDITIONS.

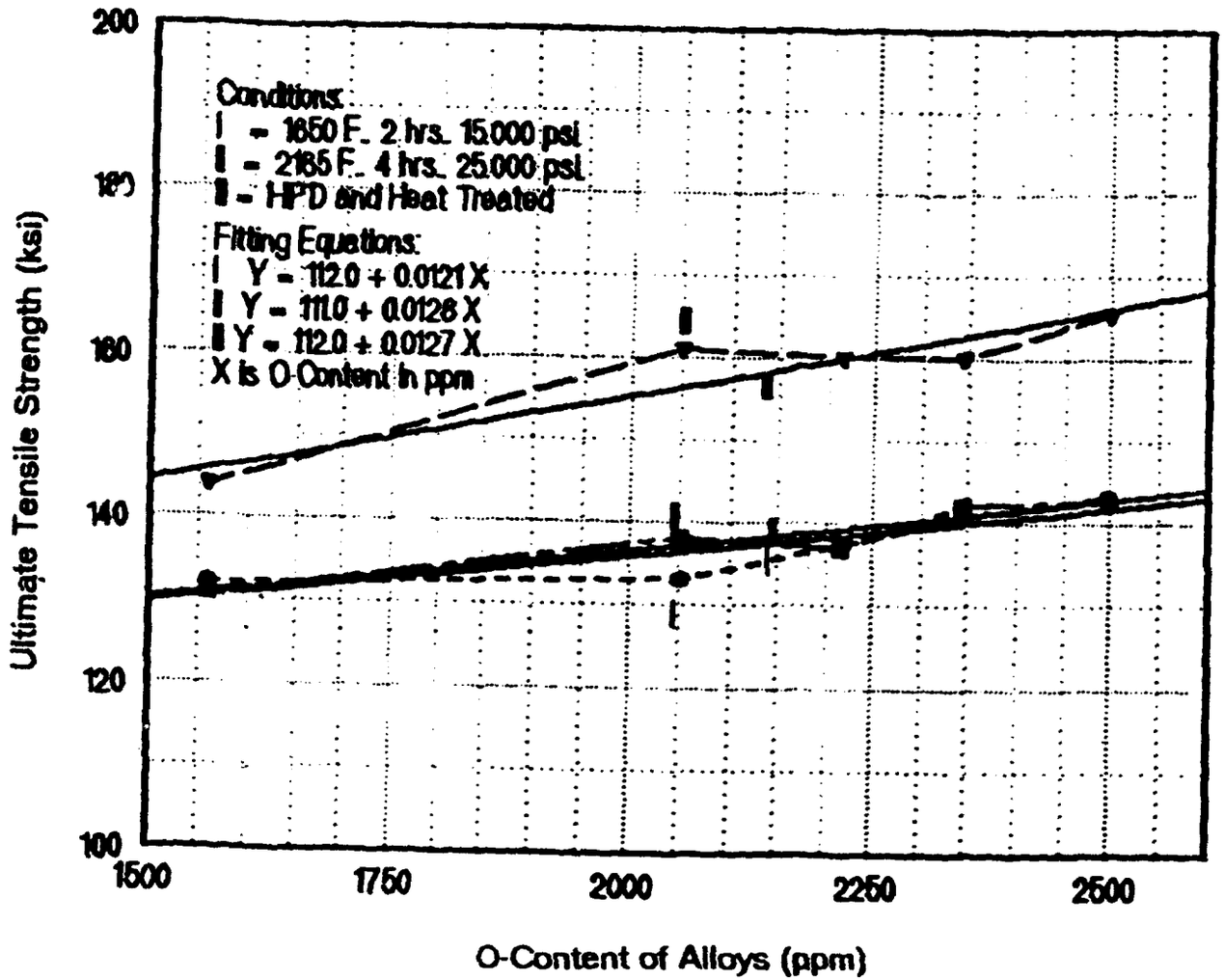

Figure 33. ULTIMATE TENSILE STRENGTH VS. O-CONTENT FOR 6 ALLOYS AT 3 DIFFERENT CONDITIONS.

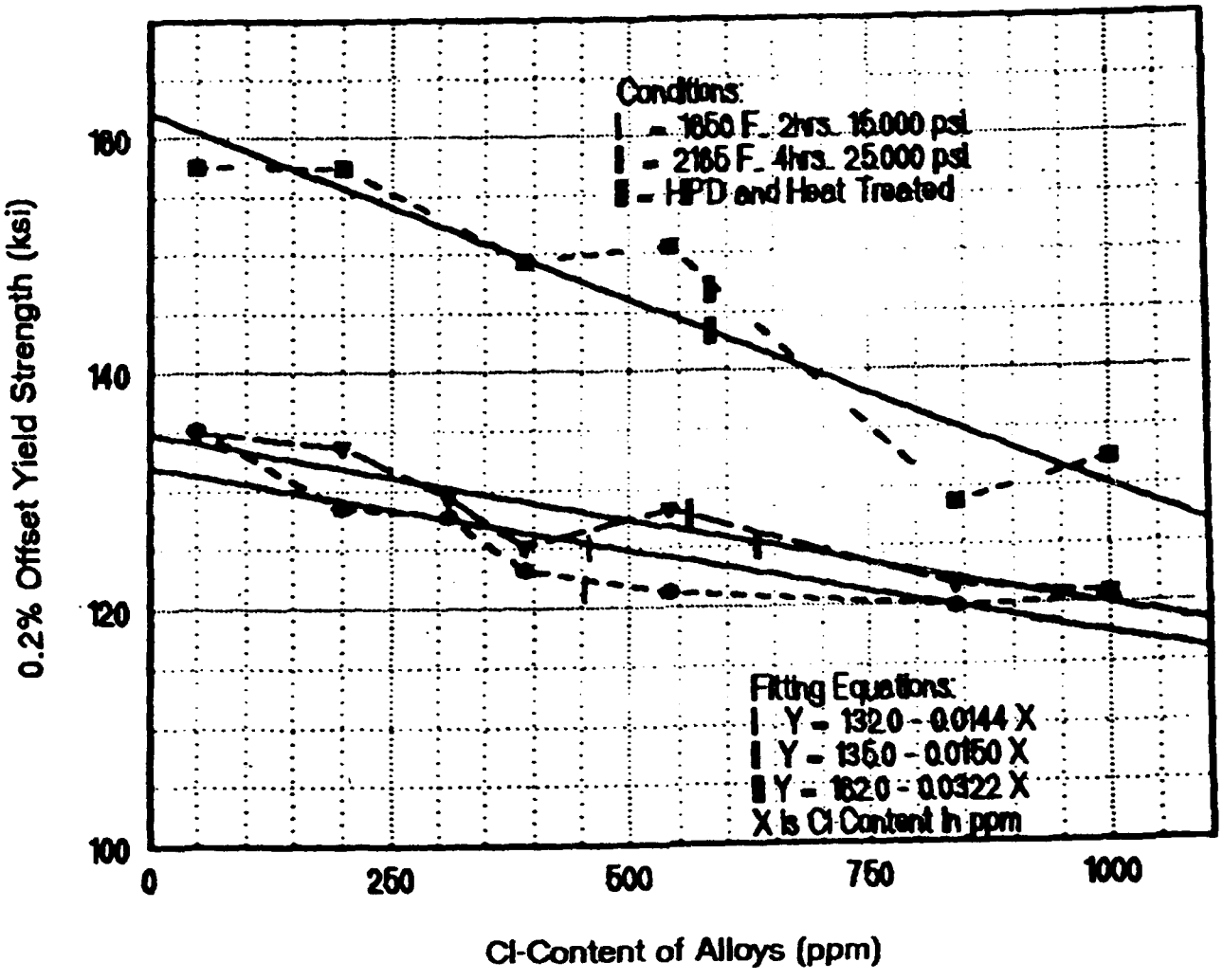

Figure 34. 0.2% OFFSET YIELD STRENGTH VS. CI-CONTENT FOR 7 ALLOYS AT 3 DIFFERENT CONDITIONS.

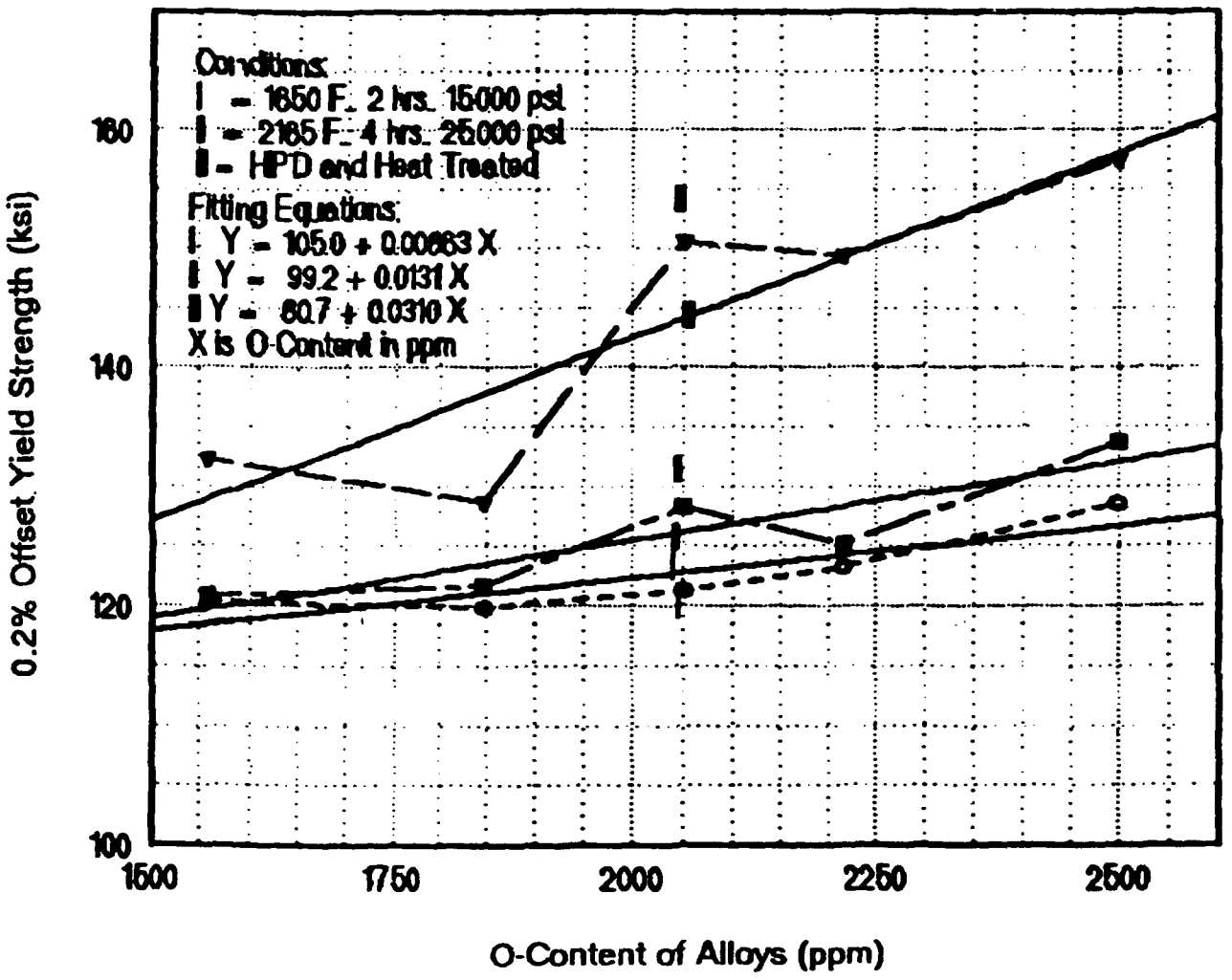

Figure 35. 0.2% OFFSET YIELD STRENGTH VS. O-CONTENT FOR 6 ALLOYS AT 3 DIFFERENT CONDITIONS.

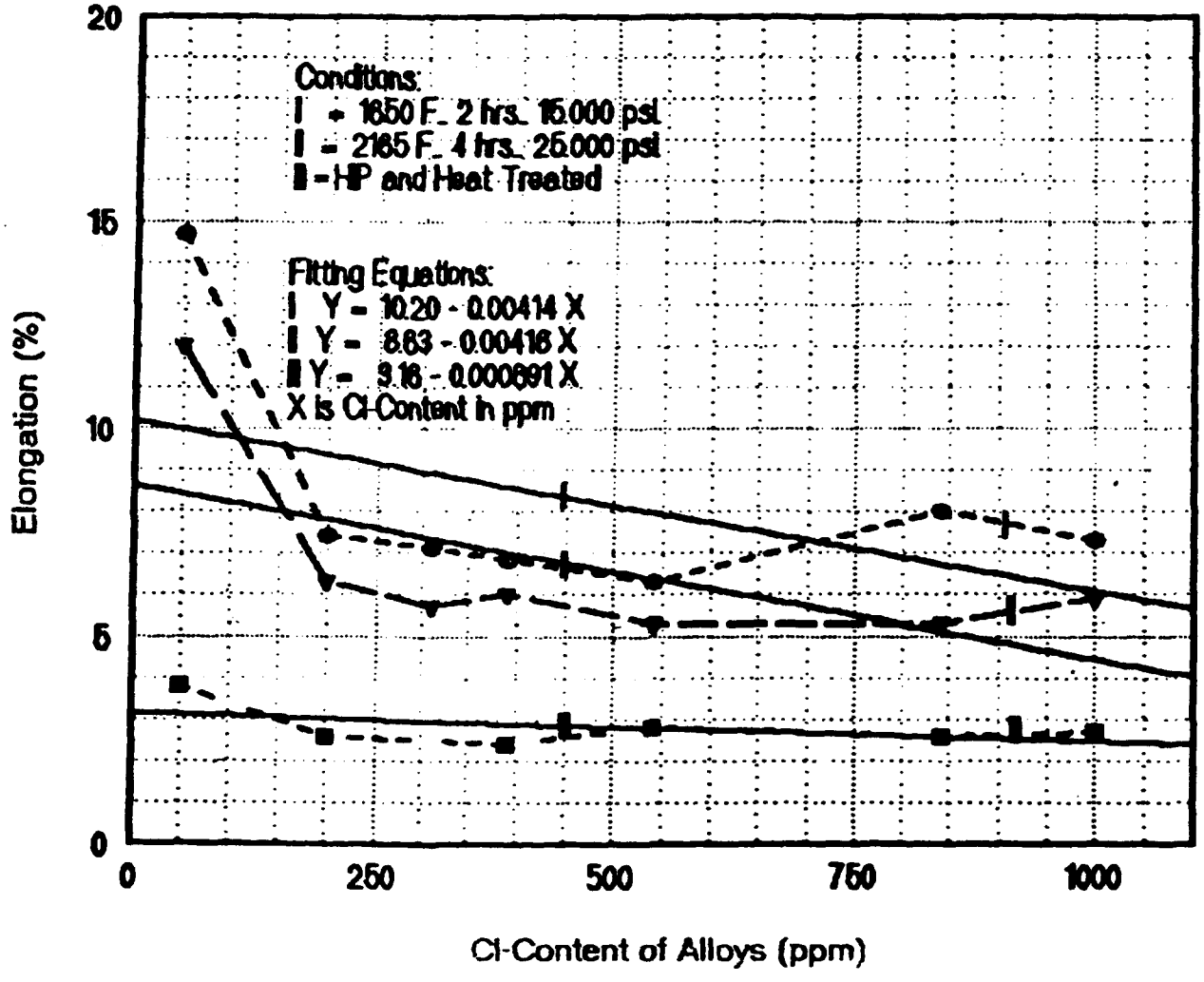

Figure 36. % ELONGATION VS. Cl-CONTENT FOR 7 ALLOYS AT 3 DIFFERENT CONDITIONS.

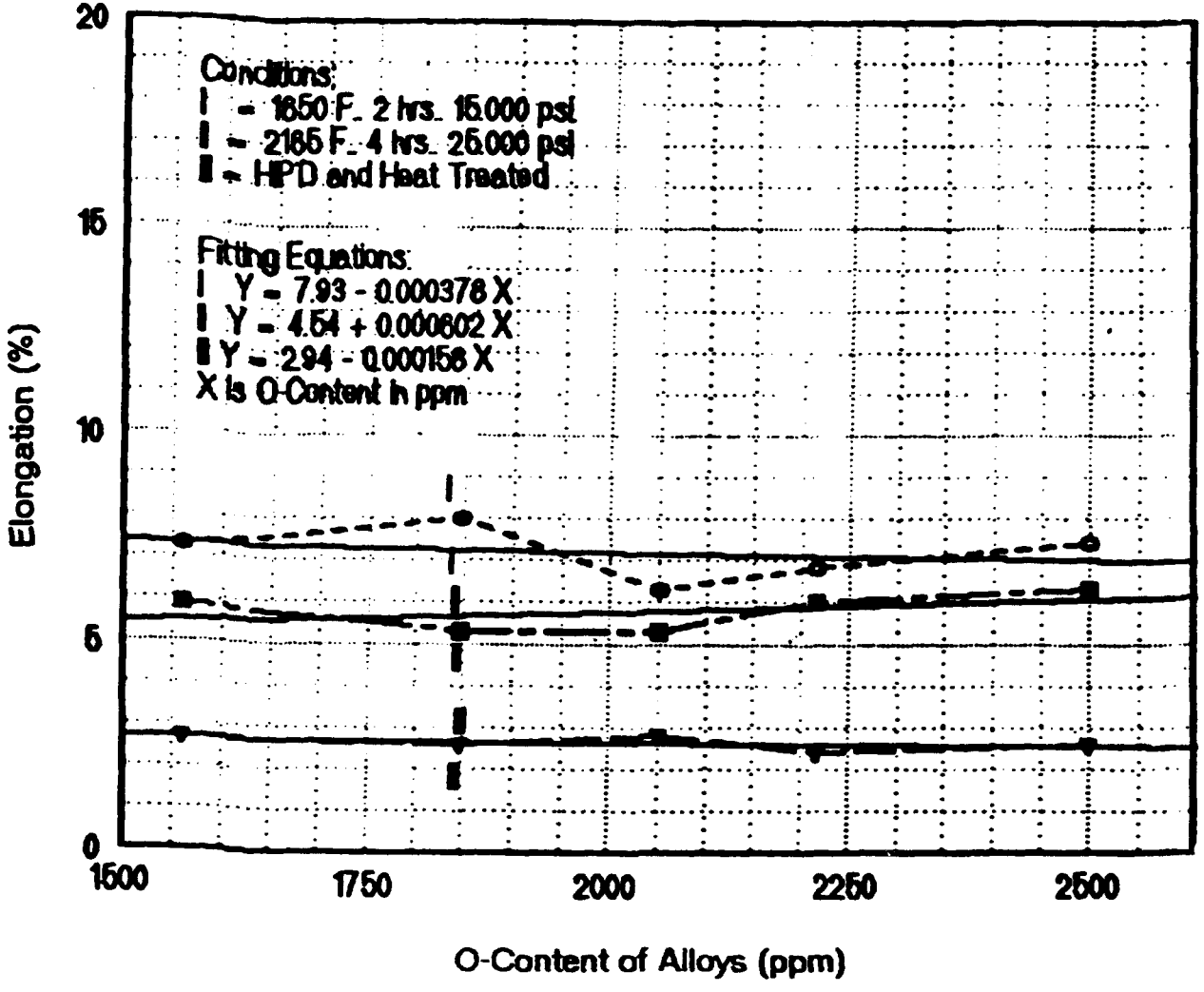

Figure 37. % ELONGATION VS. O-CONTENT FOR 6 ALLOYS AT 3 DIFFERENT CONDITIONS.

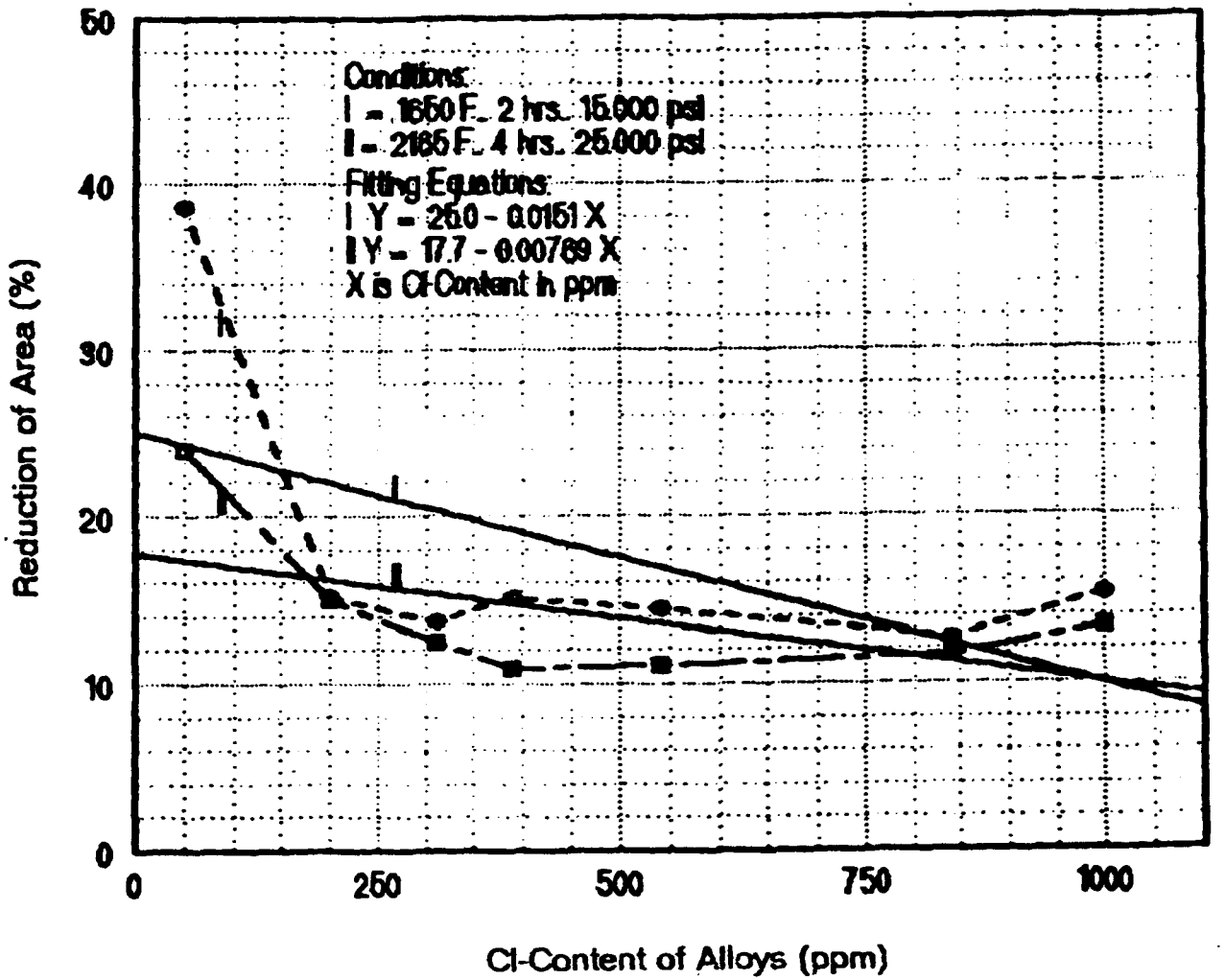

Figure 38. % REDUCTION OF AREA VS. CI-CONTENT FOR 7 ALLOYS AT 2 DIFFERENT CONDITIONS.

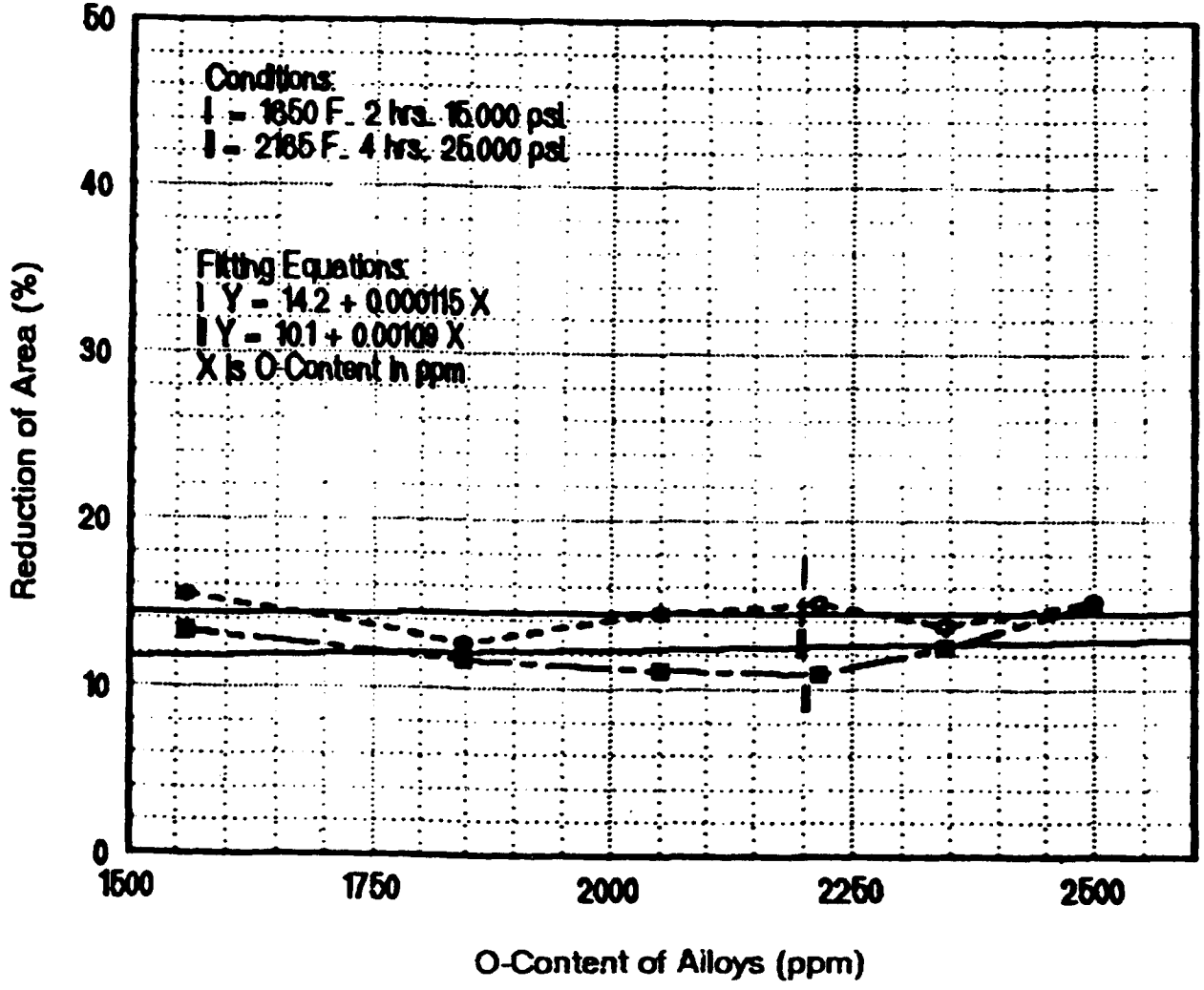

Figure 39. % REDUCTION OF AREA VS. O-CONTENT FOR 6 ALLOYS AT 2 DIFFERENT CONDITIONS.

Tensile Properties (Cont'd)

0.2% Offset Yield Strength	Y=132.0-0.0144*X X=Cl ppm Y=105.0+0.0863*X X=O ppm	1650°F,2hrs,15,000 psi
	Y=135.0-0.0150*X X=Cl ppm Y=99.2+0.0131*X X=O ppm	2165°F,4hrs,25,000 psi
	Y=162.0-0.0322*X X=Cl ppm Y=80.7+0.0310*X X=O ppm	HIPed and Heat Treated
% Elongation	Y=10.20-0.00414*X X=Cl ppm Y=7.93-0.000378*X X=O ppm	1650°F,2hrs,15,000 psi
	Y=8.63-0.00418*X X=Cl ppm Y=4.54+0.000602*X X=O ppm	2165°F,4hrs,25,000 psi
	Y=8.16-0.000691*X X=Cl ppm Y=2.94-0.000158*X X=O ppm	HIPed and Heat treated
% Reduction of Area	Y=25.0-0.0151*X X=Cl ppm Y=14.2-0.000115*X X=O ppm	1650°F,2hrs,15,000 psi
	Y=17.7-0.00769*X X=Cl ppm Y=10.1+0.00109*X X=O ppm	2165°F,4hrs,25,000 psi

In all process conditions the ultimate tensile strength (UTS) increases with decreasing Cl-content (Figure 32) and increasing O-content (Figure 33). The as-HIPed specimens display nearly identical values irrespective of the HIP cycle, and the corresponding fitting equations are also nearly identical. At a given Cl-content or O-content the highest values of UTS are found in material in the HIPed and heat treated condition.

The yield strength measured at 0.2% offset (YS) increases with decreasing Cl-content (Figure 34) and increasing O-content (Figure 35) in a manner similar to the UTS. Again, material in the HIPed plus heat treated condition displays the highest values followed by the as-HIPed samples with those HIPed at 2165°F for 4 hours at 25,000 psi pressure having higher YS than those HIPed

at 1650°F for 2 hours at 15,000 psi. The increase in YS with increasing O-content is much steeper in the HIPed plus heat treated material than in the as-HIPed material for which the plots for the two different cycles are nearly parallel.

The elongation decreases with increasing Cl-content (Figure 36) and increases slightly with increasing O-content (Figure 37). The highest values were obtained in as-HIPed samples with those HIPed at 1650°F having higher values than those HIPed at 2165°F. HIPed plus heat treated material had the lowest elongation. The reduction of area was only analyzed for the two as-HIPed conditions, since data for the HIPed plus heat treated material were not available. As with elongation, reduction of area decreases with increasing Cl-content (Figure 38), with the specimens HIPed at 1650°F showing higher values than those HIPed at 2165°F. A similar trend is displayed in plotting reduction of area against O-content, but here there is a very slight increase with increasing O-content, again with the specimens HIPed at 1650°F showing the higher values (Figure 39).

Fracture Toughness

The results of the four-point bend tests of notched test bars (Table B-4) were used to calculate an index of fracture toughness, K_{IQ}, which is considered a good estimate of the plane-strain fracture toughness, K_{IC} . K_{IQ} is given by

$$K_{IQ} = \sigma \text{ max } \sqrt{\pi a}$$

where σ max is the fracture stress and **a** is the depth of the notch.

Values of σ max and K_{IQ}, are shown in Table appended B-4. The dependence of fracture toughness on the Cl-content and O-content of material in the HIPed plus heat treated condition is shown in Figures 40 and 41, respectively. The corresponding fitting equations are as follows:

Fracture Toughness	Y = 58.2-0.0164*X X = Cl ppm
	Y = 46.9-0.000492*X X = O ppm

These results indicate that for fracture toughness the linear model of properties is not valid across the complete range of chloride concentrations. The fracture toughness is essentially constant with decreasing Cl-content to the 300 ppm level. Below 300 ppm Cl, K_{IQ} increases with a dramatic improvement below 200 ppm. Similarly, K_{IQ} is nearly constant with increasing O-content up to the 2500 ppm level.

Fatigue Testing

The HIPed and heat treated cylindrical test bars which had been low-stress machined into standard test bars were fatigue tested in reversed axial-axial fatigue (R = -1.0) under load control. The test results for each of the seven test blends are shown in appended Table B-5 and plotted as a master plot of stress vs. life (S-N) in Figure 42.

The test results show the expected improvement in fatigue properties of material with reduced levels of chloride impurity. There is a moderate increase in fatigue resistance between StCl and LCl-80 with the endurance limit, σ_f, increasing from about 50,000 psi with the StCl (1000 ppm chloride) to about 60,000 psi with the LCl-80 (200 ppm chloride) alloy blend, as shown in Figure 42. As in the case of the fracture toughness, The most dramatic increase in fatigue properties occurs between LCl-80 and ELCl with the latter blend displaying a σ_f of about 75,000 psi.

The endurance limits as a fraction of the ultimate tensile strength (σ_f/σ_{UTS}) vs. chloride content are shown in Figure 43. This plot shows a much lower (σ_f/σ_{UTS}) ratio for the heat treated ELCl material than for the as-HIPed material, indicating that the heat treatment is not as effective in increasing the dynamic (fatigue) properties as it is in increasing the static (tensile) properties.

The fatigue test results for each of the seven alloy blends were modeled using two linear regressions, as follows:

$$(1) \quad LN(N) = A + B*\sigma$$
$$(2) \quad LN(N) = C + D*LN(\sigma)$$

where:

N = Fatigue Life (Cycles)
σ = Maximum Stress (ksi)
LN = Natural Logarithm

Equations for each design point were obtained by transforming the original data into the appropriate logarithms, plotting these and curve fitting the plots. Once the equations were derived, their upper and lower confidence levels were calculated. Also calculated was the standard error of estimate, which is an indication of the "goodness of fit"; i.e., how well the calculated data fit the original data. Table IX presents the derived linear fitting equations together with their standard error of estimate. The lower the latter value, the better the "fit".

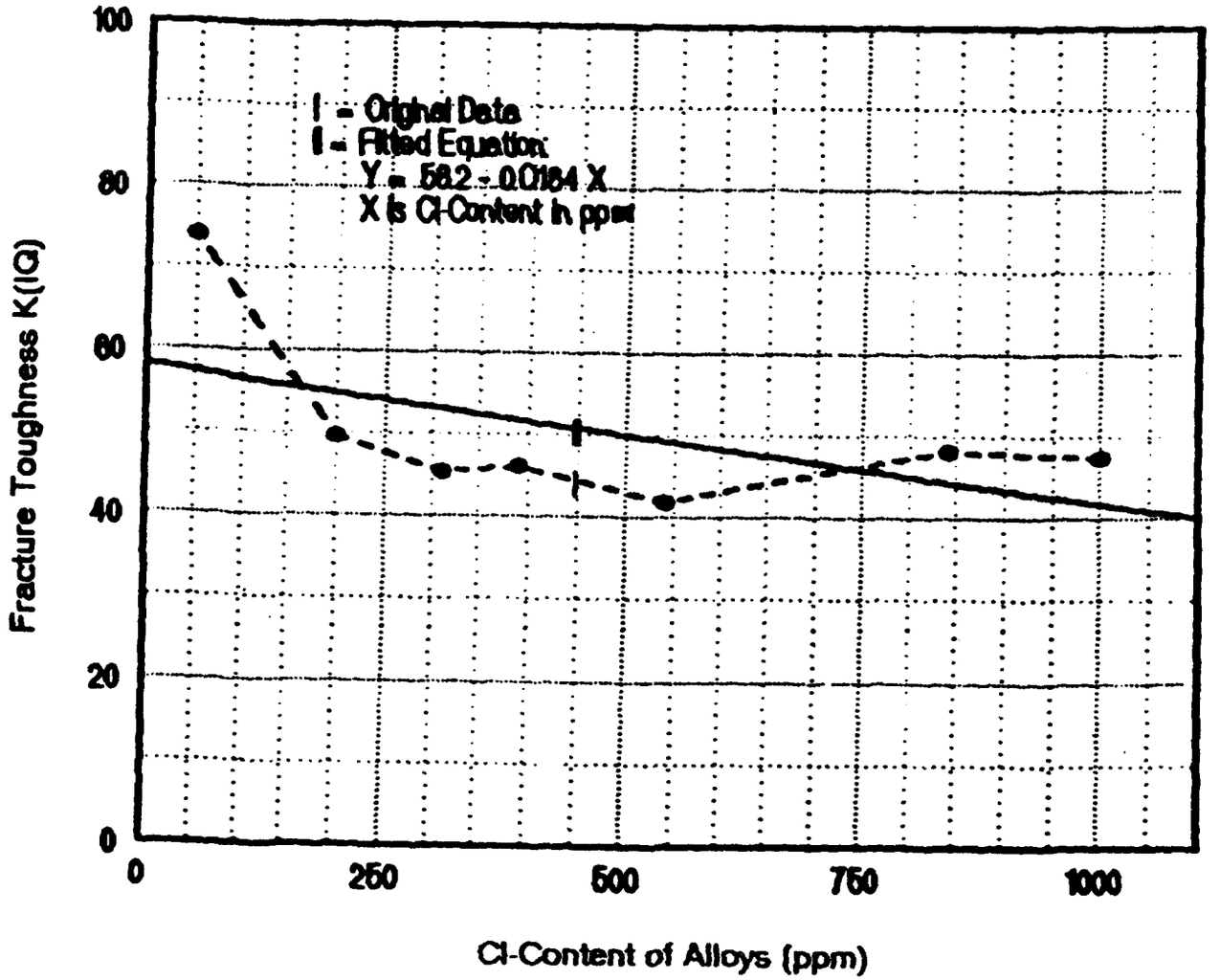

Figure 40. FRACTURE TOUGHNESS K(IQ) VS. Cl-CONTENT FOR 7 ALLOYS.

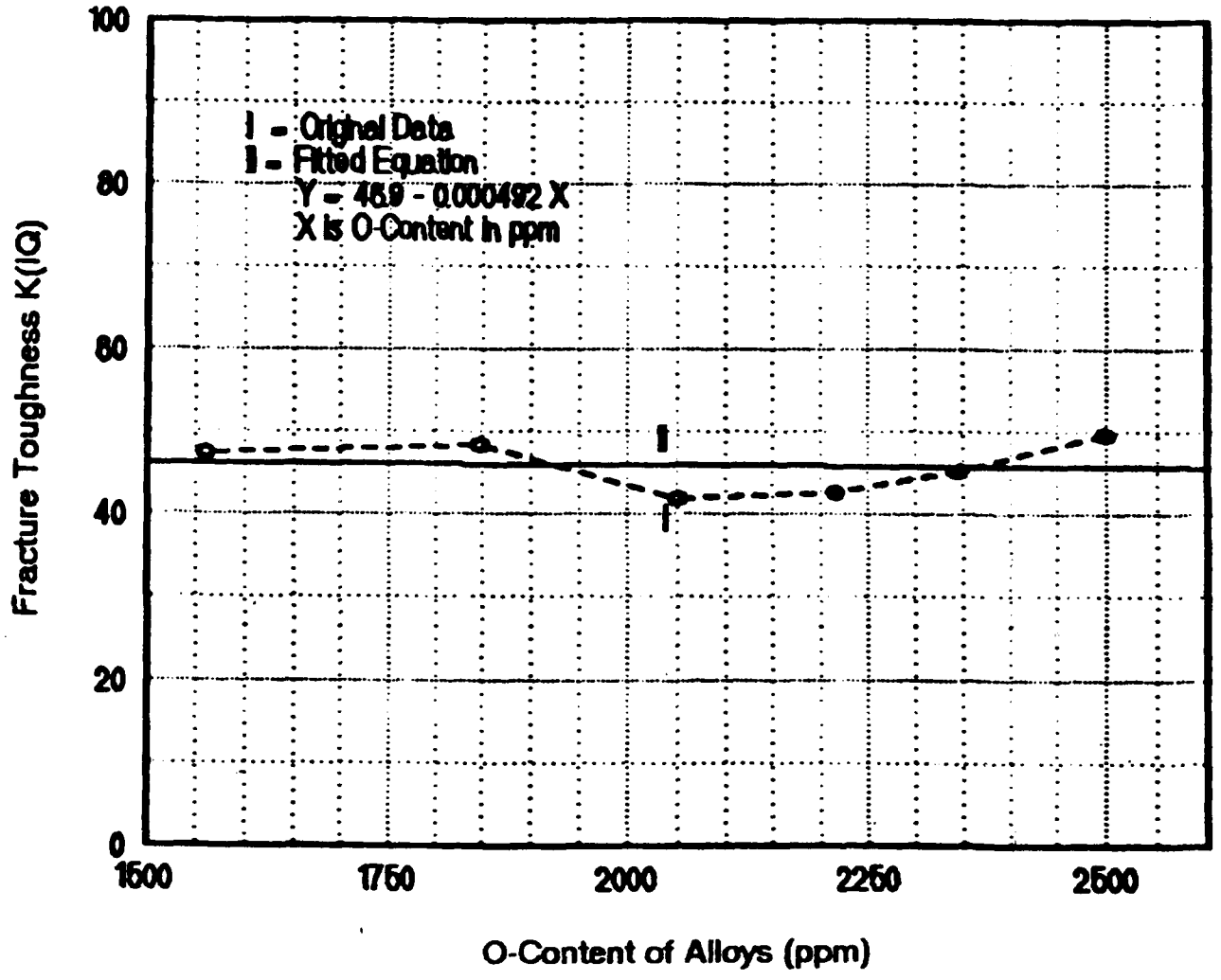

Figure 41. FRACTURE TOUGHNESS K(IQ) VS. O-CONTENT FOR 7 ALLOYS.

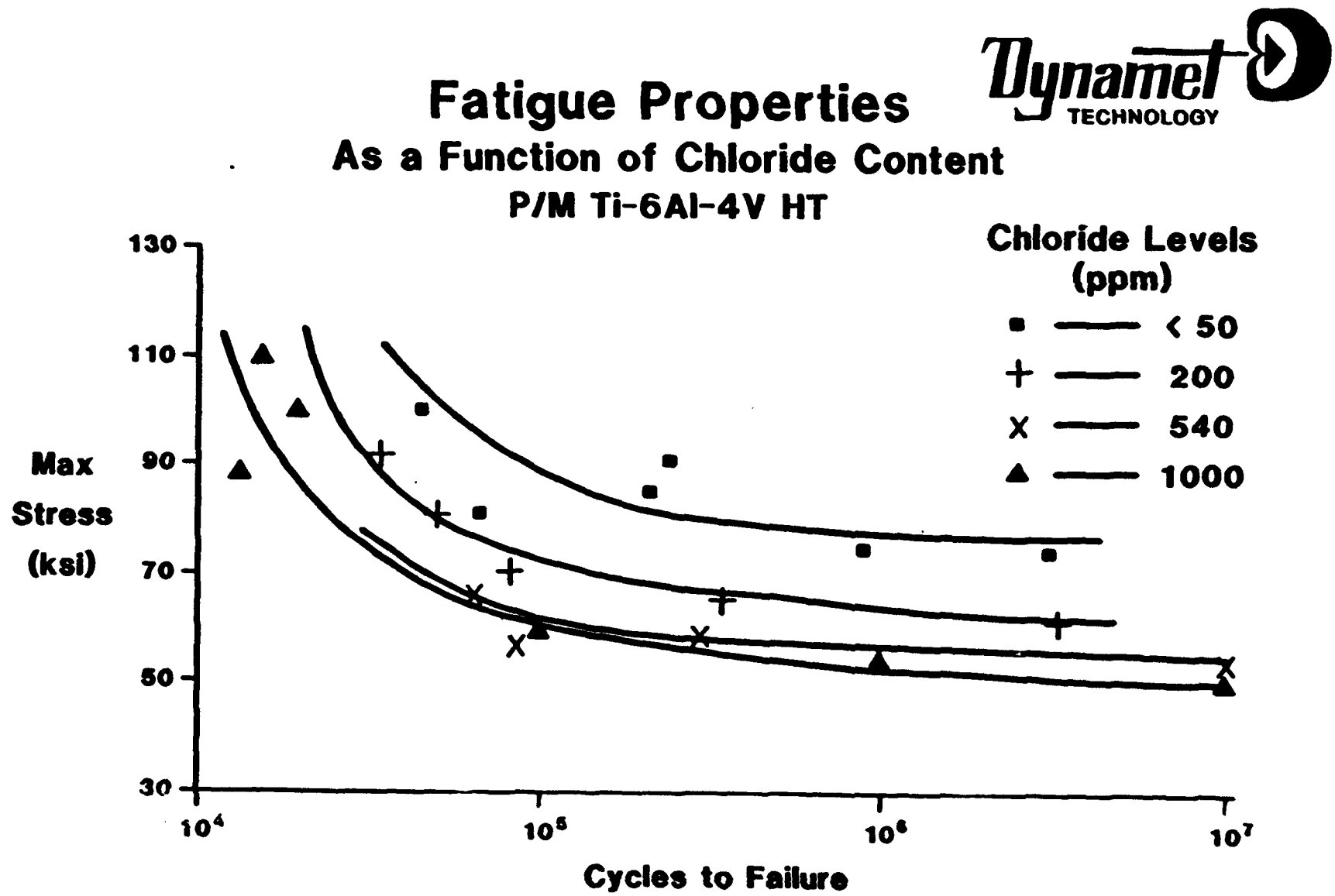

Figure 42. STRESS VS. FATIGUE LIFE, HEAT TREATED SPECIMEN RESULTS.

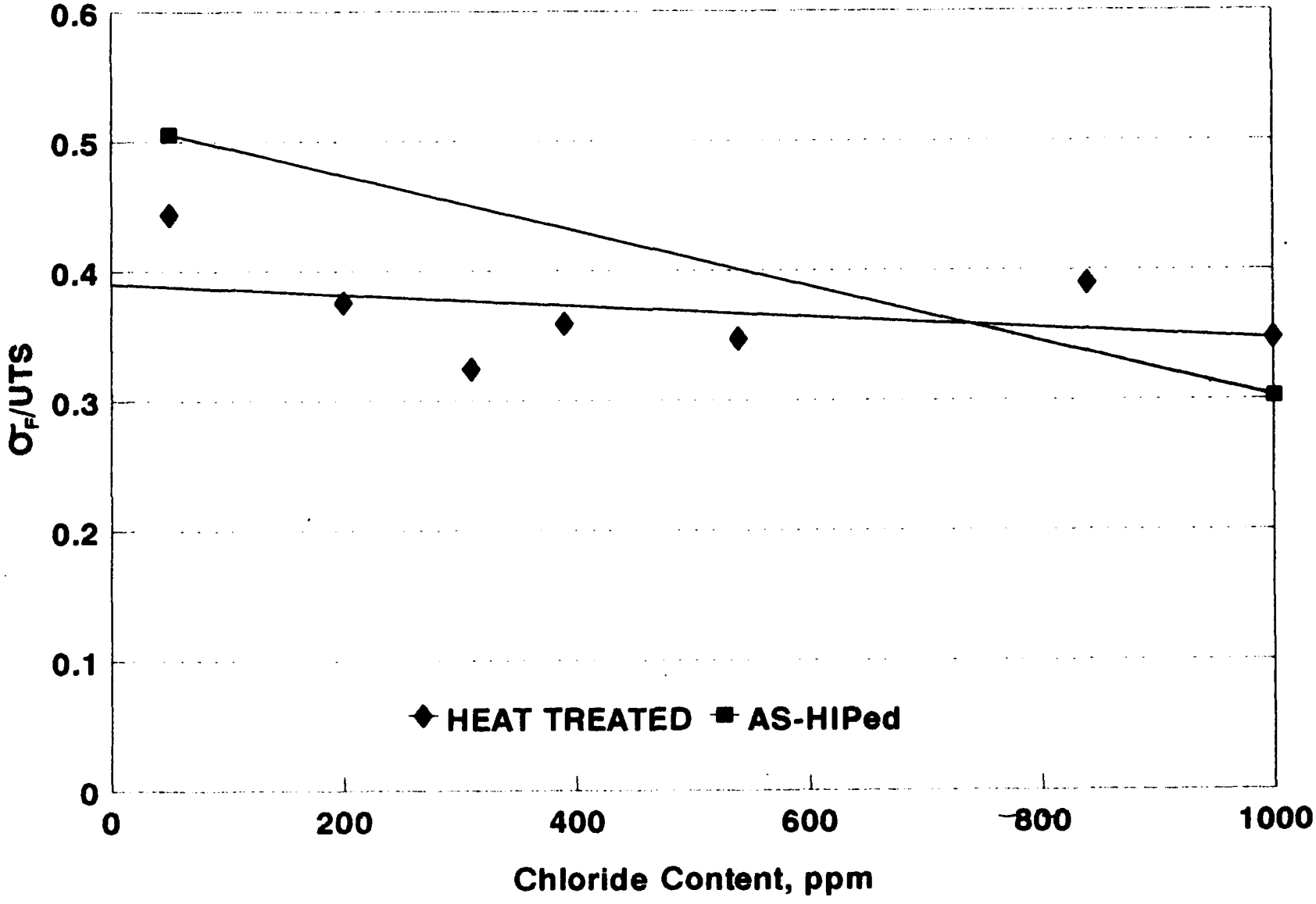

Figure 43. ENDURANCE LIMIT/UTS VS. CHLORIDE CONTENT, COMPARISON OF HEAT TREATED TO HIPed.

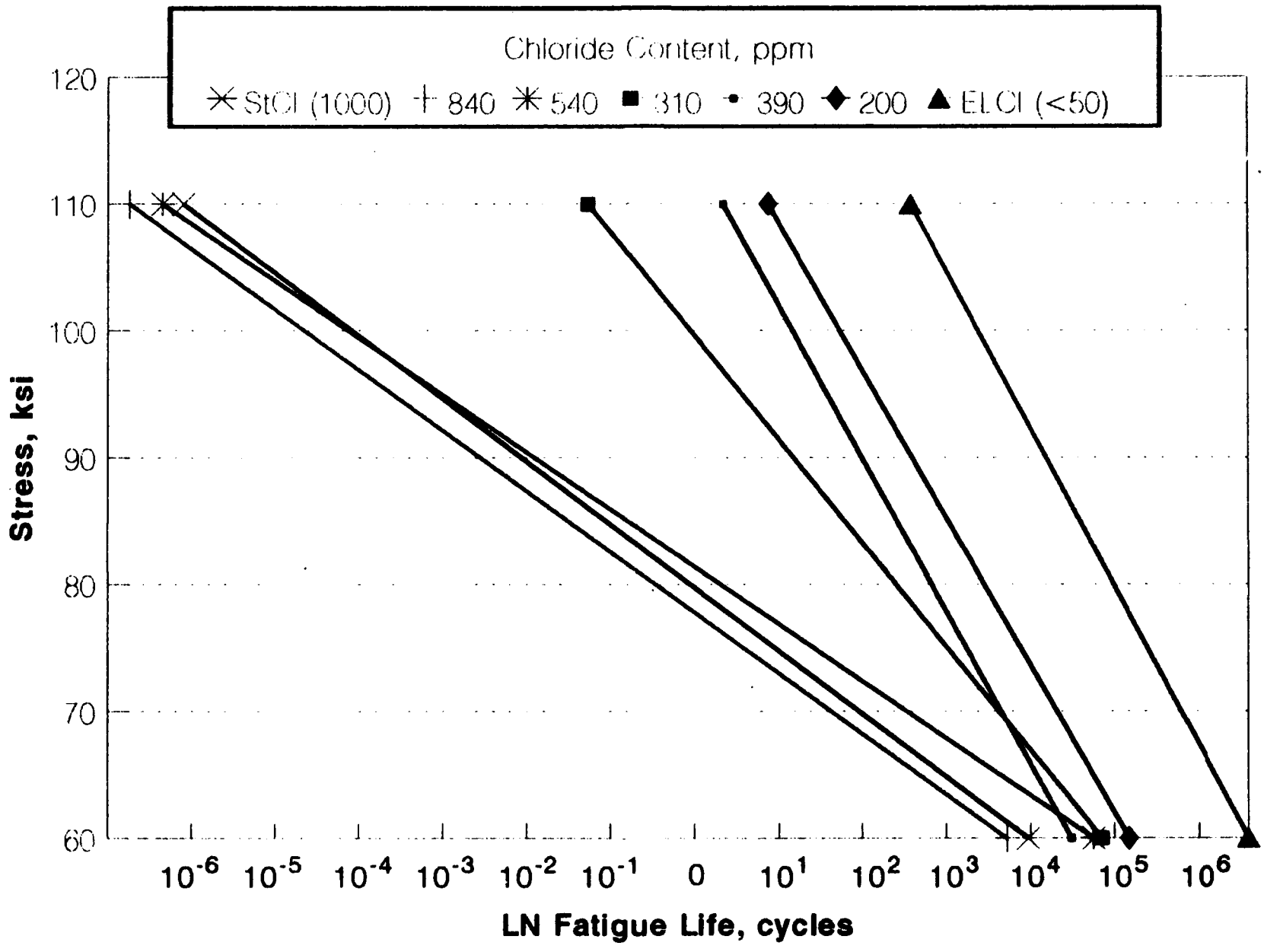

Figure 44. FATIGUE STRESS VS. LN CYCLES TO FAILURE FOR 7 ALLOYS FROM REGRESSION EQUATIONS OF TABLE IX.

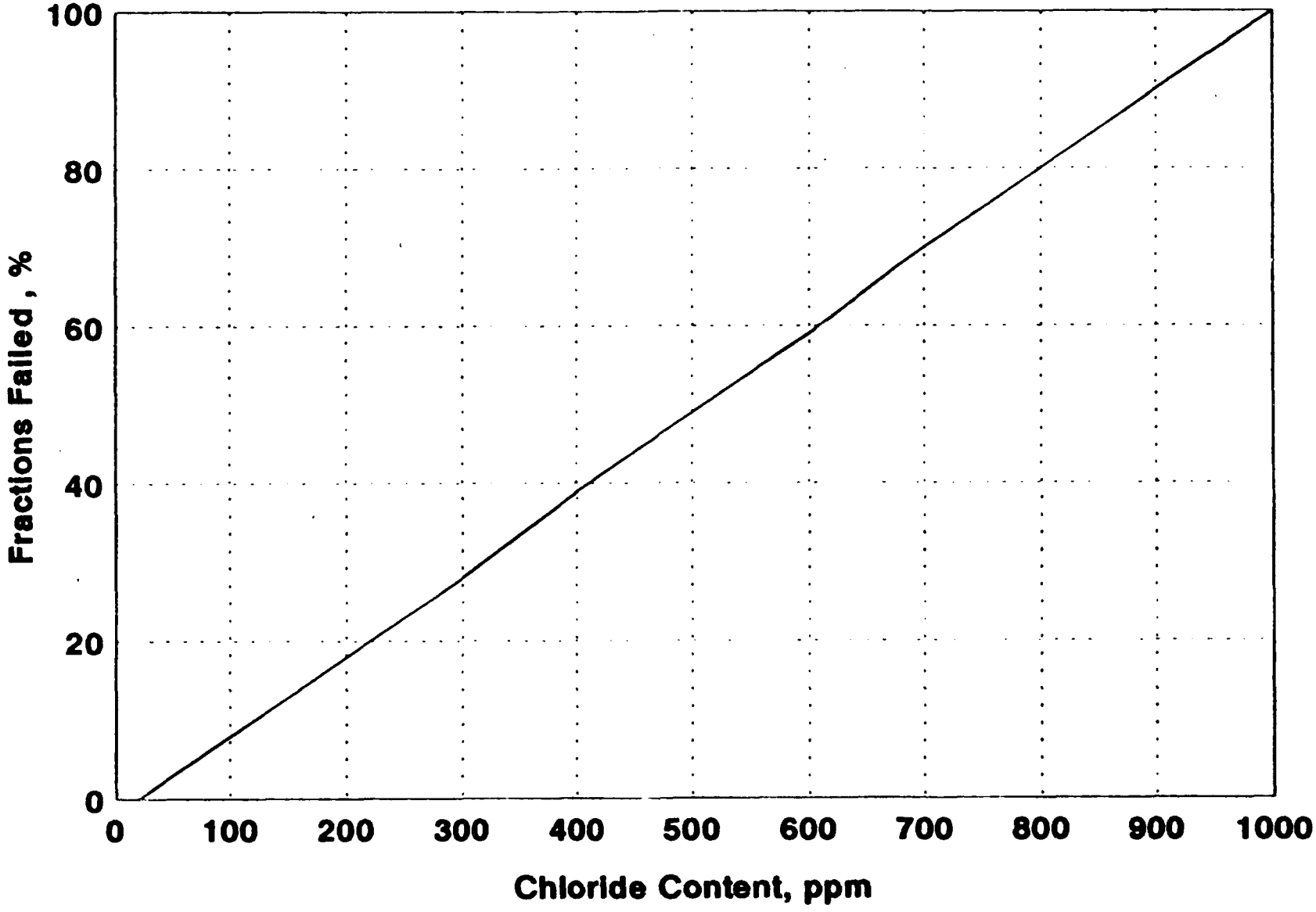

Figure 45. FRACTIONS FAILED VS. CI-CONTENT OF 7 ALLOYS AT A STRESS OF 60 KSI.

TABLE IX

LINEAR FITTING EQUATIONS FOR FATIGUE TEST RESULTS FOR SEVEN ALLOY BLENDS

		Standard Error of Estimate
1) LN Fatigue Life Cycles (N) vs. Stress (ksi)		
StCl	LN(N) = 39.3 - 0.464*S	0.03310
LCl-20	LN(N) = 39.8 - 0.482*S	0.84346
LCl-40	LN(N) = 43.9 - 0.511*S	0.81134
LCl-50	LN(N) = 30.4 - 0.282*S	2.41773
LCl-60	LN(N) = 24.1 - 0.191*S	1.76713
LCl-80	LN(N) = 26.1 - 0.198*S	1.00922
ELCl	LN(N) = 28.6 - 0.185*S	0.77753
2) LN Fatigue Life Cycles (N) vs. LN Stress (ksi)		
StCl	LN(N) = 116.0 - 25.4*LN(S)	0.84535
LCl-20	LN(N) = 120.0 - 26.7*LN(S)	0.84366
LCl-40	LN(N) = 139.0 - 30.8*LN(S)	0.85702
LCl-50	LN(N) = 87.4 - 18.1*LN(S)	2.32240
LCl-60	LN(N) = 62.4 - 12.1*LN(S)	1.63636
LCl-80	LN(N) = 72.1 - 14.1*LN(S)	0.92100
ELCl	LN(N) = 80.7 - 15.3*LN(S)	0.76038

Figure 44 is a plot of σ versus LN N (a plot of LN σ versus LN N shows essentially the same thing) and indicates as in Figure 42 that the fatigue lives of StCl, LCl-20 and LCl-40 are clustered with only a slight improvement in fatigue properties with lower chloride content. Alloys LCl-50, LCl-60 and LCl-80 form a second cluster with improved fatigue properties compared to the alloys with higher chloride. The highest fatigue lives, as expected, are exhibited by the ELCl alloy.

In addition to the regression equations, fractions failed were computed, using an approach outlined by Nelson[4]. The fractions failing calculation represents cumulative normal probabilities computed from the original data, as follows:

Cum. Norm. Prob. of [Y(I) - Y(AVE)]/Y(STD)

where:

Y(I) = individual data point in the data set
Y(AVE) = average of the data set
Y(STD) = standard deviation of the data set

Tables X and XI show the results of the fractions failed calculation. These represent cumulative normal probabilities computed from the original data. These two tables express the dependence of fractions failing either on fatigue life or on stress. The tables should either be used together or with the plot of the regression equations in Figure 44.

The fractions failed when plotted against stress shows the percentage of specimens that will fail at a given fatigue stress level. The usefulness of the fractions failing calculation is illustrated by Figure 45 which is a plot of the fractions failing vs. Cl-content at a fixed stress of 60 ksi. Whereas 100% of StCl specimens will fail at 60 ksi, the fractions failing decreases with decreasing Cl-content and at the ELCl chloride level, 0% of the specimens will fail.

---

[4] W. Nelson, Applied Life Data Analysis, Wiley, 1982, p. 222.

TABLE X

FRACTIONS FAILED (%) VS. FATIGUE LIFE (CYCLES)

	Fatigue Life (Cycles)	Fractions Failed %
StCl	10,037,617	84.18
	973,000	49.13
	97,100	15.92
LCl-20	10,000,043	87.12
	287,300	39.65
	60,200	19.04
LCl-40	10,000,043	86.43
	285,729	40.02
	60,200	19.85
LCl-50	10,000,043	87.57
	96,700	29.70
	76,000	26.74
LCl-60	10,000,043	92.47
	207,600	47.00
	45,500	25.21
	42,500	24.37
LCl-80	3,327,394	91.19
	339,700	55.57
	82,396	27.00
	49,500	18.94
ELCl	3,076,213	87.57
	236,300	29.48
	210,801	26.94

TABLE XI

FRACTIONS FAILED (%) VS. STRESS (KSI)

	Stress (ksi)	Fractions Failed %
StCl	60.0	84.13
	55.0	50.0
	50.0	15.87
LCl-20	60.0	84.13
	55.0	50.00
	50.0	15.87
LCl-40	65.0	84.13
	60.0	50.00
	55.0	15.87
LCl-50	70.0	86.24
	60.0	41.36
	55.0	19.14
LCl-60	75.0	89.26
	65.0	63.24
	55.0	28.65
	50.0	15.51
LCl-80	80.0	90.62
	70.0	55.82
	65.0	33.03
	60.0	15.28
ELCl	90.0	80.86
	85.0	58.64
	75.0	13.76

MANUFACTURE AND TEST OF OPTIMAL BEARING HOUSING

The results of the statistical analysis were used as the basis for selection of the optimal composition for the bearing housing application. Selection was based on the ability of the material to consistently meet required properties at lowest cost. The Ti-6Al-4V StCl alloy was found to fulfill this criterion.

A CHIP Ti-6Al-4V StCl preform manufactured according to Figure 13 was sent to Textron Lycoming for heat treatment and subsequent evaluation. Prior testing of witness bars manufactured with the preform using the same alloy blend indicated high performance material as shown by the results in Table II.

The bearing housing preform was solution annealed at 1750°F for 1 hour, water quenched, and aged at 1050°F for 2 hours, after which it was air cooled. Metallography, room temperature tensile tests and low-cycle fatigue tests at 400°F were performed on specimens machined from the heat treated preform.

Metallographic examination revealed a microstructure typical of heat treated Ti-6Al-4V. The uniformity of chemistry and grain size and the absence of porosity are evident in the photomicrograph of Figure 46. The structure consists of acicular alpha and transformed beta with fine alpha needles precipitated from the beta during ageing. This is the same microstructure as the heat treated test bars shown in Figure 22.

Tensile properties were also consistent with the test results of Task III (see Figures 32-35). Average tensile and yield strengths were 156 ksi and 145 ksi, respectively, exceeding the minimum specified values of AMS4998A. However, the ductility was not as high as expected.

Low cycle fatigue tests were conducted at 400°F under strain control with a fully reversed strain amplitude of 0.005. Two specimens machined from the same bearing housing preform were tested with fatigue lives of 24,195 and 39,370 cycles. These results were judged by Textron Lycoming to be more than adequate to qualify the Ti-6Al-4V StCl P/M preform for use in bearing housings and other low stress, stationary parts.

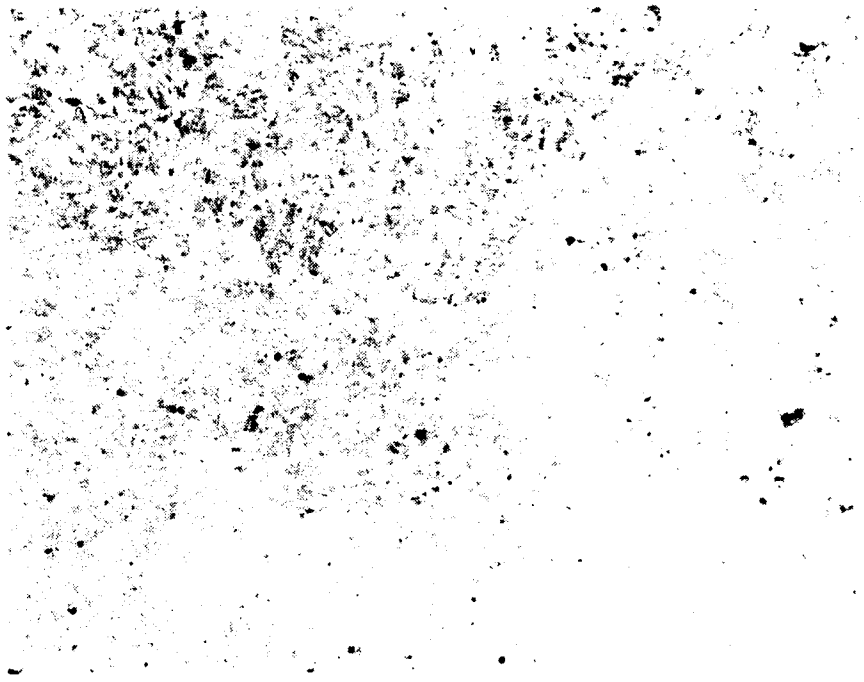

Figure 46. HEAT TREATED MICROSTRUCTURE REPRESENTING StCI Ti-6Al-4V BEARING HOUSING EVALUATED BY TEXTRON LYCOMING.

APPLICATION OF PROCESS MODEL TO NEW COMPONENT

In the original program work plan, this task was planned as a demonstration of the broader applicability of the Dynamet process to other government flight worthy components. A second bearing housing for the T55 turbine engine was tentatively identified as a potential demonstration component whose shape would lend itself to the Dynamet CHIP process and further demonstrate the cost saving benefits of the process. However, also recognized was the possibility that other Army components might later be identified which would better serve the purpose of the program.

Based on discussions with Army personnel from the Tank Automotive Command (TACOM) and the Army Research Laboratory, Materials Directorate (ARL-MD), an alternative candidate component was identified. This component is a track pin used in Army tanks (TACOM P/N 12274418) and shown in Figure 47. It is considered an ideal component for this program, because it represents a powder metal-appropriate shape for fabrication and would permit a lightweight replacement for the steel track pins currently in use which would have important benefits for the Army.

Dynamet Technology originally proposed an expanded Task V in which thirty (30) titanium alloy tank track pins would be manufactured by the CHIP process. These prototype track pins would be made from Ti-6Al-4V StCl and Ti-6Al-4V ELCl materials in as-HIPed and HIPed plus heat treated conditions and supplied to the Army as finished track pins to allow for full evaluation. However, funds were not available for the expanded Task V and, as a result, a more limited work plan, consistent with the scope in the original proposal Statement of Work, was proposed and approved by ARL-MD.

The effort consisted of the design of a tank track pin preform and the manufacture of four (4) prototype preforms according to the materials and process conditions of Table XII.

TABLE XII

TASK V PROTOTYPE TANK TRACK PIN P/M PREFORM

	Alloy Material	Process Condition	Number of PINs
A.	Ti-6Al-4V StCl	CHIP & Heat Treated	1
B.	Ti-6Al-4V StCl	CHIP	1
C.	Ti-6Al-4V LCl-70	CHIP & Heat Treated	1
D.	Ti-6Al-4V ELCl	CHIP	1

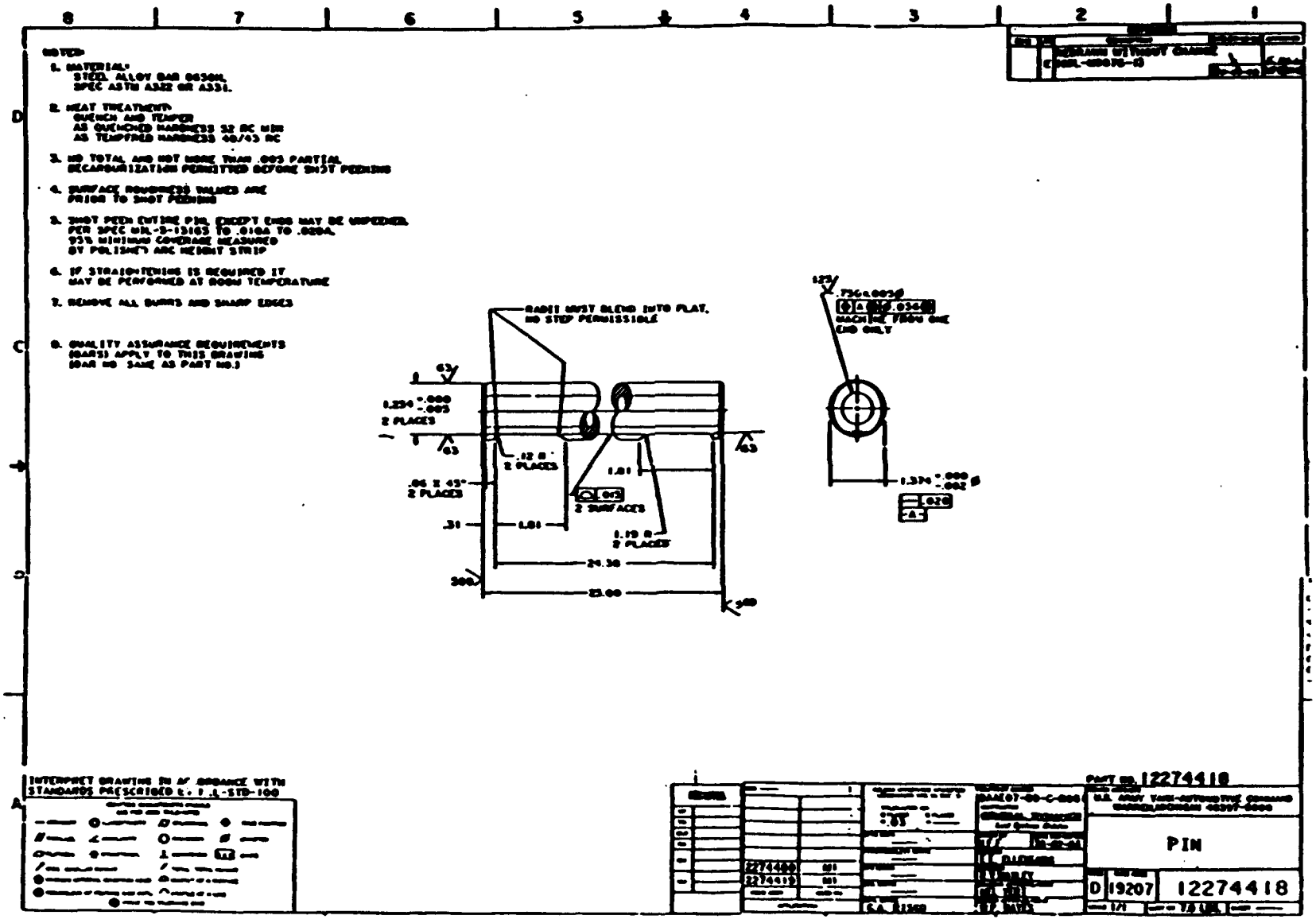

Figure 47. DRAWING OF THE TANK TRACK PIN SELECTED AS A POTENTIAL COMPONENT FOR DEVELOPMENT.

The highest (StCl) and lowest (ELCl) chloride levels comprise the end points of the mechanical performance/cost spectrum of P/M Ti-6Al-4V alloy. The intermediate Cl level may represent the most cost-effective material, since it provides near-optimum mechanical properties at a significantly reduced raw material cost. The use of the ELCl-StCl combination blend LCl-70 (70%ELCl/30%StCl ratio) fulfills a major objective of the program, namely, the manufacture of a part from an optimum blend based on the results of Task III.

For this preliminary development effort, Dynamet designed the track pin preform shown in Figure 48. A track pin made from this Ti-6Al-4V preform will provide a significant weight reduction to the currently used steel pins; the calculated preform weight is 7½ pounds with the final machined Ti-6Al-4V part weighing slightly under 4¼ pounds. This compares to a finished steel track pin weight of about 7½ pounds, resulting in a projected weight reduction of over 40% by the material substitution.

The necessary CIP tooling for pin fabrication, consisting of a steel mandrel and an elastomeric mold, was designed and manufactured. Because of the high aspect ratio of the track pin and the possibility of bending (leading to part distortion) at the high CIP pressure, a hardened steel was selected for the mandrel material. Conventional elastomeric materials were selected for the mold.

Because of the high aspect ratio of the P/M preform and the possibilities of non-uniform powder fill and shrinkage, further precautions against distortion were taken. These included the use of specially designed fixturing to ensure uniform powder fill of the mold and supports to hold the CIPed preforms rigid during sintering. No additional accessories were needed for HIPing or heat treating since most of the distortion would likely occur during sintering, because the largest volume shrinkage occurs during sintering.

A single track pin preform was manufactured according to each of the material and process conditions of Table XII. Preforms were fabricated from Ti-6Al-4V StCl, Ti-6Al-4V ELCl, and the Ti-6Al-4V LCl-70. Two process conditions were used; as-CHIPed, representing the maximum ductility, and a heat treated condition (solution annealed at 1750°F, water quenched and aged for 2 hours at 1050°F), a higher strength but lower ductility condition.

The two blends containing ELCl material utilized titanium powder from a pre-qualified powder lot. The ELCl titanium, designated R1596, was blended with 60Al-40V master alloy in

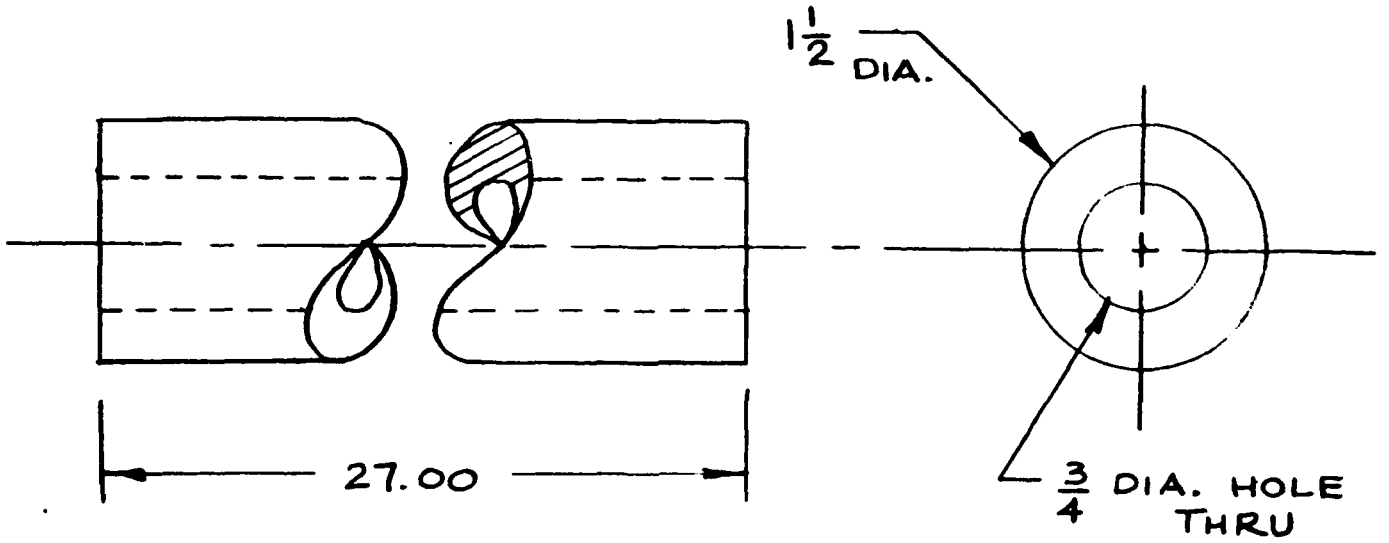

Figure 48. DYNAMET PREFORM DESIGN OF PROPOSED Ti-6Al-4V TRACK PIN TO REPLACE TRACK PIN OF FIGURE 47.

mat'l: Ti 6AL 4V	Dynamet TECHNOLOGY
tolerances: xx ± .01 .xxx ± .005 fractions ± angles ±	
SCALE: NONE	APPROVED BY
DATE: 4 AUG 92	DRAWN BY T.C. sheet 1 of 1
REF DWG 12274418	PIN BLANK
proj. no. IQ183	U.S. ARMY TANK-AUTOMOTIVE COM'D
job no.	DRAWING NUMBER

preparation of Ti-6Al-4V. Representative tensile blanks (approximately 5 inch diameter x 5½ inch long) were made from each blend, CIPed at 55 ksi and vacuum sintered. These were fully densified using a standard 1650°F HIP cycle at a pressure of 15 ksi for 2 hours, and two were selected to be tested. Results showed the materials to be compositionally uniform, and the measured mechanical properties, shown below, confirmed the material to be acceptable, qualifying the titanium powder for use in this program.

Sample No.	Ultimate Tensile Strength (ksi)	0.2% Offset Yield Strength (ksi)	(%) Elongation	Reduction of Area (%)
1	140,000	123,000	13.8	42.2
2	142,000	125,000	17.9	44.0

All parts were vacuum sintered, HIPed and heat treated using the same standard cycles developed for manufacturing the bearing housing preforms. Dimensional measurements of the pin preforms were measured after each processing step and are recorded in Figure 49.

All of the preforms achieved full 100% density (adjusted for the differences in chloride level) and displayed uniform dimensions along both the outside and inside surfaces and from end to end. The flaring of the ends was minimal, particularly for a first time tool design, and the preforms required no straightening prior to machining. This was a significant manufacturing achievement which will enhance producibility of these components in a production mode.

Preform B was manufactured with the lowest amount of starting material, less than 6½ pounds of Ti-6Al-4V StCl powder. The high weight of preform D (8.6 pounds) is due to the much higher tap density of ELCl titanium and the fact that only a single set of prototype tooling was built and designed to accommodate the full range of tap densities which results across the StCl to ELCl titanium grades.

From the Preform B result, it is anticipated that a P/M titanium alloy track pin preform manufactured with optimized tooling could eventually achieve a weight of as little as 5½ pounds, for whichever titanium grade is determined to be optimal.

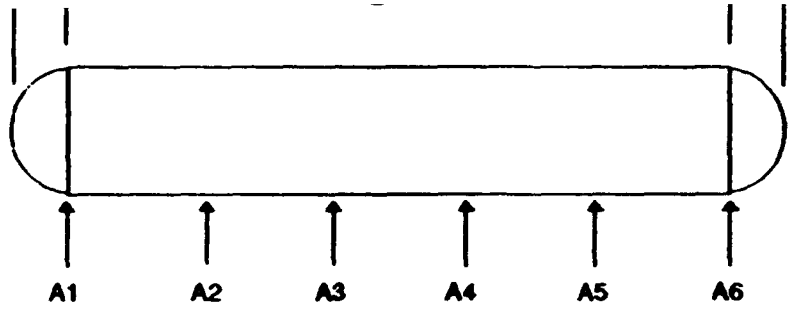

PREFORM (A) DIMENSIONS	PRESSED	SINTERED	HIPED
A1 DIA.	1.791	1.689	1.618
A2 DIA.	1.645	1.580/1.575	1.575/1.559
A3 DIA.	1.639	1.570/1.575	1.553/1.550
A4 DIA.	1.640	1.570/1.560	1.549/1.558
A5 DIA.	1.648	1.570/1.575	1.554/1.564
A6 DIA.	1.754	1.630/1.635	1.568/1.575
B	29.00	28.187	27.860
C1	0.768	0.625	0.600
C2	0.544	0.540	0.490
I.D.	0.790	0.763/0.765	0.754/0.755
	WEIGHT: 3007.4 g	DENSITY: 96.77%	DENSITY: 99.84%

PREFORM (B) DIMENSIONS	PRESSED	SINTERED	HIPED
A1 DIA.	1.755	1.689	1.671
A2 DIA.	1.614	1.543	1.525
A3 DIA.	1.633	1.564	1.545
A4 DIA.	1.612	1.544	1.527
A5 DIA.	1.614	1.537	1.523
A6 DIA.	1.711	1.653	1.635
B	28.937	28.1875	27.810
C1	0.608	0.505	0.505
C2	0.633	0.580	0.580
I.D.	0.890	0.761	0.749
	WEIGHT: 2885.8 g	DENSITY: 96.92%	DENSITY: 99.81%

PREFORM (C) DIMENSIONS	PRESSED	SINTERED	HIPED
A1 DIA.	1.909	1.800	1.792/1.785
A2 DIA.	1.796	1.706/1/715	1.682/1.690
A3 DIA.	1.801	1.717/1.715	1.664/1.680
A4 DIA.	1.802	1.695/1.710	1.667/1.684
A5 DIA.	1.791	1.696/1.704	1.670/1.678
A6 DIA.	1.909	1.800	1.770/1.775
B	29.125	27.75	27.716
C1	0.806	0.500	0.500
C2	0.844	0.56	0.56
I.D.	0.789	0.759/0.757	0.745/0.746
	WEIGHT: 3007.4 g	DENSITY: 96.77%	DENSITY: 99.97%

PREFORM (D) DIMENSIONS	PRESSED	SINTERED	HIPED
A1 DIA.	1.951	1.858	1.835
A2 DIA.	1.856	1.761	1.738
A3 DIA.	1.869	1.770	1.746
A4 DIA.	1.859	1.761	1.748
A5 DIA.	1.883	1.780	1.750
A6 DIA.	1.946	1.858	1.835
B	29.063	27.500	26.890
C1	0.521	0.485	0.475
C2	0.637	0.610	0.583
I.D.	0.790	0.749	0.741
	WEIGHT: 3919.1 gms	DENSITY: 95.09%	DENSITY: 99.84%

Figure 49. WEIGHTS, DIMENSIONAL MEASUREMENTS AND DENSITIES OF 4 TRACK PIN PREFORMS AFTER CIP, SINTER AND HIP PROCESSING STEPS.

Track pin preforms A and C of Table XII were rough machined and heat treated. Pin C was then finish machined in accordance with the applicable requirements (Figure 47), including requirements for surface finish and shot peening. Figure 50 shows 2 photographs representing (a) finish machined Pin C and unfinished Preform A, both heat treated, alongside as-HIPed Preforms B and D and (b) a before-and-after comparison of Preform B to finish machined Pin C.

Pin C, along with witness bars (5/8 inch diameter x 5 inch minimum length) representing each of the material/process combinations identified in Table XII and processed along with the related track pins, is being furnished by Dynamet to the Army for further evaluation. The other rough-machined tank track pin and two preforms along with test bars from each alloy blend and process condition are also being retained by Dynamet for later evaluation.

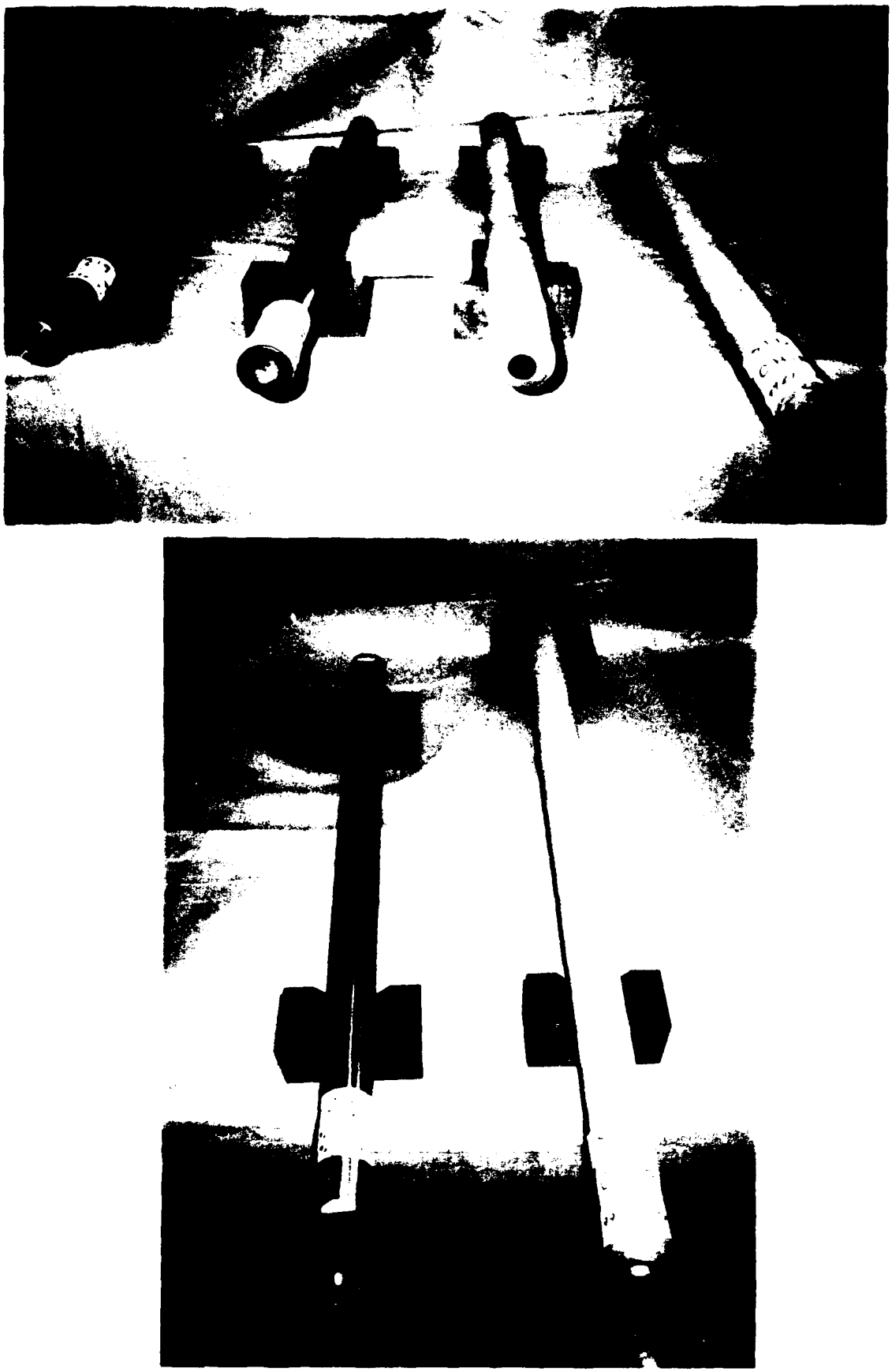

Figure 50 PHOTOGRAPHS SHOWING (a) FINISH-MACHINED PIN C AND ROUGH-MACHINED PIN A (BOTH HEAT TREATED) ALONGSIDE CHIP'D PREFORMS B AND D AND (b) PREFORM B PRIOR TO MACHINING AND FINISH-MACHINED PIN C

ECONOMIC EVALUATION

The advantages of the powder metal manufacturing approach have become increasingly apparent with the progress of this program. Refinement of the CHIP process technology and the development of a model to characterize the relationship between chloride impurity level and mechanical properties are the best means to optimize this P/M technology to meet the requirements of a particular application. The translation of the modeling to a cost-performance relationship indicates the economical practicality of applying the P/M approach to an expanded range of production circumstances. What follows are the economic considerations, benefits and tradeoffs, of the CHIP fabrication of components based on the Phase II work.

The cost relationship of chloride level to the mechanical properties is simple enough: enhanced properties with lower chloride but at greater expense. The relationship of properties to chloride is not linear and, generally, improvement can be marginal until Cl levels are reduced by over 60%. Depending on the application and requirements, the increased material cost may or may not be warranted.

Figures 51 and 52 depict fatigue endurance limit stress and fracture toughness, respectively, as a function of chloride content, as well as raw material cost (price per pound). Expectedly, properties deteriorate as the Cl level increases but, plateau or bottom out when the chloride content is at a 400 ppm or more level. This implies that the use of the higher priced material is usually not justified except in cases where requirements for performance are most demanding. However, future developments in the titanium industry are expected to lead to the availability of higher purity titanium powder, with Cl-content below 200 ppm, at significantly lower cost than ELCl powder. The results of this program will be useful in determining if the cost reduction will be sufficient to justify the use of this improved performance material.

Based on economic considerations and fatigue test results, StCl Ti-6Al-4V was judged the optimal material for the bearing housing application. The specific bearing housing component studied in the Phase II investigation is currently manufactured as a forging and finish machined to final configuration. The forging is produced as a 16 pound ring forging which must then be finish machined to the final dimensions of the housing. The P/M prototype preform produced in this program had target shape and configuration and a weight of 7 to 7¼ pounds, a marked improvement over the 9-10 pound preforms produced in Phase I.

Based upon the reduced preform size and acceptable properties of the StCl material, the estimated cost to manufacture this bearing housing preform in production is $177 (not including the expense of finish machining). In comparison, the cost to produce the 16 pound ring forging is estimated at

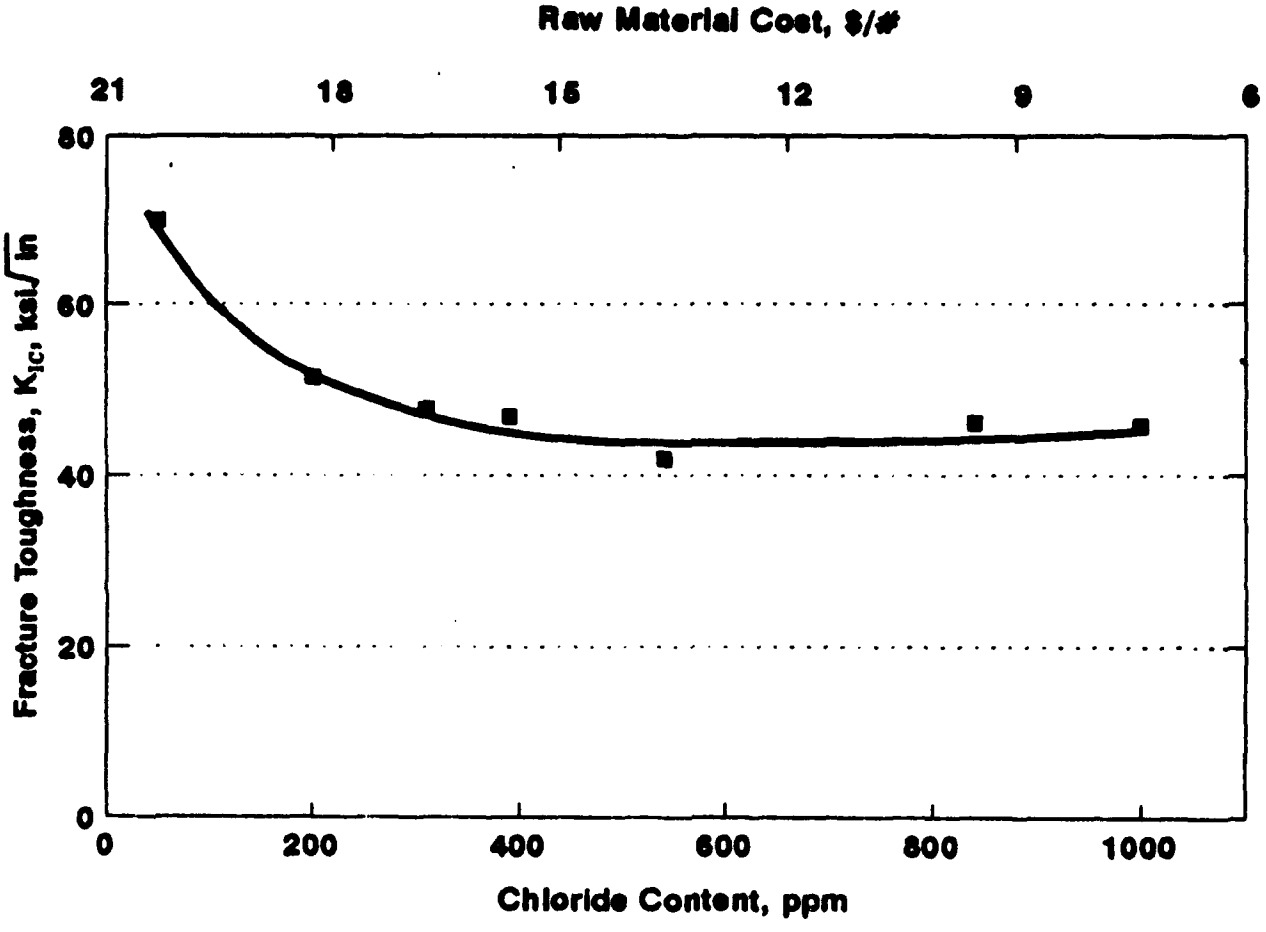

Figure 51. FRACTURE TOUGHNESS OF P/M Ti-6Al-4V IN HEAT TREATED CONDITION AS A FUNCTION OF CHLORIDE CONTENT AND RAW MATERIAL COST ($/POUND)

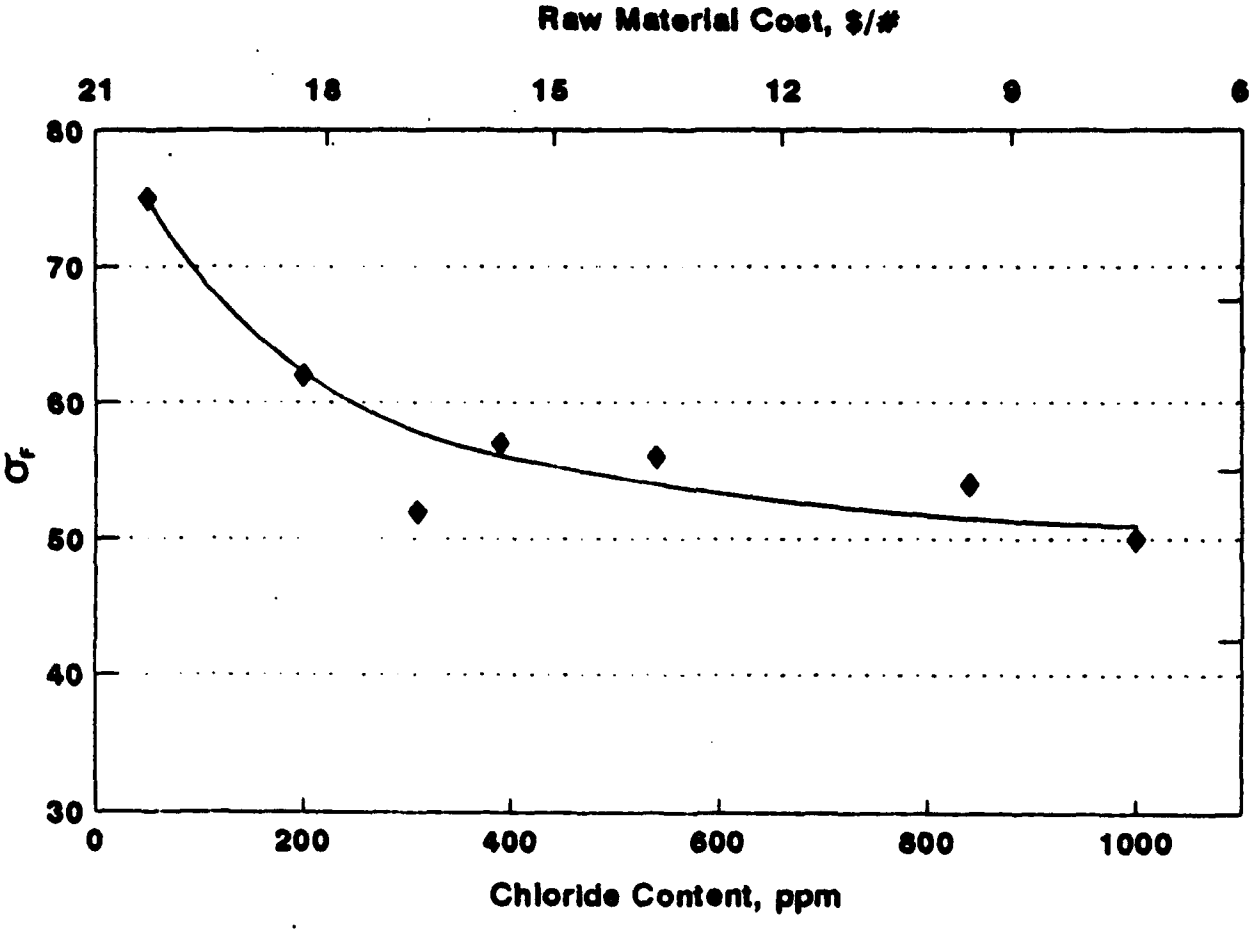

Figure 52. ENDURANCE LIMIT (σ_f) AS A FUNCTION OF CHLORIDE CONTENT AND RAW MATERIAL COST ($/POUND) FOR HEAT TREATED Ti-6Al-4V.

about $300 (not including the machining costs, which would be greater than for the P/M part, because more excess material is to be removed). Therefore, by employing the P/M preform, a cost savings representing at least 40% of the cost of the current forging is anticipated, as well as additional cost savings in the reduced machining to remove the additional 9 lbs. of excess weight of the forging over the P/M preform.

The bearing housing represents a clear example of the advantages of Dynamet's P/M process over conventional manufacturing methods. Maintaining near-net shapes in producing initial part configurations reduces material usage and the labor content of machining the preform to final dimensions. Furthermore, the flexibility in the CHIP process is broad and relevant to diverse component shapes ranging from closed-end dome shapes to high-aspect ratio tubular components such as the tank track pin. The technology also lends itself to introducing shaped features on the interior of parts, as illustrated in Task II of the program by the demonstration of the inside-out pressing. Conventional fabrication technologies such as forging cannot provide the flexibility of this type of near-net dimensional and shape control. On the other hand, cast products cannot generally provide the high performance fatigue properties of fully dense, CHIP fabricated P/M components.

THE ABILITY OF THE CHIP PROCESS TO ECONOMIZE ON A NUMBER OF LEVELS WITHOUT COMPROMISING THE END-PRODUCT QUALITY AS WELL AS ITS ADAPTABILITY TO A WIDE RANGE OF PART APPLICATIONS, PLACES IT AS A HIGHLY COMPETITIVE ALTERNATIVE AMONG THE MORE CONVENTIONAL TECHNOLOGIES AVAILABLE FOR COMPONENT MANUFACTURE.

SUMMARY AND CONCLUSIONS

This SBIR Phase II program has achieved all of its technical objectives and more. Significant accomplishments have been made in the development of economical P/M fabrication and metal processing methods to obtain microstructural uniformity and property uniformity in fully dense, near-net shape structural quality preforms. In addition, a comprehensive and reliable mechanical property data base has been obtained and used to model the important mechanical properties, including fatigue and fracture toughness, as they relate to the chloride impurity level of the starting elemental titanium powders and the corresponding powder costs. However, the linear modeling of properties vs. chloride content was not valid for all properties measured. With fatigue endurance limit and fracture toughness there was a sharp change in performance between ELCl (<50ppm) and LCl-80 (200ppm). Above 200 ppm chloride these properties were essentially constant.

Specific conclusions and achievements of the program are as follows:

1. A P/M bearing housing preform for a helicopter gas turbine engine was designed and produced at less than 7.5 lbs, a 50% weight saving compared to the forging currently used in its manufacture.

2. Statistically significant improvements in fatigue properties were achieved when chloride content was reduced to approximately 400 PPM. At 540 PPM or more there was no significant difference in the fatigue properties vs. the StCl level.

3. A 200 to 400 PPM chloride level provides a range where improved properties can be achieved to meet specific demands at reduced cost relative to producing P/M ELCl parts equivalent to conventional wrought product.

4. A significant improvement in fatigue properties was achieved between 0 and 200 PPM chloride, indicating that for the most demanding fatigue-critical applications, near chloride-free material is required.

5. Fracture toughness properties closely correlated with fatigue properties, indicating that modest improvements can be achieved through chloride level control.

6. Static properties indicated consistent results across the design points (as adjusted for oxygen level variation), and achieved properties comparable to wrought materials.

7. The experimental design provides a model and data base to permit utilization of this economical P/M technology in applications requiring more demanding fatigue requirements.

8. Titanium Army tank track pin preforms have been produced as a potential application of these results to a new component. This demonstrates the applicability of this P/M technology to components of widely varied size and configuration.

RECOMMENDATIONS

With the successful completion of Phase II, the program has clearly demonstrated that the CHIP P/M manufacturing technology achieves technical performance comparable to conventional forged titanium components. In addition, the CHIP technology clearly offers substantial savings for those component applications which take full advantage of the near-net shape making offered by CHIP fabrication. This is evident from the conservative cost projection calculated for the helicopter bearing housing and, more importantly, from the record of performance achieved by Dynamet Technology over the past few years in the production and delivery of components for missile applications. The only obstacle that remains to commercialize the use of CHIP processed titanium alloy components is to identify a component requirement in early prototype development that is approaching production status. Therefore our recommendations are as follows:

1. It is strongly recommended that the Army communicate as promptly as possible to its suppliers of fatigue critical components, that there now exists a new technology which has proven itself both technically feasible and economically advantageous for the production of structural titanium alloy components. In this way final prototype and production manufacture will most rapidly be introduced and applied to meeting requirements of existing or newly planned systems.

2. Introduction of the P/M Bearing Housing as a substitute for the Ring Forging should be pursued as a Value Engineering (VE) change.

3. The prototype CHIP fabricated tank track pins manufactured in this program should be fully evaluated to determine which material(s) have static and dynamic mechanical properties sufficient to meet the requirements of tank service. Based on these results a tank track pin development program should be undertaken to select the optimum alloy composition, refine the CHIP manufacturing of track pin preforms, and qualify this material for use (perhaps through a Phase III SBIR, see recommendation 5).

4. Review other candidate components and select a current production design which could utilize the Ti-6Al-4V CHIP preform technology developed under this program. Address required preform design modifications and qualify through first article preproduction for substitution into existing or future production.

5. Additional work should be performed which would increase the technical options offered by the CHIP titanium alloy technology and thereby expand the future opportunities for this near-net shape fabrication process. Suggested tasks could include the development of other high performance titanium alloys such as those for higher temperature use, and component preform shapes for specific applications in which these alloys are specified.

RECOMMENDATIONS (con't)

6. The successful results of this program demand the prompt undertaking of a Phase III program aimed at one or more potential production components (perhaps Tank components). The Phase III program will ensure that the innovative technology confirmed here will result in production cost benefit to the military. In addition this technology has been demonstrated to offer "dual use" application and thus such an Army program will as a by-product contribute to U.S. industrial competitiveness.

APPENDIX A

CERTIFICATE OF CONFORMANCE OF Ti-6Al-4V BEARING HOUSING MACHINED FROM DYNAMET PHASE I PREFORM

TEXTRON Lycoming

Certificate of Conformance

Lycoming Purchase Order No.	Packing Slip No.	Shipping Date
E296338	11582	11/21/90

Part Name	Part No.	Rev. Letter	Quantity
HSG BRG	2-141-073-25SP1		1

I. This is to certify that all material and/or processes used in the manufacture of this detail or assembly has been fully tested (including functional testing) and processed in accordance with the applicable specifications and Material Quality Requirements for the Inspection of Engine Parts as supplied to us.

II. This is to certify that all listed parts meet the requirements of B/P, Specifications and/or Clauses which are part of the Purchase Order and which are substantiated by appropriate records which are maintained on file and will be supplied on request.

III. For all special processes, such as heat treating, welding, magnetic particle inspection, penetrant inspection, radiographic inspection, surface treatment, etc., the following information is submitted in accordance with QAPI 65-30.

PROCESS SPECIFICATION	REV. LETTER	PROCESS DESCRIPTION	NAME OF PROCESSING FACILITY	LYCOMING CERT. NO.
P6808	K	FPI	MQS, TREVOSE, PA	Cert #0532
P6820	D	Acceptance Stds FPI	MQS, TREVOSE, PA	N/A
MATERIAL LYCOMING SUPPLIED		VT-34908		
(Dynamet)				

COMPANY NAME

KMS CORPORATION (06773)
2693 PHILMONT AVE.
HUNTINGDON VALLEY, PA. 19006

SIGNATURE AND TITLE OF COMPANY OFFICIAL

William Schoenlein

William Schoenlein, General Manager

SEE REVERSE SIDE FOR SERIAL NUMBERS

DATE

11/21/90

APPENDIX B
MEASURED PROPERTIES OF TASK III TEST BARS

TABLE B-1
DENSITIES OF TEST BARS AFTER SINTERING AND AFTER HIPING

BLEND	FORM	SINTERED DENSITY	% THEOR. DENS. (SINTERED)	HIP'D DENSITY	% THEOR. DENS. (HIP'D)
ELC1	CYLINDER	4.250	95.94	4.443	100.29[1]
ELC1	CYLINDER	4.255	96.05	4.446	100.35[2]
ELC1	CYLINDER	4.257	96.09	4.448	100.41
ELC1	CYLINDER	4.259	96.13	4.448	100.41
ELC1	CYLINDER	4.258	96.12	4.450	100.46
ELC1	CYLINDER	4.254	96.03	4.451	100.46
ELC1	CYLINDER	4.261	96.18	4.449	100.43
ELC1	CYLINDER	4.253	96.02	4.452	100.50
ELC1	CYLINDER	4.259	96.14	4.450	100.45
ELC1	CYLINDER	4.244	96.79	4.452	100.51
ELC1	CYLINDER	4.247	96.88	4.455	100.56
ELC1	RECTANGLE	4.245	95.83	4.445	100.35
ELC1	RECTANGLE	4.255	96.05	4.446	100.36
ELC1	RECTANGLE	4.254	96.02	4.447	100.38
ELC1	RECTANGLE	4.261	96.19	4.453	100.51
ELC1	RECTANGLE	4.261	96.19	4.453	100.52
ELC1	RECTANGLE	4.255	96.04	4.453	100.52
LCL-20	CYLINDER	4.310	97.30	4.435	100.11[1]
LCL-20	CYLINDER	4.312	97.33	4.434	100.09[2]
LCL-20	CYLINDER	4.306	97.20	4.433	100.07
LCL-20	CYLINDER	4.305	97.18	4.433	100.08
LCL-20	CYLINDER	4.311	97.31	4.435	100.12
LCL-20	CYLINDER	4.317	97.45	4.438	100.18
LCL-20	CYLINDER	4.314	97.39	4.434	100.08
LCL-20	CYLINDER	4.313	97.35	4.439	100.21
LCL-20	CYLINDER	4.307	97.22	4.434	100.10
LCL-20	CYLINDER	4.313	97.37	4.435	100.12
LCL-20	CYLINDER	4.307	97.23	4.432	100.05
LCL-20	CYLINDER	4.318	97.48	4.438	100.18
LCL-20	CYLINDER	4.312	97.33	4.436	100.14
LCL-20	CYLINDER	4.318	97.46	4.433	100.07
LCL-20	CYLINDER	4.312	97.35	4.434	100.08

BLEND	FORM	SINTERED DENSITY	% THEOR. DENS. (SINTERED)	HIP'D DENSITY	% THEOR. DENS. (HIP'D)
LCL-20	RECTANGLE	4.303	97.14	4.431	100.01
LCL-20	RECTANGLE	4.315	97.40	4.430	100.01
LCL-20	RECTANGLE	4.314	97.38	4.431	100.03
LCL-20	RECTANGLE	4.319	97.49	4.431	100.03
LCL-20	RECTANGLE	4.312	97.34	4.434	100.09
LCL-20	RECTANGLE	4.322	97.55	4.432	100.05
LCL-40	CYLINDER	4.311	97.32	4.438	100.19[1]
LCL-40	CYLINDER	4.303	97.13	4.437	100.16[2]
LCL-40	CYLINDER	4.310	97.29	4.435	100.10
LCL-40	CYLINDER	4.350	97.40	4.437	100.15
LCL-40	CYLINDER	4.306	97.20	4.436	100.14
LCL-40	CYLINDER	4.308	97.24	4.436	100.14
LCL-40	CYLINDER	4.308	97.25	4.434	100.09
LCL-40	CYLINDER	4.304	97.15	4.435	100.11
LCL-40	CYLINDER	4.310	97.29	4.434	100.09
LCL-40	CYLINDER	4.312	97.34	4.437	100.17
LCL-40	CYLINDER	4.307	97.22	4.433	100.06
LCL-40	CYLINDER	4.306	97.21	4.435	100.11
LCL-40	CYLINDER	4.307	97.21	4.436	100.14
LCL-40	CYLINDER	4.303	97.13	4.434	100.10
LCL-40	RECTANGLE	4.309	97.28	4.429	99.98
LCL-40	RECTANGLE	4.316	97.43	4.434	100.09
LCL-50	CYLINDER	4.297	96.99	4.441	100.26[1]
LCL-50	CYLINDER	4.297	97.00	4.447	100.39[2]
LCL-50	CYLINDER	4.304	97.16	4.433	100.07
LCL-50	CYLINDER	4.303	97.13	4.433	100.07
LCL-50	CYLINDER	4.300	97.06	4.432	100.05
LCL-50	CYLINDER	4.338	97.93	4.435	100.12
LCL-50	CYLINDER	4.301	97.09	4.431	100.02
LCL-50	CYLINDER	4.309	97.27	4.431	100.03
LCL-50	CYLINDER	4.309	97.28	4.432	100.05
LCL-50	CYLINDER	4.304	97.16	4.430	100.00
LCL-50	CYLINDER	4.304	97.16	4.431	100.04
LCL-50	CYLINDER	4.299	97.04	4.430	100.00
LCL-50	CYLINDER	4.299	97.04	4.433	100.06
LCL-50	CYLINDER	4.305	97.17	4.435	100.11

BLEND	FORM	SINTERED DENSITY	% THEOR. DENS. (SINTERED)	HIP'D DENSITY	% THEOR. DENS. (HIP'D)
LCL-50	RECTANGLE	4.303	97.14	4.438	100.18
LCL-50	RECTANGLE	4.306	97.21	4.440	100.21
LCL-50	RECTANGLE	4.299	97.03	4.437	100.15
LCL-50	RECTANGLE	4.306	97.20	4.437	100.17
LCL-50	RECTANGLE	4.300	97.06	4.440	100.22
LCL-50	RECTANGLE	4.304	97.16	4.435	100.12
LCL-60	CYLINDER	4.278	96.56	4.438	100.17[1]
LCL-60	CYLINDER	4.289	96.81	4.432	100.04[2]
LCL-60	CYLINDER	4.283	96.69	4.442	100.27
LCL-60	CYLINDER	4.280	96.61	4.441	100.26
LCL-60	CYLINDER	4.282	96.65	4.442	100.28
LCL-60	CYLINDER	4.279	96.59	4.442	100.28
LCL-60	CYLINDER	4.277	96.55	4.444	100.32
LCL-60	CYLINDER	4.284	96.70	4.444	100.31
LCL-60	CYLINDER	4.287	96.77	4.443	100.29
LCL-60	CYLINDER	4.284	96.72	4.442	100.28
LCL-60	CYLINDER	4.289	96.81	4.443	100.29
LCL-60	CYLINDER	4.298	97.02	4.444	100.32
LCL-60	CYLINDER	4.293	96.92	4.444	100.33
LCL-60	RECTANGLE	4.298	97.03	4.437	100.17
LCL-60	RECTANGLE	4.300	97.07	4.440	100.22
LCL-60	RECTANGLE	4.296	96.98	4.439	100.21
LCL-60	RECTANGLE	4.298	97.02	4.440	100.22
LCL-60	RECTANGLE	4.302	97.10	4.442	100.27
LCL-60	RECTANGLE	4.296	96.97	4.439	100.20
LCL-80	CYLINDER	4.258	96.12	4.443	100.30[1]
LCL-80	CYLINDER	4.280	96.62	4.434	100.08[2]
LCL-80	CYLINDER	4.278	96.57	4.447	100.38
LCL-80	CYLINDER	4.275	96.51	4.447	100.39
LCL-80	CYLINDER	4.265	96.28	4.448	100.42
LCL-80	CYLINDER	4.277	96.55	4.449	100.43
LCL-80	CYLINDER	4.275	96.50	4.448	100.40
LCL-80	CYLINDER	4.274	96.49	4.447	100.37
LCL-80	CYLINDER	4.252	95.99	4.448	100.41
LCL-80	CYLINDER	4.269	96.37	4.450	100.46
LCL-80	CYLINDER	4.273	96.45	4.449	100.43
LCL-80	CYLINDER	4.266	96.30	4.448	100.41
LCL-80	CYLINDER	4.271	96.41	4.450	100.46

BLEND	FORM	SINTERED DENSITY	% THEOR. DENS. (SINTERED)	HIP'D DENSITY	% THEOR. DENS. (HIP'D)
LCL-80	RECTANGLE	4.277	96.55	4.433	100.07
LCL-80	RECTANGLE	4.285	96.72	4.448	100.40
LCL-80	RECTANGLE	4.271	96.41	4.446	100.36
LCL-80	RECTANGLE	4.279	96.60	4.444	100.32
LCL-80	RECTANGLE	4.279	96.58	4.444	100.32
LCL-80	RECTANGLE	4.267	96.32	4.444	100.31
STC1	CYLINDER	4.316	97.43	4.427	99.94[1]
STC1	CYLINDER	4.313	97.36	4.435	100.12[2]
STC1	CYLINDER	4.318	97.48	4.428	99.97
STC1	CYLINDER	4.320	97.52	4.430	100.01
STC1	CYLINDER	4.314	97.38	4.429	99.97
STC1	CYLINDER	4.307	97.23	4.426	99.91
STC1	CYLINDER	4.319	97.49	4.429	99.98
STC1	CYLINDER	4.315	97.40	4.428	99.96
STC1	CYLINDER	4.320	97.51	4.429	99.97
STC1	CYLINDER	4.314	97.38	4.427	99.93
STC1	CYLINDER	4.313	97.35	4.428	99.96
STC1	CYLINDER	4.313	97.35	4.429	99.99
STC1	CYLINDER	4.322	97.56	4.430	100.00
STC1	CYLINDER	4.311	97.32	4.429	99.98
STC1	CYLINDER	4.328	97.69	4.433	100.07
STC1	CYLINDER	4.314	97.38	4.430	100.00
STC1	RECTANGLE	4.308	97.24	4.419	99.74
STC1	RECTANGLE	4.308	97.25	4.398	99.27
STC1	RECTANGLE	4.314	97.37	4.425	99.89
STC1	RECTANGLE	4.309	97.28	4.423	99.85
STC1	RECTANGLE	4.319	97.48	4.428	99.95
STC1	RECTANGLE	4.309	97.27	4.431	100.03

[1] Evaluation HIP cycle at 1650°F for 2 hours at 15,000 psi

[2] Evaluation HIP cycle at 2165°F for 4 hours at 25,000 psi

TABLE B-2

ROCKWELL C HARDNESS (Rc) VALUES FOR HIP'D AND HIP'D PLUS HEAT TREATED TEST BARS

% ELCI	HIP @ 1650 F	HIP @ 2165 F	HEAT TREATED*
0	30	33	37
20	32	32	36
40	32	33	40
50	31	33	39
60	32	32	39
80	33	35	41
100	33	37	42

*Heat Treatment after 1650F HIP by Solution Anneal at 1750F for 1 hr,Water Quench, and Age 1050F for 4 hrs.

TABLE B-3

TENSILE PROPERTIES OF HIP'D AND HIP'D PLUS HEAT TREATED TEST BARS COMPARING PROCESSES

PROCESS	BLEND	Ultimate Tensile Strength (psi)	0.2% Offset Yield Strength (psi)	Elongation (%)	Reduction of Area (%)
#1	StCl	132,100	120,400	7.3	15.3
	LCI-20	135,200	119,800	8.0	12.7
1650F HIP	LCI-40	133,100	121,200	6.3	14.4
2 HR	LCI-50	137,300	123,200	6.8	15.1
15,000 psi	LCI-60	140,800	127,800	7.1	13.7
	LCI-80	143,400	128,500	7.4	15.2
	ELCI	148,300	135,200	14.7	38.6
#2	StCl	130,800	120,900	5.9	13.3
	LCI-20	133,000	121,700	5.3	11.7
2165F HIP	LCI-40	138,200	128,300	5.3	11.1
4 HR	LCI-50	136,900	125,100	6.0	10.9
25,000 psi	LCI-60	142,300	129,400	5.7	12.5
	LCI-80	142,700	133,700	6.3	15
	ELCI	147,600	135,000	12.0	24
#3	StCl	143,760	132,320	2.7	unavailable
	LCI-20	138,480	128,570	2.6	unavailable
1650F HIP	LCI-40	161,050	150,480	2.8	unavailable
plus	LCI-50	158,660	149,360	2.4	unavailable
HEAT	LCI-60	160,190	*	*	unavailable
TREAT	LCI-80	165,500	157,410	2.6	unavailable
	ELCI	169,020	157,590	3.8	unavailable

* Broke out of gage length before reaching 0.2% offset strain.

TABLE B-4
FOUR POINT BEND TEST RESULTS
FOR SEVEN ALLOY BLENDS

BLEND	S/N	MAX. LOAD (lbs.)	DISPLACEMENT (in.)	K_{IQ} (ksi$\sqrt{in.}$)
ELC1	3	1376.6	0.038	50.03
ELC1	4	1809.2	0.048	65.75
ELC1	5	1965.0	0.071	71.41
LC1-80	3	1169.9	0.036	42.51
LC1-80	4	1216.8	0.036	44.22
LC1-80	5	1390.0	0.043	50.51
LC1-60	3	1071.5	0.032	38.94
LC1-60	4	1108.7	0.034	40.29
LC1-60	5	1329.1	0.041	48.30
LC1-50	3	1131.5	0.034	41.12
LC1-50	4	1044.4	0.033	37.95
LC1-50	5	1262.3	0.040	45.87
LC1-40	4	1051.5	0.034	38.21
LC1-40	5	1001.5	0.033	36.39
LC1-20	3	1082.9	0.030	39.35
LC1-20	4	1186.0	0.036	43.10
LC1-20	5	1177.1	0.035	42.78
STC1	3	958.8	0.028	34.84
STC1	4	1161.3	0.032	42.20
STC1	5	1246.2	0.037	45.29

TABLE B-5
FATIGUE TEST RESULTS FOR SEVEN ALLOY BLENDS

BLEND	S/N	STRESS (ksi)	FATIGUE LIFE (CYCLES)
ELC1	4	100.0	44,700
ELC1	5	90.0	236,300
ELC1	6	85.0	210,800
ELC1	7	80.0	65,200
ELC1	8	75.0	3,076,200
ELC1	9	75.0	856,200
LC1-80	4	90.0	34,300
LC1-80	5	80.0	49,800
LC1-80	6	70.0	82,400
LC1-80	7	60.0	3,327,400
LC1-80	8	60.0	3,300,600
LC1-80	9	65.0	339,700
LC1-60	4	75.0	45,500
LC1-60	5	65.0	42,500
LC1-60	6	55.0	207,600
LC1-60	7	50.0	>10,000,000
LC1-60	8	53.0	78,700
LC1-60	9	50.0	>10,000,000
LC1-50	4	70.0	76,000
LC1-50	5	60.0	96,700
LC1-50	6	55.0	>10,000,000
LC1-50	7	58.0	9,693,500
LC1-50	8	60.0	331,600
LC1-50	9	63.0	79,200
LC1-40	4	65.0	60,200
LC1-40	5	60.0	287,300
LC1-40	7	55.0	>10,000,000
LC1-40	8	58.0	85,500
LC1-40	9	60.0	169,600
LC1-20	4	60.0	80,400
LC1-20	5	55.0	218,900
LC1-20	7	50.0	>10,000,000
LC1-20	8	53.0	>10,004,800
LC1-20	9	58.0	76,100
STC1	4	110.0	15,300
STC1	5	100.0	19,100
STC1	6	88.0	13,000
STC1	7	55.0	973,300
STC1	8	50.0	>10,037,600
STC1	9	60.0	97,100

DISTRIBUTION LIST

No. of Copies	To
1	Office of the Under Secretary of Defense for Research and Engineering, The Pentagon, Washington, D.C. 20301
	Director, U.S. Army Research Laboratory, 2800 Powder Mill Road, Adelphi, MD 20783-1197
1	ATTN: AMSRL-OP-CI-AD, Technical Publishing Branch;
1	AMSRL-OP-CI-AD, Records Management Administration
	Commander, Defense Technical Information Center, Cameron Station, Building 5, 5010 Duke Street, Alexandria, VA 22304-6145
2	ATTN: DTIC-FDAC
1	MIA/CINDAS, Purdue University, 2595 Yeager Road, West Lafayette, IN 47905
	Commander, Army Research Office, P.O. Box 12211, Research Triangle Park, NC 27709-2211
1	ATTN: Information Processing Office
	Commander, U.S. Army Materiel Command, 5001 Eisenhower Avenue, Alexandria, VA 22333
1	ATTN: AMCSCI
	Commander, U.S. Army Materiel Systems Analysis Activity, Aberdeen Proving Ground, MD 21005
1	ATTN: AMXSY-MP, Mr. H. Cohen
	Commander, U.S. Army Missile Command, Redstone Scientific Information Center, Redstone Arsenal, AL 35898-5241
1	ATTN: AMSMI-RD-CS-R/Doc
	Commander, U.S. Army Armament, Munitions and Chemical Command, Dover, NJ 07801
1	ATTN: SMCAR-AET
	Director, U.S. Army Ballistic Research Laboratory, Aberdeen Proving Ground, MD 21005
1	ATTN: SLCBR-TSB-S (STINFO)
	Director, Benet Weapons Laboratory, LCWSL, USA AMCCOM, Watervliet, NY 12189
1	ATTN: AMSMC-LCB-TL
	Commander, U.S. Army Tank-Automotive Command, Warren, MI 48397-5000
1	ATTN: AMSTA-TSL, Technical Library
	Commander, U.S. Army Foreign Science and Technology Center, 220 7th Street, N.E., Charlottesville, VA 22901-5396
1	ATTN: AIFRTC, Applied Technologies Branch, Gerald Schlesinger
	U.S. Army Aviation Training Library, Fort Rucker, AL 36360
1	ATTN: Building 5906-5907
	Commander, USADC Air Defense Agency, Fort Bliss, TX 79916
1	ATTN: Technical Library
	Naval Research Laboratory, Washington, D.C. 20375
1	ATTN: Code 5830
	Chief of Naval Research, Arlington, VA 22217
1	ATTN: Code 471
	NAVCADTRN, P.O. Box 7176, Code PE34, Trenton, NJ 08628-0176
1	ATTN: Mr. Andrew Culbertson
	Naval Surface Warfare Center, 10901 New Hampshire Avenue, Silver Springs, MD 20912
1	ATTN: Mr. David Divecha
	Naval Air Warfare Center, Aircraft Division, Code 6063, Warminster, PA 18974-5000
1	ATTN: Mr. Joseph Kozol
	Commander, U.S. Air Force Wright Research & Development Center, Wright-Patterson Air Force Base, OH 45433-6523
1	ATTN: WRDC/MLLP, Mr. M. Forney, Jr.

DISTRIBUTION LIST

No. of Copies	To
	NASA - Marshall Space Flight Center, MSFC, AL 35812
1	ATTN: Mr. Paul Schuerer/EH01
	General Dynamics, Convair Aerospace Division, P.O. Box 748, Fort Worth, TX 76101
1	ATTN: Mfg. Engineering Technical Library
	Department of the Army, Aerostructures Directorate, MS-266, U.S. Army Aviation R&T Activitin, AVSCOM, Langley
1	Research Center, Hampton, VA 23665-5225
	U.S. Army Vehicle Propulsion Directorate, NASA Lewis Research Center, 2100 Brookpark Road, Cleveland, OH 44135-3191
1	ATTN: AMSRL-VP
1	NASA- Lewis Research Center, 2100 Brookpark Road, Cleveland, OH 44135-3191
	Director, Defense Intelligence Agency, Washington, D.C. 20340-6053
1	ATTN: ODT-5A (Mr. Frank Jaeger)
	Atlantic Research, 5945 Wellington Road, Coainesville, VA 22312
1	ATTN: Ms. Michele Abraham
	Ford Motor Company, Room S-2065 Science Lab, Dearborn, MI 48124-2053
1	ATTN: Dr. John Allison
	Pratt & Whitney, P.O. Box 109600, MS 707-26, West Palm Beach, FL 33410-9600
1	ATTN: Mr. Ralph Anderson
	Rockwell International Corporation, 201 N. Douglas Street, El-Segunda, CA 90245
1	ATTN: Mr. Sami El-Soudani
	GE Aircraft Engine, 1000 Western Avenue, M/S 37403, Lynn, MA 01910
1	ATTN: Mr. James Fleck
	ARC Amercom, 8928 Fullbright Avenue, Chatsworth, CA 91311
1	ATTN: Mr. Vincent Fry
	Lockheed Aeronautical Systems Co., 86 S. Cobb Dr., D73/73 20150 Bldg. B1, Marietta, GA 30056
1	ATTN: Mr. Timothy Ginter
	General Dynamics, MZ 5860, P.O. Box 748, Fort Worth, TX 76101-0748
1	ATTN: Mr. David Gordon
	Rockwell International Science Center, 1049 Camino dos Rios, P.O. Box 1085, Thousand Oaks, CA 91360
1	ATTN: Dr. Jeffrey Graves
	Garrett Engine Division, 111 S. 34th St., P.O. Box 5217, MS 5034V, Phoenix, AZ 85010
1	ATTN: Dr. James Hall
	Titanium Metals Corp., P.O. Box 2128, Henderson, NV 89009
1	ATTN: Dr. Paul J. Bania
	GM Corp Advanced Engineering Staff, 30300 Mound Rd., A/MD-31, Warren, MI 48090-9040
1	ATTN: Ms. Susan Hartfield-Wunsch
	Howmet Corp/Applied Research Div - CTL, 1500 South Warner Street, Whitehall, MI 49461-1895
1	ATTN: Mr. Blair London
	Crucible Materials Corporation, P.O. Box 88, Pittsburgh, PA 15230
1	ATTN: Mr. John Moll
	Textron Specialty Materials, Two Industrial Avenue, Lowell, MA 01851
1	ATTN: Mr. Peter Nagy

DISTRIBUTION LIST

No. of Copies	To
	Textron Lycoming, 550 S. Main Street, Stratford, CT 06497-2452
1	ATTN: Dr. Vinod Nangia
	United Technologies Corporation, 400 Main Street, East Hartford, CT 06108
1	ATTN: Mr. Paul Nisson
	GM Corp/Allison Gas Turbine, 333 W. First Street, Ste 200, Dayton, OH 45402
1	ATTN: Dr. John Petrusha
	Allied-Signal Aerospace Co., 717 N. Bendix Drive, Southbend, IN 46620
1	ATTN: Mr. Richard Rateick Jr.
	MSNW Inc., P.O. Box 865, San Marcos, CA 92069-0300
1	ATTN: Dr. George Reynolds
	GM Corp/Allison Gas Turbine, P.O. Box 420, Speed Code W06, Indianapolis, IN 46206-0420
1	ATTN: Mr. Ronald Roessler
	GE Corp R&D, P.O. Box 8, Bldg. K-1, MB-265, Schenectady, NY 12301
1	ATTN: Dr. R. Grant Rowe
	McDonnell Douglas Corporation, P.O. Box 516, MC 1021322, St. Louis, MO 63166
1	ATTN: Ms. Catherine Sabinash
	RMI Titanium Co., 1000 Warren Avenue, Niles, OH 44446
1	ATTN: Mr. John Schley
	Allied Signal Aerospace, 3000 Presidential Drive, Ste 300, Fairborn, OH 45324
1	ATTN: Mr. David Stanforth
	Dynamet Technology, Inc., Eight A Street, Burlington, MA 01803
1	ATTN: Dr. Stanley Abkowitz
	Director, U.S. Army Research Laboratory, Watertown, MA 02172-0001
1	ATTN: AMSRL-OP-WT-IS, Technical Library
1	AMSRL-OP-WT-IS, Visual Information
1	AMSRL-OP-PR-WT
5	AMSRL-MA-CC, Dr. Martin G.H. Wells, COR